ABSTRACT

NOVEL INTERNALLY-ULTRAFILTRATION FOR PROTEIN PURIFICATION

by

Meredith Ann Feins

A new ultrafiltration technique based on a multimembrane stack has been developed to fractionate proteins closer in molecular weight than conventionally possible. The technique is illustrated here by obtaining a pure protein product from a binary protein mixture. By employing membranes in series using the same membrane without any gaskets or spacers in-between, ultrafiltration is carried out to separate two proteins relatively close in molecular weight. Flat membranes, of the same molecular weight cutoff (MWCO) 30,000 or 100,000, are stacked together in the desired number, and ultrafiltration takes place. The membrane rejection of a protein is amplified with each additional membrane, ultimately resulting in a completely rejected species. Complete purification of the more permeable protein may be achieved by operating under a physicochemical condition that is optimal for selective separation by a single membrane. Three systems; myoglobin and β-lactoglobulin (molecular weight ratio 2.05), myoglobin, and α-lactalbumin (molecular weight ratio 1.22), and hemoglobin and bovine serum albumin (molecular weight ratio 1.03) were studied under various operating conditions. Complete rejection was achieved using three membranes one on top of the other for all three systems. To achieve complete rejection in a multimembrane stack, the single membrane rejection must be considerable. Cleaning *in situ* was achieved with reproducible experimental results before and after on-line cleaning. Flux decreased by a factor equal to the number of membranes when a multimembrane composite was used.

However, the lost flux may be recovered by increasing the pressure by the same factor. The results clearly demonstrate that multimembrane stacks can be used for effective fractionation of proteins that are quite close in molecular weight. Internally-staged ultrafiltration (ISUF) with one flat membrane on top of the other may therefore overcome some of the limitations of conventional ultrafiltration (UF). Two types of models have been explored, one based on a lumped model, the other based on a convection-diffusion model with concentration polarization to explain the potential amplification of retention with each added membrane.

NOVEL INTERNALLY-STAGED ULTRAFILTRATION FOR PROTEIN PURIFICATION

by
Meredith Ann Feins

A Dissertation
Submitted to the Faculty of
New Jersey Institute of Technology
In Partial Fulfillment of the Requirements for the Degree of
Doctor of Philosophy

Otto H. York Department of Chemical Engineering

May 2004

APPROVAL PAGE

NOVEL INTERNALLY-STAGED ULTRAFILTRATION FOR PROTEIN PURIFICATION

Meredith Ann Feins

Dr. Kamalesh K. Sirkar, Advisor — Date
Distinguished Professor of Chemical Engineering, NJIT
Foundation Professor, Membrane Separations

Dr. Piero Armenante, Committee Member — Date
Distinguished Professor of Chemical Engineering, NJIT

Dr. Gordon A. Lewandowski, Committee Member — Date
Distinguished Professor of Chemical Engineering, NJIT

Dr. Dana E. Knox, Committee Member — Date
Associate Professor of Chemical Engineering, NJIT

Dr. Barbara Kebbekus, Committee Member — Date
Professor of Chemistry, NJIT

BIOGRAPHICAL SKETCH

Author: Meredith Ann Feins

Degree: Doctor of Philosophy

Date: May 2004

Undergraduate and Graduate Education:

- Doctor of Philosophy in Chemical Engineering
  New Jersey Institute of Technology, Newark, NJ 2004

- Bachelor of Science in Biology
  Syracuse University, Syracuse, NY 1990

Major: Chemical Engineering

Presentations and Publications:

Meredith Feins, K.K. Sirkar, 2004, "Highly Selective Membranes in Protein Ultrafiltration." *Biotechnology and Bioengineering*, in press (Accelerated Publication).

Meredith Feins and K.K. Sirkar, 2003, "Novel Internally-Staged Ultrafiltration Membranes for Protein Purification." Submitted.

Meredith Feins and K.K. Sirkar, 2003 Highly Selective Membranes in Protein Ultrafiltration, AIChE Annual Meeting, San Francisco, CA.

Meredith Feins and K.K. Sirkar, 2003 Highly Selective Membranes in Protein Ultrafiltration, 14th NAMS Annual Meeting, Jackson Hole, WY.

Meredith Feins and K.K. Sirkar, 2002 A New Ultrafiltration Technique for Biomolecule Isolation and Purification, AIChE Annual Meeting, Indianapolis, IN.

To my beloved husband Ed

ACKNOWLEDGMENTS

I would like to express my deepest appreciation to Dr. Kamalesh K. Sirkar, who has been a dedicated advisor and mentor. He has provided essential guidance and leadership throughout my Ph.D. study. He has continually challenged me and has provided me with an invaluable education.

I am very grateful to Dr. Piero Armenante, Dr. Barbara Kebbekus, Dr. Dana E. Knox, and Dr. Gordon A. Lewandowski, who served on my dissertation committee. I am appreciative for their useful advice and insight on the proposal and the dissertation.

I thank the Center for Membrane Technologies at NJIT, and Otto H. York Department of Chemical Engineering for financial support during my Ph.D. study. I would like to thank all the members of the membrane separation group for their friendship and assistance during my time at NJIT.

Deepest thanks to my family, especially my husband, Ed, for keeping me inspired and motivated. He has encouraged me to reach for my dreams and helped me to achieve my goals. His unconditional support and love have been a constant source of strength and guidance.

TABLE OF CONTENTS

TABLE OF CONTENTS
(Continued)

Chapter **Page**

TABLE OF CONTENTS
(Continued)

Chapter **Page**

LIST OF TABLES

LIST OF FIGURES

LIST OF FIGURES
(Continued)

Figure **Page**

LIST OF FIGURES
(Continued)

Figure **Page**

LIST OF FIGURES
(Continued)

Figure **Page**

LIST OF FIGURES
(Continued)

Figure **Page**

LIST OF FIGURES
(Continued)

Figure **Page**

LIST OF FIGURES
(Continued)

Figure **Page**

NOMENCLATURE

a	Area of the membrane (cm^2)
A	Water permeation parameter (cm/psig/min)
C	Protein concentration in the liquid (mg/ml or μg/ml)
J_v	Permeate flux (μm/s or cm/min)
D_0	Protein diffusivity in free solution (m^2/s)
D_{eff}	Effective protein diffusivity in the pore (m^2/s)
k	Mass transfer coefficient (m/s)
K_c	Convective hindrance factor
K_d	Diffusive hindrance factor
M	Molecular weight (Da)
N_s	Protein flux (kg/cm^2-min)
P	Pressure (psig)
Pe_m	Peclet number for the membrane, $S_\infty J_v \delta_m / D_{eff}$
Q	Flow rate (cm^3/min)
R	Rejection coefficient for membrane
S_a	Actual sieving coefficient
S_o	Observed sieving coefficient
S_∞	Intrinsic sieving coefficient
t	time (min or s)
T	Temperature (K)
V_o	Initial volume in ultrafiltration cell (ml)
V	Volume of retenate (ml)

Greek letters

δ	Thickness (m or μm)
ε	Membrane skin layer porosity
ϕ	Protein partition coefficient between the solution and the membrane
Ψ	Selectivity

Subscripts

b	Bulk solution
i	Species i
w	Membrane wall on feed side
f	Feed side
m	Membrane
p	Permeate side
z	At any point from $z=0$ (for the feed)
1	Membrane 1
2	Membrane 2
3	Membrane 3

CHAPTER 1

BACKGROUND

1.1 Introduction

In the production of biopharmaceuticals, cell-culture and fermentation processes are utilized to produce target drug molecules (e.g., interferons, hormones, immunoglobulins, DNAs, growth factors). Biomolecules are either intracellular or extracellular products. Intracellular proteins require cell lysis, which creates complex mixtures containing cell debris that are difficult to separate. Extracellular proteins are excreted into the broth and the whole cells are separated from the broth. After the cell debris or whole cells are removed, a complex mixture containing the target biomolecule is obtained. Regardless of intracellular or extracellular method, downstream protein purification requires many purification steps.

Due to the complex broth / mixture, many bioseparation steps are required to isolate the target molecule. The processes utilized for protein purification contribute to the high costs associated with downstream purification. The cost for downstream recovery and purification accounts for 50-80% of the total production cost (Harrison 1994; Sofer and Hagel 1997). Overall manufacturing costs in the production of biopharmaceuticals is crucial in today's market to overall profit margin (Rathore 2004). Therefore, the development of techniques that increase the selectivity and reduce the cost, are highly desirable, making them the current focus of research.

The downstream purification processes that are currently utilized include: chromatography, membrane adsorption or membrane chromatography, and ultrafiltration

(UF) (Harrison 1994). Chromatographic processes realize very high selectivities based on solute interaction with specific beads in a column (Scopes 1994). In this process as generally implemented, separation is often limited by diffusion in and out of the resin particles (Figure 1.1). Gigaporous particles have been recently developed to facilitate convective flow through the particles which is expected to mitigate this problem (Pfeiffer, Chen, and Hsu 1996). However, the buffer volume employed in such processes is very high. Moreover, scaleup is problematic making column chromatography costly. Regeneration and elution steps are needed, which add to the overall process time and cost. Specifically, chromatography may account for two-thirds of the total downstream processing costs (Myers 2000). Therefore alternatives to conventional chromatography are desired to reduce downstream processing costs.

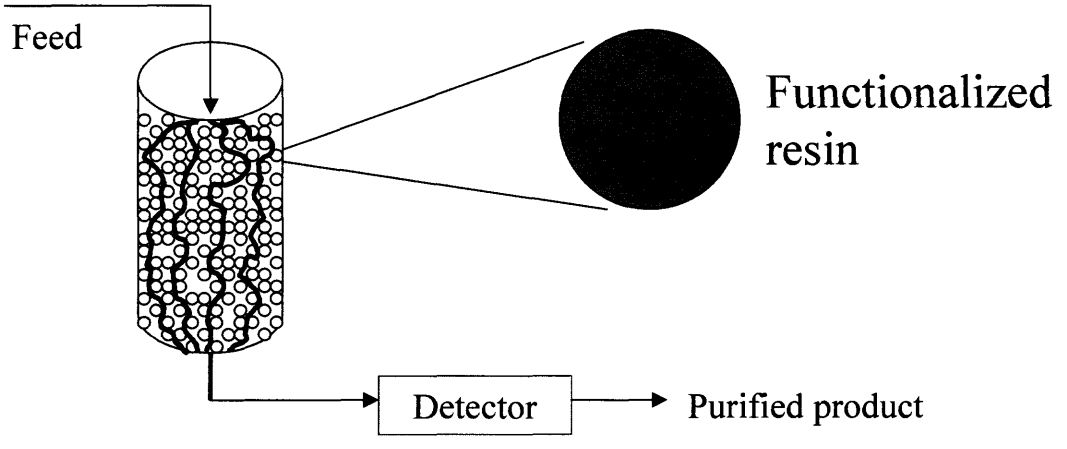

Figure 1.1 Schematic of a chromatographic process.

Membrane adsorption processes were developed as an alternative to column chromatography in order to increase the flux and reduce the cost. Figure 1.2 illustrates a schematic of a membrane adsorption process. In this process, specific ligands are grafted onto the surface of pores in membranes traditionally employed in microfiltration; biomolecule binding with the ligands occurs during convection through the membrane pores (Thömmes, Halfar, Lenz and Kula 1995). The large pore size in microfiltration membranes makes this process attractive, since it allows much easier and convective access to the binding sites on the pore wall rather than diffusion in conventional beads packed in chromatography columns. The ligand utilization has been shown to be orders of magnitude higher. But it is an unsteady cyclic process. In a given cycle, the overall capacity for adsorption is low; consequently, multiple cycles are needed.

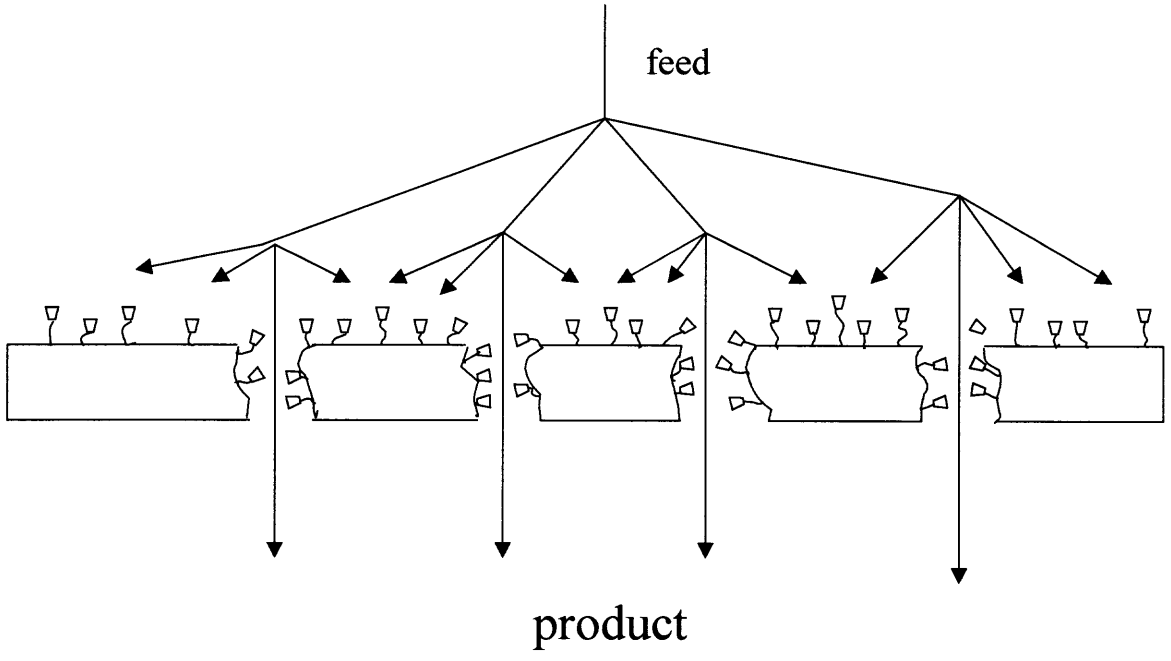

Figure 1.2 Schematic of a membrane adsorption process.

The membrane adsorption process mentioned above requires specially designed adsorbents and unusual operating conditions; for example, rapid cyclic procedures are employed spanning many cycles: each cycle consists of an adsorption, elution, and regeneration step. Membrane adsorption processes are not immune from dispersion in current device designs (Gebauer, Thömmes and Kula 1997); protein binding capacities comparable with conventional chromatographic beads have not been achieved (Sarfert and Etzel 1997).

1.2 Ultrafiltration Processes

Ultrafiltration is a pressure-driven process used for size-exclusion-based separation of macromolecules (500 to 500,000 daltons). The membranes used in UF are asymmetric membranes containing a microporous / mesoporous skin that is permselective and a more porous substrate for support. The pore sizes of UF membranes range from 10 to 1000 Å (Kulkarni, Funk, and Li 2001).

Rejection relates the concentration of solute in the permeate to that in the feed solution. The rejection of the membrane is expressed by:

$$R = 1 - \frac{C_p}{C_f} \tag{1.1}$$

Where R is the rejection coefficient, C_p is the concentration of solute going through the membrane (permeate), and C_f is the solute concentration upstream of the membrane (feed). When a solute is completely retained by a membrane, its rejection equals 1.0. If a solute permeates through the membrane freely, the rejection is equal to zero. The sieving coefficient S, is used to evaluate solute sieving or transport and is related to rejection as follows:

$$S = 1 - R = \frac{C_p}{C_f} \tag{1.2}$$

The sieving coefficient and the rejection coefficient are both used to describe the performance of a membrane for a given solute.

The characterization of ultrafiltration membranes reveals a pore size distribution (Merin and Cheryan 1980; Fane, Fell, and Waters 1981; Chan and Matsuura 1983). The pore size distribution of an ideal membrane compared to that of an actual membrane is illustrated in Figure 1.3. Because of the pore size distribution that exists in all membranes, there are smaller and larger pores present in actual membranes. Due to these smaller and larger pores, small as well as large molecules can permeate through the membrane.

The result of such a pore size distribution on which molecules pass through the membrane to what extent is illustrated in Figure 1.4. Membrane manufacturers characterize their ultrafiltration membranes by using a molecular weight cutoff (MWCO), which is where 95% of proteins / solutes of that particular molecular weight are rejected by the membrane (e.g., if a 30,000 molecular weight protein is rejected 95% by a membrane, this membrane has a MWCO of 30,000). Solutes / proteins will permeate through the larger pores that are present resulting in incomplete separation. In particular, wide pore size distributions can significantly limit the membrane resolving power (Mochizuki and Zydney 1993). In order to guarantee complete rejection of a certain solute, a much smaller MWCO membrane (compared to the size of the solute) must be chosen. For example, for complete rejection of a protein having a molecular weight of 30,000, a membrane with a MWCO of 10,000 is utilized. This membrane is chosen to ensure that no unwanted protein will permeate through the "imperfections" present in the

membrane due to the pore size distribution. However, when using a smaller molecular weight membrane, a large flux reduction will be observed, as well as a loss of yield for the more permeable protein in a binary mixture.

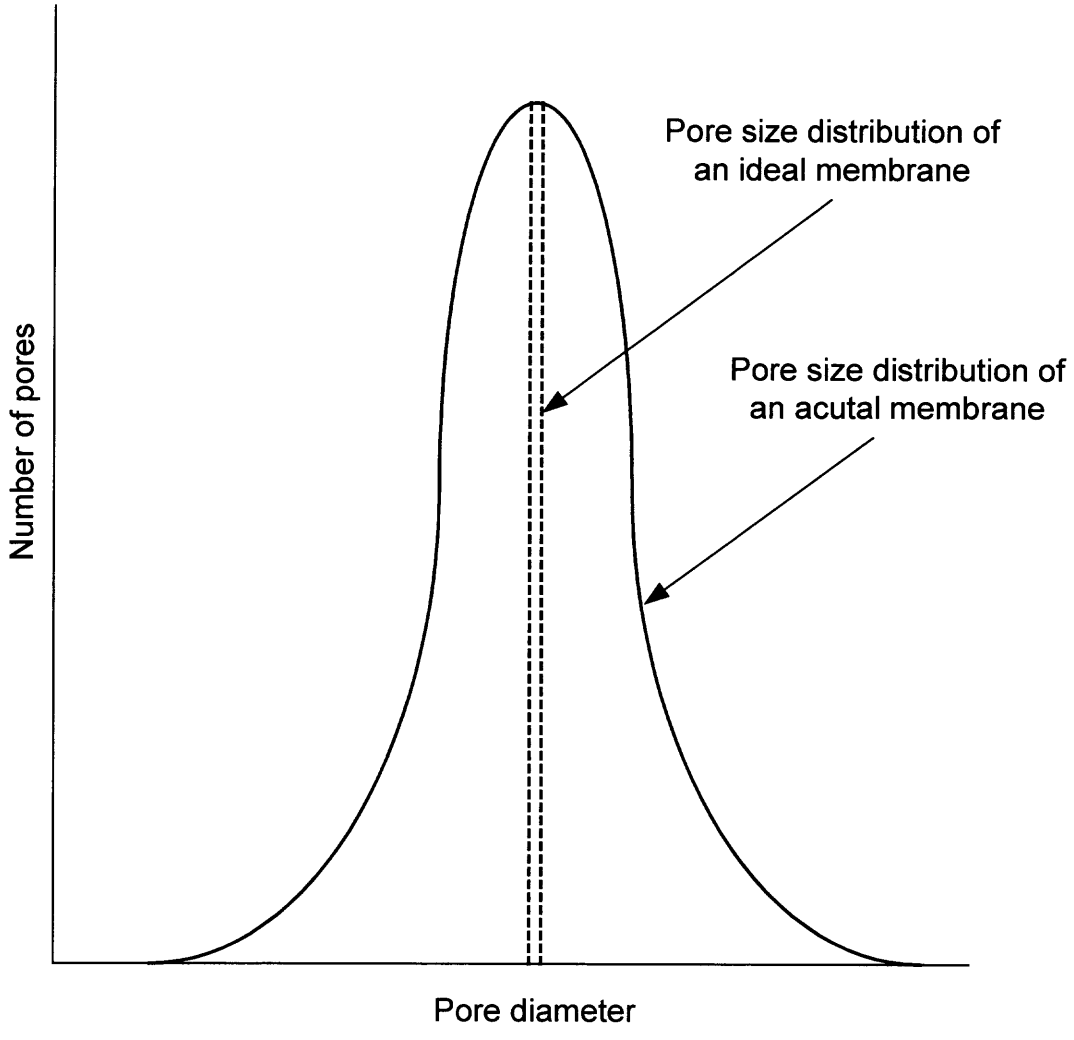

Figure 1.3 Illustration of a pore size distribution for an actual membrane compared to an ideal membrane.

Osmotic pressure of larger macromolecules, in most cases, is negligible because of the large size of macromolecules. However, fouling and concentration polarization are factors that affect the transport of solutes / proteins. Fouling results from pore plugging

and adsorption on the membrane surface and inside the membrane pores. Concentration polarization is caused by an increased concentration of protein / solute at the wall of the membrane. This wall concentration reaches a constant level due to convective flow of the solvent toward and through the membrane and diffusive flux of solute back into the bulk solution from the near-membrane region.

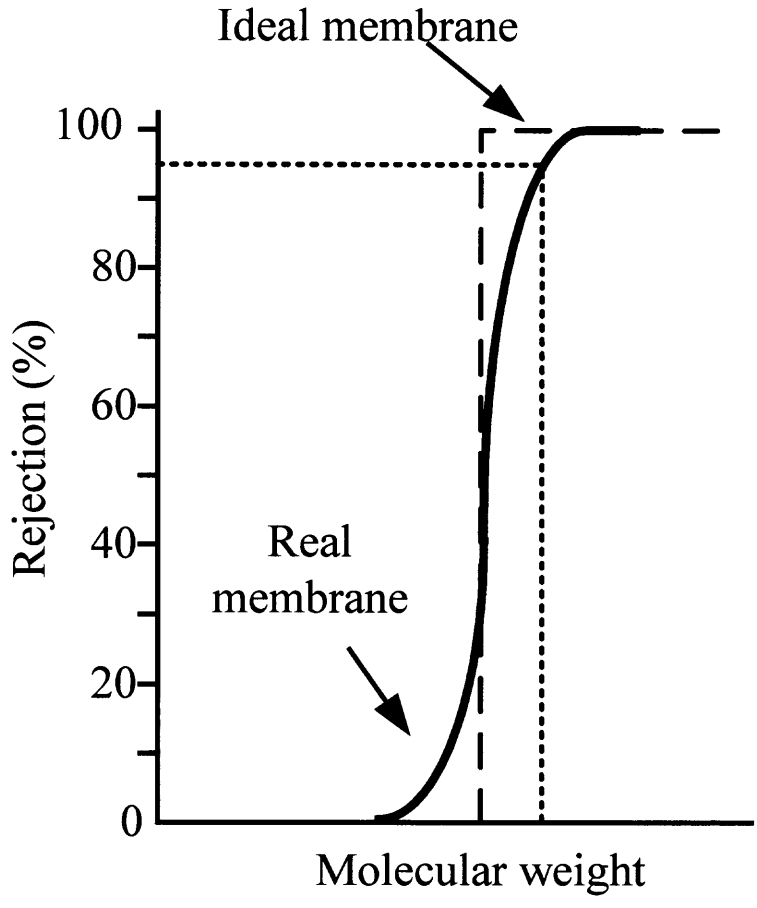

Figure 1.4 Illustration of the effect of a pore size distribution on the extent of rejection of solutes of various molecular weights through an ultrafiltration membrane.

Both fouling and concentration polarization can affect the performance of a given ultrafiltration operation. A flux decline is often observed (which is irreversible in the case of fouling). Due to higher concentrations of solute on the surface of the membrane, the rejection of a given solute is affected. This change in rejection behavior can be undesirable or desirable. The presence of higher concentration of solutes at the membrane wall will enhance solute transmission. However, the presence of a "cake" will reduce transmission (or increase rejection) by reducing the pore sizes and adding a layer of resistance.

Traditionally ultrafiltration has been employed for size-based separation of protein mixtures where the ratio of the protein molecular masses is at least around 7-10 (Cherkasov and Polotsky 1996). For protein concentration and buffer exchange, UF has become the preferred method of choice, replacing size-exclusion chromatography (Kurnik, Yu, Blank, Burton, Smith, Athalye and van Reis 1995). Ultrafiltration membranes can also be used to fractionate proteins of different sizes (Ghosh and Cui 2000). To achieve better purification of similarly sized biomolecules, considerable research has taken place focusing on "fine tuning" the operating and physicochemical conditions to attain higher selectivity (Saksena and Zydney 1994; van Eijndhoven ,Saksena and Zydney 1995; van Reis, Goodrich, Yson, Frautschy, Whiteley and Zydney 1997; Nyström, Aimar, Luque, Kulovaara and Metsämuuronen 1998; Zydney and van Reis 2001). These researchers have allowed the size difference between two proteins to be exploited via the increased or decreased hydrodynamic radius that results from changes in buffer conditions (i.e., ionic strength and pH). Saksena and Zydney (1994) showed that adjusting the pH from 7 to 4.8 and lowering the ionic strength could achieve

20-fold selectivity increase during the ultrafiltration-based separation of BSA and IgG. Cheang and Zydney (2003) investigated the fractionation of α-lactalbumin and β-lactoglobulin and found that, by adjusting pH and ionic strength, a selectivity of 55 could be attained.

Ionic strength and pH are important operating conditions that affect the characteristics of the proteins. When the pH of the buffer is equal to the pI of the protein, the protein carries a zero net charge. When the pH of the buffer is below the pI of the protein, the protein carries a net positive charge. If the pH of the buffer is above the pI of the protein, the protein has a net negative charge. Further, high ionic strength of the buffer results in the presence of a large amount of salt ions that shield the charges present on the protein. Such conditions influence the solvent flux / solute flux in different ways. For example, at the pI, the protein molecules will have higher tendency to precipitate and therefore the flux would be the lowest (Swaminathan, Chaudhuri and Sirkar 1981). On the other hand, at the pH=pI, the effective protein molecule dimensions will be the smallest; therefore its rejection is likely be minimized vis-à-vis another protein whose pI is different from the solution pH.

Operating in an optimized physicochemical environment (i.e., pH and ionic strength) enhances separation by exploiting the charge and hydrodynamic radius of the protein. In a binary mixture, operating at the pH=pI of the protein of interest results in permeation of this protein due to its lack of a net charge especially if the membrane has a net charge; further the effective hydrodynamic radius is lower due to lack of ions surrounding the protein. The other protein in the mixture is either positively or negatively charged, depending on the operating pH, which increases its hydrodynamic

radius and its transport through the membrane is hindered. Further, at low ionic strength, the charges present on the protein are minimally shielded and the hydrodynamic radius is at a maximum. The physicochemical properties of the proteins enhance the separation significantly. This is evident in the reverse separation of immunoglobulin G (IgG, MW 155,000) and BSA (MW 66,430), attaining selectivities as high as 50 for IgG over BSA (Saksena and Zydney 1994) when utilizing optimized physicochemical conditions corresponding to the pI of IgG (pH 7.4) and an ionic strength of 0.0015 M NaCl.

Van Reis et al. (1997) have utilized these concepts along with a preliminarily determined optimal operating flux or transmembrane pressure drop to develop the technique called high-performance tangential flow filtration (HPTFF). These HPTFF units can also be used in series to improve separation. Separation of the binary system of bovine serum albumin (BSA) and IgG was investigated, as well as that of the BSA monomer and dimer. Selectivities as high as 70 were achieved using a two stage HPTFF process. However, low fluxes and large buffer volumes were encountered.

Transferring the permeate from one membrane device into a second device as the feed is the current mode of membrane cascade operations (Kulkarni, Funk, and Li 2001). An illustration of three UF cells in series is shown in Figure 1.5. The permeate from the first cell is the feed for the second cell and the permeate from the second cell is the feed for the third cell. Barker and Till (1992) investigated the use of multistage techniques to improve the fractionation of dextran. A cascade of four ultrafiltration devices was implemented for the fractionation of dextran. The fractionation efficiency was improved by 18% (Barker and Till 1992). The use of a cascade operation introduces large buffer volumes and a lot of extra equipment (i.e., valves, pumps, reservoirs). The extra

equipment can introduce unwanted shear that can affect the activity of the protein as well as a loss in yield of the target protein.

Conventional multistage ultrafiltration is grossly inefficient in fractionating / purifying proteins having molecular mass ratios less than 5 (Ghosh 2003). Novel cascade configurations in separate devices with individual pumps have therefore been investigated to achieve protein purification by Ghosh (2003) who numerically illustrated such a 3-stage process for protein fractionation using two proteins whose apparent sieving coefficients were 0.5 (preferentially transmitted) and 0.01 (preferentially retained). The proteins investigated were not actual proteins.

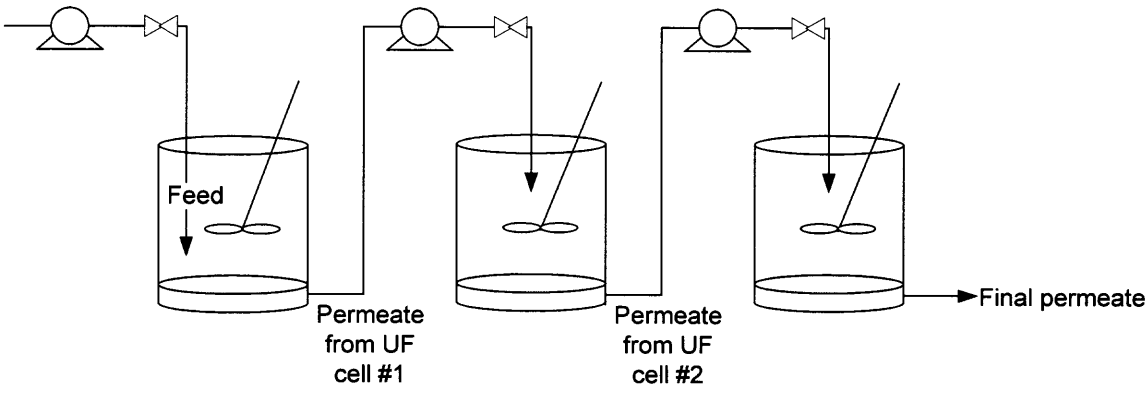

Figure 1.5 Illustration of three ultrafiltration cells in series.

Sequentially-staged ultrafiltration membrane processes have been investigated (Burba, Aster, Nifant'eva, Shkivnev and Spivakov 1998) for the separation of aquatic humic substances. In this study, tangential flow filtration was allowed to take place through UF membranes placed in series in different compartments with decreasing

molecular weight cut offs (MWCOs); ultrafiltrate was collected in a reservoir after each stage. A multi-channel pump controlled the flow rate across each membrane.

Ultrafiltration, under optimized physicochemical and operating conditions, only improves the selectivities, resulting not necessarily in a pure product. Extensive system optimization and buffer volume is needed in HPTFF. An extraordinarily large amount of equipment is required in sequentially-staged ultrafiltration due to the multiple stages and pumps; it has not been greeted by significant interest.

In general, membrane devices have advantages over chromatographic systems due to lower capital cost and steady-state operation, which allow efficient transfer to large-scale operation. One device that yields a completely purified biomolecule by completely rejecting the unwanted species is highly desirable.

1.3 Multistage Ultrafiltration in One Device

An analogy between multistage ultrafiltration and size-exclusion chromatography was examined theoretically by Prazeres (1997). A stack containing many membranes was theoretically analyzed and compared to column chromatography for fractionation of solutes according to their size. He suggested that this multistage ultrafiltration-based chromatography process behaves in a fashion opposite to that of size-exclusion chromatography by eluting solutes in increasing order of their size. This analysis concluded that all of the solutes pass through the column at different rates depending on their size. No experimental test of these conclusions was ever attempted. The number of ultrafiltration (UF) membranes to be used in a stack could also be as high as 2500.

Boyd and Zydney (1997) had made limited studies in ultrafiltration where two asymmetric Omega 30K and 50K MWCO membranes were used in a sandwich fashion, either with their support substructures together (i.e., the skin layers on the two outer surfaces) or with the skin layers together (with the porous substructures at the upstream and downstream surfaces). The purpose of their research was to study the transport of solutes, not protein fractionation.

In the research described in this thesis, multiple flat membranes are sandwiched together and housed in one device. The permeate from the first membrane will be the feed for the second membrane, and the permeate from the second membrane will be the feed for the third membrane, etc. (Figure 1.6). Therefore, the rejection of one protein through one membrane is likely to be substantially increased with each additional membrane eventually resulting in, on an overall basis, essentially complete rejection of one species. It may be possible to achieve an essentially completely pure product by using a stack of, say, three, four, or five membranes. The system configuration of the present study is completely different from that of Boyd and Zydney (1997). The composite membrane of this thesis uses the same membrane throughout. Further, the configuration of skin-backing-skin-backing-skin-backing is proposed.

When membranes are stacked one on top of another, the deficiencies present in the UF membranes due to the pore size distribution are likely to be removed. Therefore with each additional membrane added in the stack, the pore size distribution is potentially narrowed, bringing it closer to an ideal membrane (Figure 1.7). The solutes / proteins that permeate through the first membrane are rejected by the second membrane and

subsequently, by the third membrane. The concept of stacking membranes together potentially results in considerable rejection amplification.

The concept of rejection amplification by internally-staged ultrafiltration (ISUF) can be expressed by amplifying the rejection described by equation (1.1) for multiple membranes in series. Consider the schematic of the illustration of a multimembrane stack consisting of a 3-membranes composite as shown in Figure 1.8.

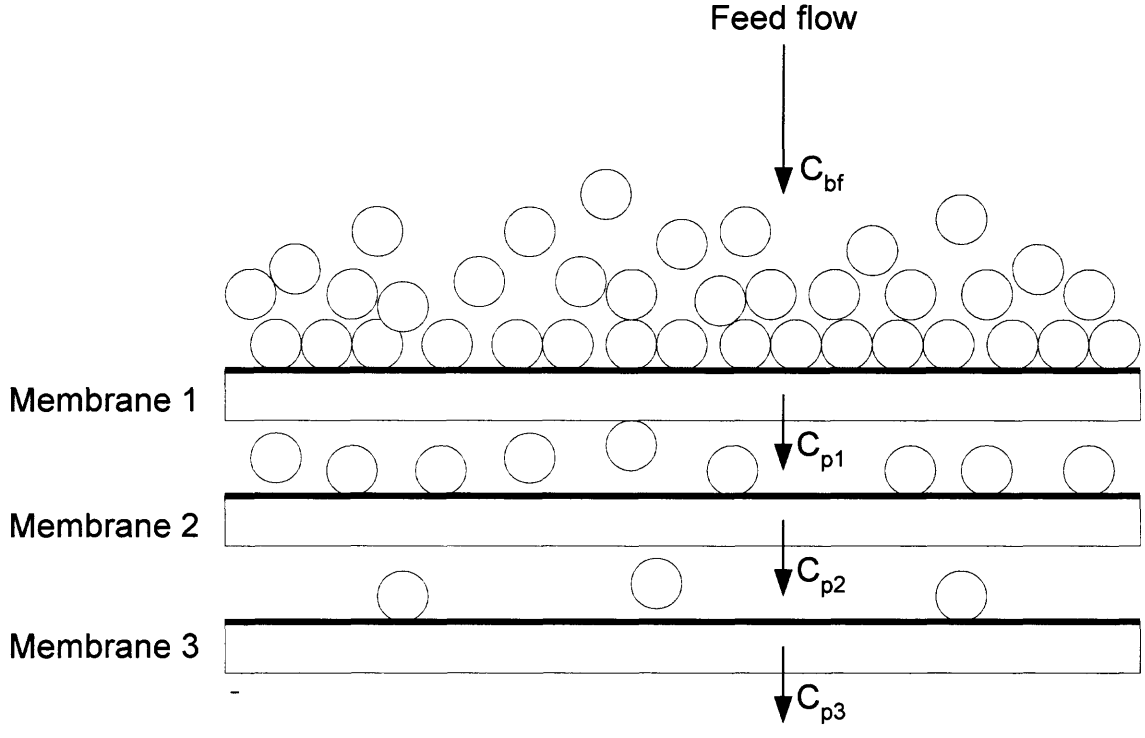

Figure 1.6 Illustration of multistage ultrafiltration in one device: internally-staged ultrafiltration (ISUF).

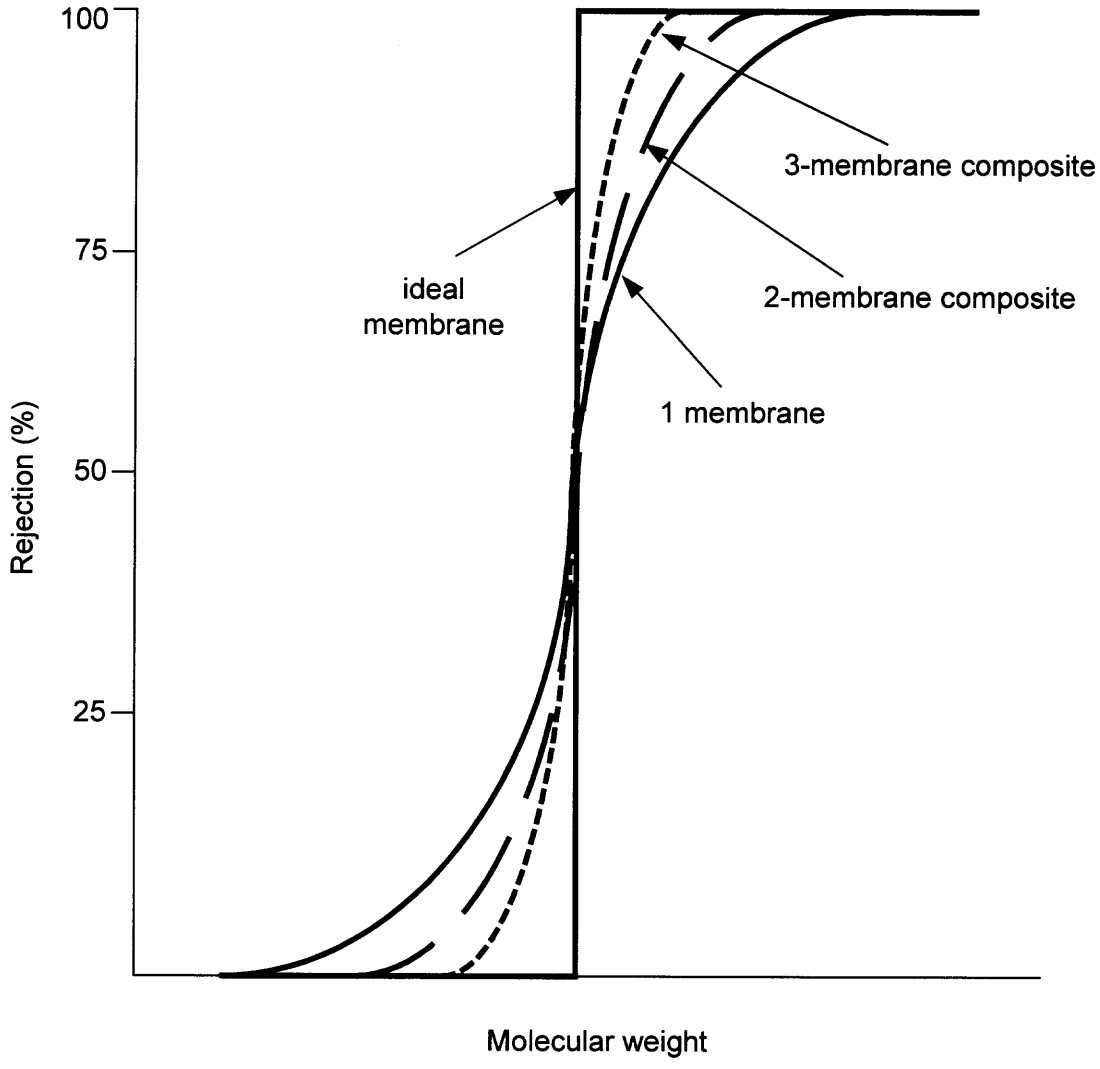

Figure 1.7 Illustration of the effect of multiple membranes on the rejection behavior of UF membrane compared to an ideal UF membrane.

The solute rejection, R_1, for the first membrane is given by

$$R_1 = 1 - \frac{C_{p1}}{C_{f1}} \tag{1.3}$$

Where C_{p1} is the solute concentration on the permeate side of membrane 1 and C_{f1} is the solute concentration on the feed side of membrane 1 exposed to the feed solution. Rejection values can be calculated for a system of multiple membranes by assuming that

the feed to the second membrane is the permeate from the previous membrane, etc.. The rejection for a two-membrane system can be calculated by rearranging equation 1.3 and assuming a rejection value valid for a single membrane system; the feed to the second membrane C_{f2} is C_{p1}, the permeate from the first membrane. Correspondingly, the feed to the third membrane, C_{f3}, is really C_{p2} which is the concentration of the permeate from membrane 2. Consequently

$$C_{p1} = (1 - R_1) C_{f1} \tag{1.4a}$$

$$C_{p2} = (1 - R_1) C_{p1} \tag{1.4b}$$

The overall rejections R_2, R_3 respectively for the systems of two membranes and three membranes in series are defined as

$$R_2 = 1 - \frac{C_{p2}}{C_{f1}} \tag{1.5}$$

$$R_3 = 1 - \frac{C_{p3}}{C_{f1}} \tag{1.6}$$

Therefore, R_2 and R_3 may be calculated respectively by the following equations

$$R_2 = 1 - (1 - R_1)^2 \tag{1.7}$$

$$R_3 = 1 - (1 - R_1)^3 \tag{1.8}$$

These relationships show how high the rejection can be when it is amplified with each additional membrane.

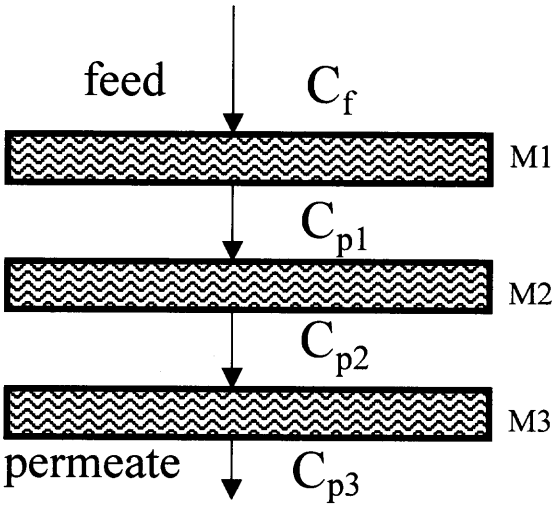

Figure 1.8 Schematic of 3-membrane composite.

Consider a solute having a single membrane rejection value of 0.7. When a 2-membrane composite is used, plugging 0.7 into equation 1.7, the rejection is amplified to 0.91. Further when a 3-membrane composite is used, from equation 1.8, the rejection is amplified to 0.97. This simple calculation illustrates the concept of rejection amplification in ISUF using a multimembrane stack.

Due to the increased resistance encountered with each membrane added, the flux may be approximately cut in half for a 2-membrane composite and by a factor of three for a 3-membrane composite. This can be considered in the context of a resistances-in-series model, with each membrane contributing to the total resistance of the stack. Potentially, the first membrane may throw up a higher resistance than the other two. However, the buffer volume is likely to be quite low compared to conventional cascade operations. The membrane stack is small and compact and utilizes conventional UF membranes. There is no regeneration step or elution step (as in chromatographic membranes). The

cost of this process is likely to be considerable cheaper than a chromatographic process if, in fact, such high purification can be achieved.

The flux loss encountered in the multimembrane stack is much smaller than that achieved when a smaller MWCO membrane is used. When YM30 regenerated cellulose membranes (having a MWCO of 30,000) are utilized in the multimembrane composite, switching to the next available smaller size regenerated cellulose membrane (YM10) having a MWCO of 10,000, a seven fold flux reduction will be encountered (Amicon 1995) without a guarantee of complete rejection. The flux reduction in a multimembrane stack for YM30 membrane may be only two times lower for two membranes and three times lower for three membranes.

Changes in the physicochemical environment can be applied to the multimembrane stack. Increasing the already high selectivity may result in a pure permeate product. Pulse injections through the stack may allow the conservation of a precious solute. By using a cascade operation in one internally staged device, a single-staged optimized separation may be exploited to achieve very high selectivities characteristic of multiple stages that, until now, were only possible using conventional column chromatographic methods.

The experimental details of this proposed technique and other associated techniques are provided in Chapter 2. The results and discussion of the performances of a single membrane and multimembrane composites are illustrated in Chapter 3. Three systems of binary protein mixtures were investigated: myoglobin and β-lactoglobulin (System 1), α-lactalbumin and myoglobin (System 2), and hemoglobin and bovine serum albumin (System 3). The membranes used were regenerated cellulose YM30 (MWCO

30,000) and YM100 (MWCO 100,000) and polyethersulfone Omega 100K (MWCO 100,000). The effects of rejection amplification will be presented.

In Chapter 4, the concept of rejection amplification was modeled first using a general lumped model. Experimental rejection data were compared to the calculated rejection values. A convection diffusion model was also developed for a 2-membrane composite and is presented in Chapter 4. The data used for the simulation were obtained from the literature. The nature of the observed sieving coefficients, the effect of mass transfer, membrane pore size, and actual sieving coefficient were analyzed as a function of solvent flux. Further, the two models were compared. The concluding remarks and recommendations for future work are provided in Chapter 5.

CHAPTER 2

EXPERIMENTAL MATERIALS AND METHODS

2.1 System Selection

2.1.1 Membranes

Flat ultrafiltration membrane disks were used in this study. A description of the membranes used is shown in Table 2.1. All information was obtained from the membrane manufactures. Regenerated cellulose flat membrane disks (YM30, MWCO 30,000, diameter 76 mm and YM100, MWCO 100,000, diameter 76 mm) from Millipore (Bedford, MA) and polyethersulfone flat membrane disks (Omega 100K, MWCO 100,000, diameter 76 mm) from Pall Corporation (East Hills, New York) were chosen for this study. Prior to use, these membranes were soaked in buffer for one hour (immediately before use). In certain experiments, the membranes were soaked overnight to equilibrate the membranes with the protein and appropriate buffer solution.

Table 2.1 Membranes Used and Their Properties*

Membrane	Material	MWCO	Pore size (nm)	Skin thickness (nm)	Charge
YM30	Regenerated cellulose	30,000	3-5	100	Slightly negative
YM100	Regenerated cellulose	100,000	6-8	100	Slightly negative
Ω100K	Polyethersulfone	100,000	-	500	Slightly negative

*Obtained from manufacturer

2.1.2 Buffer Solutions

The buffers used were: 20 mM tris-HCL buffer at pH 7.3, 20 mM citric acid buffer at pH 6.0, 20 mM citric acid buffer at pH 4.35, 20 mM phosphate buffer at pH 6.8 and 2.3 mM sodium phosphate buffer at pH 6.8. Each buffer was prepared using deionized (DI) water. Buffer recipes are shown in Table 2.2.

Table 2.2 Buffers Used and Their Characteristics

Buffer	pH	Molarity (mM)	Preparation (1 liter)
tris	7.3	20	0.884g tris-HCl*
			1.744g tris-base*
citric acid	4.35	20	4.2g citric acid* titrated with NaOH** to pH 4.35
citric acid	6.0	20	4.2g Citric acid* titrated with NaOH** to pH 6.0
sodium phosphate	6.8	20	1.988g Na_2HPO_3*
			0.409ml H_3PO_3**
sodium phosphate	6.8	2.3	0.288g Na_2HPO_3*
			0.047ml H_3PO_3**

*Sigma, St Louis, MO
**Fisher Scientific, Pittsburgh, PA

Buffers were prepared by dissolving the appropriate amount of acid and base components of buffer in DI water. The solution was allowed to stir on a stir plate for one hour, or until the salt was completely dissolved. The pH was monitored using a Thermo

Orion pH meter (Waltham, MA), model 710A, which was calibrated bi-monthly. The desired pH of the buffer was adjusted by adding acid or base until the pH was reached.

Citric acid buffer was made by dissolving citric acid in DI water and was then titrated with sodium hydroxide until appropriate pH was reached. All buffer solutions were filtered through 0.45μm pore size Durapore membranes (Millipore) to remove any particulates. Buffer solutions were kept up to 1 month at room temperature (22 ± 2°C).

2.1.3 Model Proteins

Experiments were performed using α-lactalbumin (α-LA, MW 14,175 (Vanaman, Brew and Hill 1970)), myoglobin (Mb, MW 17,566 (Darbre, Romero-Herrera, and Lehmann 1975)), β-lactoglobulin (β-LG, MW 35,500 (Townend, Weinberger, and Timasheff 1960)), hemoglobin (Hb, MW 64,677 (Dickerson and Geis 1969), and bovine serum albumin (BSA, MW 66,430 (Hirayama, Akashi, Furuya, and Fukuhara 1990)) all purchased from Sigma (St. Louis, MO). The pI values for α-LA, Mb, β-LG, Hb, and BSA are respectively 4.2-4.5 (Kronman and Andreotti 1964), 7.3 (Radola, 1973), 5.3 (Kaplan and Forester 1971), 6.8 (Lehninger 1975), and 4.7 (Longsworth and Jacobsen 1949). Three binary mixtures studied are indicated in Table 2.3.

2.1.4 Other Materials and Instruments

All other chemicals and materials were obtained commercially and were of the highest available quality. Tris-HCl (20 mM) at pH 7.3, citric acid buffer (20 mM) at pH 4.35 and at pH 6.0, and sodium phosphate buffer (20 mM and 2.3 mM) at pH 6.8 were used as buffer. All protein solutions were prepared using the appropriate buffer.

Table 2.3 Systems Studied and Their Molecular Weight Ratios

System	Proteins (molecular weight (Daltons))	Molecular weight ratio
1	Mb (17,566)	2.05
	β-LG (35,500)	
2	Mb (17,566)	1.22
	α-LA (14,175)	
3	Hb (64,677)	1.03
	BSA (66,430)	

A model U-2000 (Hitachi, Danbury, CT) UV-VIS spectrophotometer was used to measure the protein concentration. Quartz cuvets (S-10C) (Sigma, St. Louis, MO) having a 10 mm path length were used in the spectrophotometer.

2.2 Experimental Methods

2.2.1 Pretreatment of the New Membranes

Ultrafiltration (UF) membranes purchased from Millipore and Pall were supplied pretreated with glycerol. This solution is present inside the pore structure and is used to keep the membrane from drying while also maintaining the integrity of the pores. This solution must be removed prior to use (Millipore 2000; Pall 2001). The YM30 and YM100 membranes were soaked in deionized water for one hour changing the water at least three times. The Omega 100K membranes were restored by passing 5.0 mL/cm^2 of deionized water through the membranes while they were in a stirred cell. This assured complete removal of the solution. After pretreatment, the membranes were subjected to ultrafiltration of pure deionized water and the fluxes are measured. This is the virgin

pure water flux of the membrane. The fluxes were measured at different pressures. Fluxes were plotted versus pressure. The slope obtained was the membrane permeance.

2.2.2 Protein Solution Preparation

Protein solutions were prepared by dissolving the desired protein in the appropriate buffer solution at room temperature. Buffer solutions were prefiltered through a 0.45 μm pore size Durapore membrane (Millipore, Bedford, MA) prior to use. The protein solutions were then prefiltered through 0.45 μm pore size Durapore membranes (Millipore) to remove any undissolved proteins and large particulates. Protein solutions were stored at 4°C and used within 24 hours in order to ensure no bacterial contamination.

The concentrations of the proteins used in the feed solution are, unless otherwise mentioned, are indicated in Table 2.4.

Table 2.4 System Protein Concentrations

System	Protein concentrations
1	1.0 mg/ml β-LG and 0.2 mg/ml Mb
2	0.2 mg/ml α-LA and 0.2 mg/ml Mb
3	1.0 mg/ml BSA and 0.2 mg/ml Hb

2.2.3 Ultrafiltration Methods

2.2.3.1 Batch Ultrafiltration Experiments. The experimental setup used is shown in Figure 2.1. Prior to use, these membranes were soaked in buffer solution for 1 hour for Systems 1 and 2. For System 3, the membranes were soaked overnight in feed solution. All filtration experiments were conducted using a 76 mm stirred ultrafiltration cell (model 8400, Amicon Corporation) with a 400 ml maximum volume capacity and 10 ml minimum volume capacity. Two solvent reservoirs were used. One buffer reservoir of stainless steel was filled with a pure specific buffer of an appropriate pH. The other acrylic reservoir (500 ml capacity) contained cleaning solution when cleaning *in situ;* it was left empty when off-line cleaning was used, or contained a concentrated feed solution for pulse injection experiments. All were batch ultrafiltration experiments with fresh buffer replacing the lost solvent volume, essentially in continuous diafiltration mode.

The ultrafiltration cell is shown in Figure 2.2. The membranes were placed on the polypropylene screen, all skin side up, on top of one another; the o-ring was placed over the top membrane, as shown in Figure 2.3. The cell was then sealed from the top and the port 2 (corresponding to Figure 2.2) of the UF cell was opened. Using a syringe, the room temperature feed solution was introduced into the cell chamber through port 2 (corresponding to Figure 2.2). This technique ensured that the membranes were sealed and there would be minimal leakage of the protein solution. Port 2 (corresponding to Figure 2.2) was closed and system was allowed to pressurize for 5 minutes to ensure constant pressure throughout the whole setup. Valve 4 (corresponding to Figure 2.2) was opened to the solvent reservoir 1 (corresponding to Figure 2.1), which contained pure buffer, and valve 5 was opened to begin UF. Stirring was initiated and kept constant. All

experiments were performed at constant pressure and were performed at room temperature (22 ± 2°C). Fractions were collected and assayed for the protein concentration. The membranes were then cleaned according to the cleaning protocols discussed in Section 2.2.4.

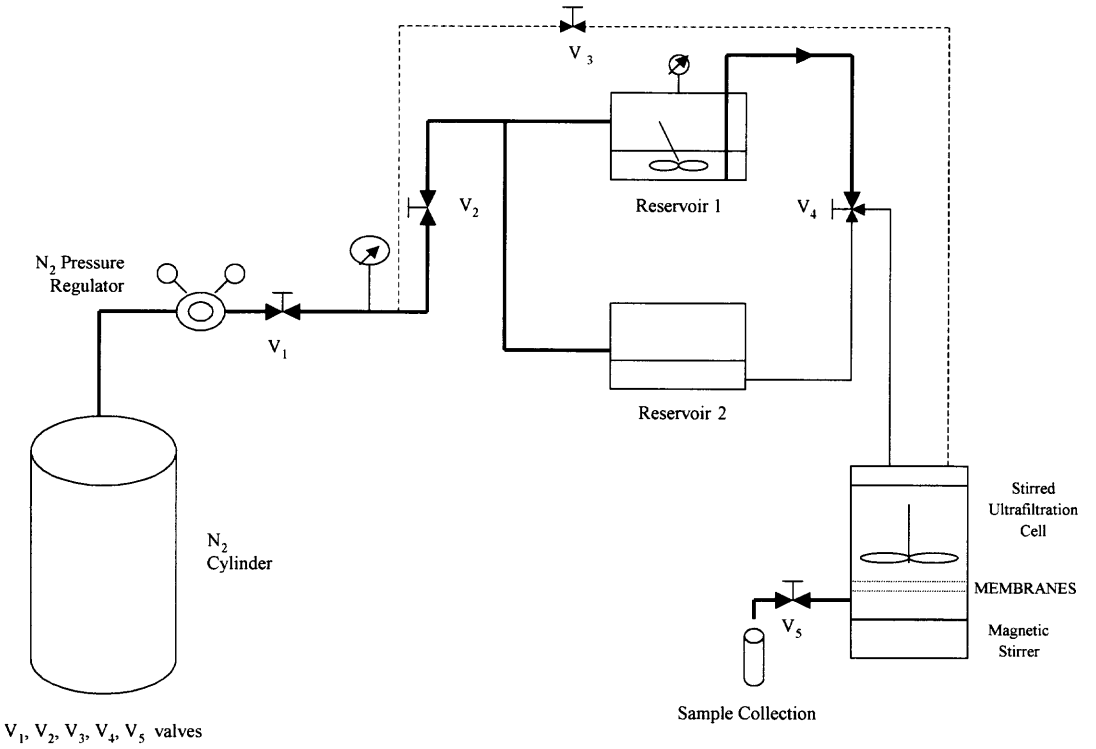

Figure 2.1 Experimental setup.

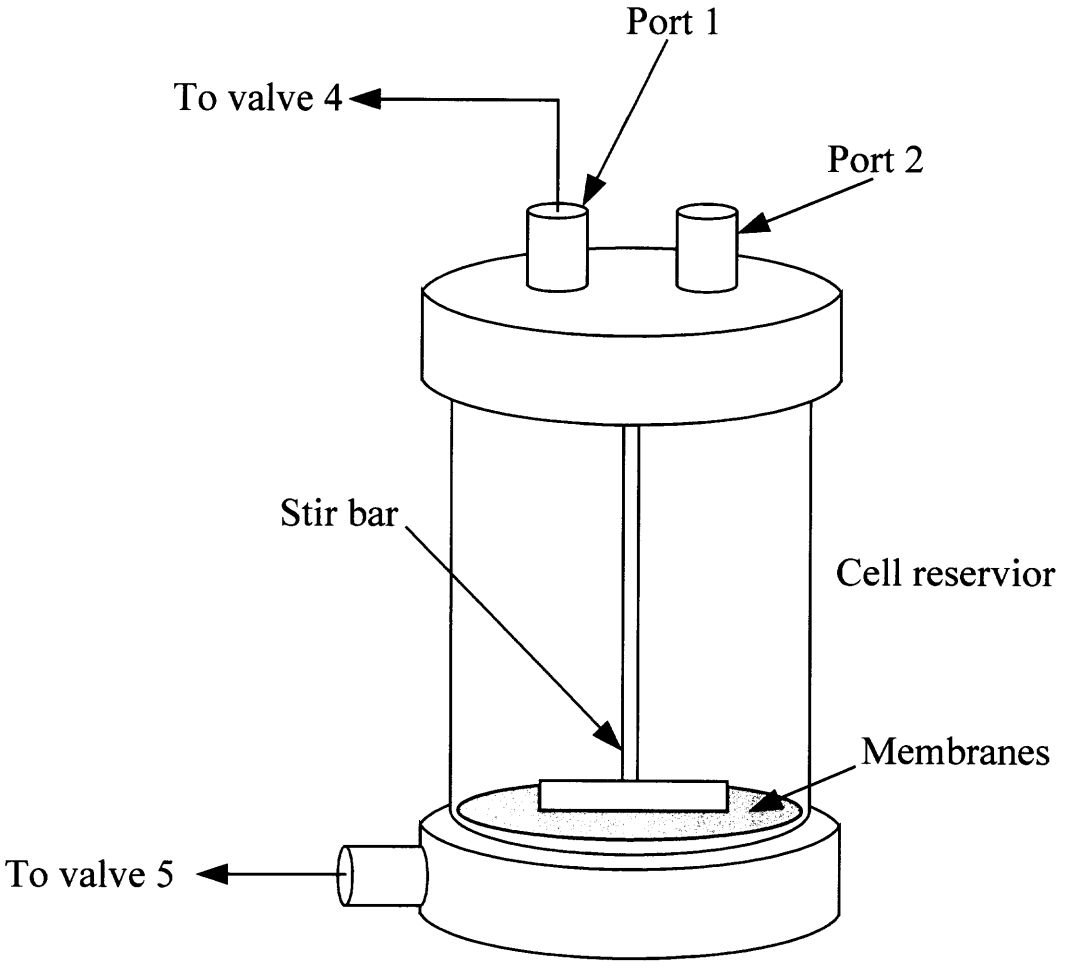

Figure 2.2 Amicon ultrafiltration cell.

2.2.3.2 Pulse Experiments. Pulse experiments were performed by placing a highly concentrated feed solution (that was prepared so as to have the desired final concentration in the ultrafiltration cell) in the second acrylic reservoir (corresponding to Figure 2.1), while an appropriate buffer was placed in the cell. The membranes were placed in the ultrafiltration cell, all skin side up, on top of one another and the o-ring was placed over the top membrane. The UF feed reservoir shell was then placed over the

membranes and the o-ring and buffer was poured into the chamber. Because only pure buffer was in the cell, leakage was not a concern and the method discussed in Subsection 2.2.3.1 using the syringe to fill the cell was not used. The system was allowed to pressurize for 5 minutes to ensure constant pressure throughout the whole setup; valve 4 (corresponding to Figure 2.1) was turned toward solvent reservoir 1 (corresponding to Figure 2.1), which contained pure buffer, and valve 5 was opened to begin UF.

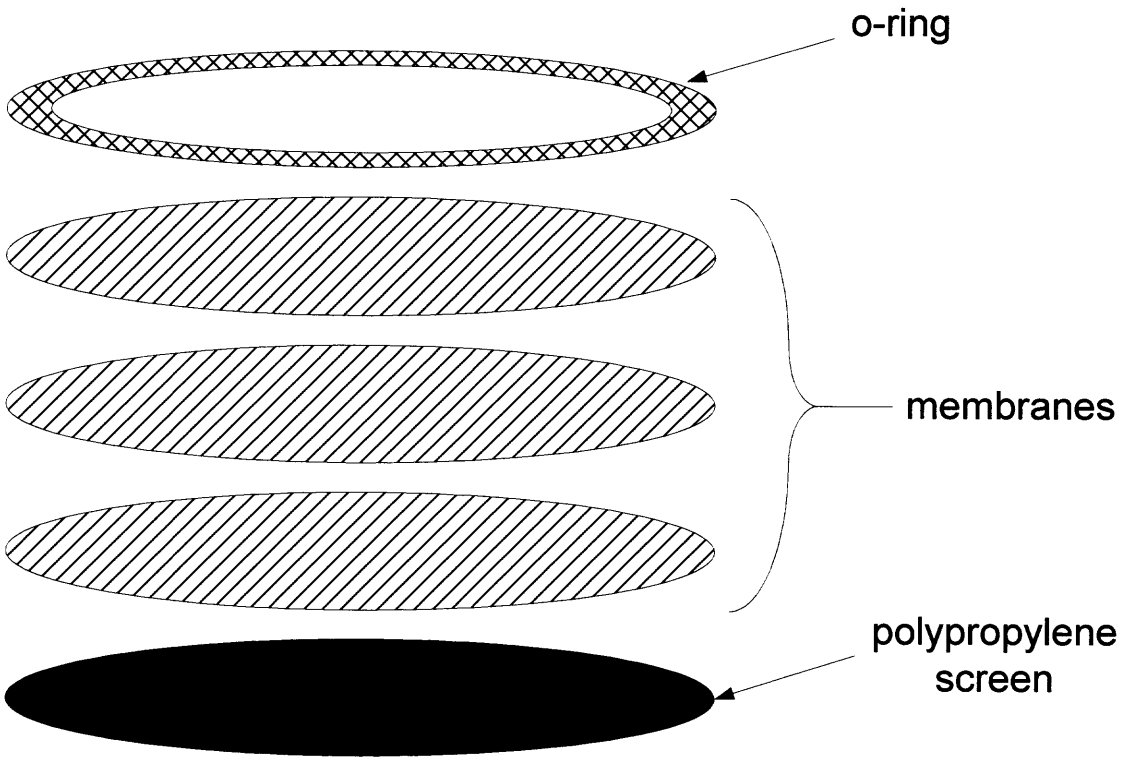

Figure 2.3 Standard membrane stack arrangement.

The buffer flow rate was monitored. From the flow rate, the injection time for a specific volume of feed was calculated and an "injection" was made by turning valve 4 (corresponding to Figure 2.1) toward solvent reservoir 2 (corresponding to Figure 2.1), which contained a concentrated feed solution. After the injection, valve 4 (corresponding to Figure 2.1) was turned toward solvent reservoir 1 (corresponding to Figure 2.1) and the experiments proceeded in diafiltration mode. All experiments were performed at constant pressure and room temperature (22 ± 2°C). Fractions were collected and assayed for the protein concentration. The membranes were then cleaned according to the cleaning protocols discussed in section 2.2.4.

2.2.3.3 Continuous Feed Experiments. Certain experiments were not performed in continuous diafiltration mode with fresh buffer coming from reservoir 1 (corresponding to Figure 2.1), but rather with the feed solution. Feed solution was placed in reservoir 1 (corresponding to Figure 2.1), as well as in the Amicon cell reservoir, and ultrafiltration was initiated. The same procedure discussed in Subsection 2.2.3.1 under "Batch Ultrafiltration Experiments" was followed. All experiments were performed at constant pressure and were performed at room temperature (22 ± 2°C). Fractions were collected and assayed for the protein concentration. The membranes were then cleaned according to the cleaning protocols discussed in Section 2.2.4.

2.2.3.4 Other Membrane Stack Arrangements. In order to investigate an optimal membrane stack design, some initial experiments were performed with rubber gaskets, o-rings, and filter paper separating each membrane in the membrane stack (different from the arrangement shown in Figure 2.3). Experiments were performed with plain rubber gaskets made from sheets of 0.0625 inch thick natural rubber (McMaster-

Carr, Dayton, NJ). Punched gaskets were made with a 3 inch outside diameter punch. The inside diameter was 2.67 inches. Because the inside cut did not need to achieve a perfect seal, it was cut with a razor blade. The gaskets were then placed between the membranes. Some experiments were also performed in which the gaskets were sealed along the outside perimeter with silicone rubber in order to ensure a better seal. The silicone was applied in a thin bead and was allowed to cure for 24 hours before use.

Certain experiments were performed with polypropylene support screens, in addition to an o-ring, in between the membrane stack. Experiments investigating o-rings alone separating the membranes were performed. Use of filter papers between the membranes in addition to sealing the membrane stack (without gaskets, polypropylene screens, or o-rings) along the outside edge with silicone (by applying a thin bead of silicone rubber and allowing it to cure for 24 hours), was also investigated. UF experiments were performed in batch mode and the experimental procedure is discussed in Subsections 2.2.3.1 and 2.2.3.2. In all alternate stack arrangement experiments, the top of the stack was always sealed with an o-ring to prevent leakage and damage from the ultrafiltration cell reservoir shell to the skin of the topmost ultrafiltration membrane.

2.2.3.5 Cyclic Processes. For cyclic processes, ultrafiltration was carried out as described in Subsection 2.2.3.1. After completion of ultrafiltration, valve 4 (corresponding to Figure 2.1) was turned off and all of the retentate was allowed to exit the ultrafiltration cell via valve 5 (corresponding to Figure 2.1). The *in situ* cleaning protocol was utilized (described later in Figure 2.4). The pure water flux of the membranes was then monitored and when the membrane's pure water flux was restored (see Section 2.2.4), repeat of the ultrafiltration was performed.

2.2.3.6 Protein Adsorption on Membranes after Ultrafiltration. Occasionally after ultrafiltration experiments were completed, the membranes were soaked in deionized water overnight (prior to cleaning). The membranes were brought to room temperature and placed on a shaker for approximately one hour. The water solution was then analyzed to measure the amount of protein that was desorbed from the membrane.

2.2.4 Cleaning Operations

2.2.4.1 Regenerated Cellulose Membranes. After completion of the experiments, cleaning was conducted in two ways: *in situ* or off-line. Off-line cleaning procedures required dissembling the apparatus and briefly rinsing the membranes with tap water. Then the membranes were allowed to soak in 0.1 M NaOH at room temperature for 30 minutes.

The *in situ* cleaning protocol for regenerated cellulose YM30 membranes is shown in Figure 2.4. After this procedure, water fluxes were returned to their original level and ultrafiltration could be performed reproducibly, allowing cyclic processes to be performed without disassembling the ultrafiltration cell. This cleaning procedure was repeated if the desired pure water flux could not be obtained. However, maximum exposure of caustic solution to the membranes must be $\leq$ 30 minutes. If the membranes were soaked any longer, the membrane skin, according to the manufacturer, would be damaged.

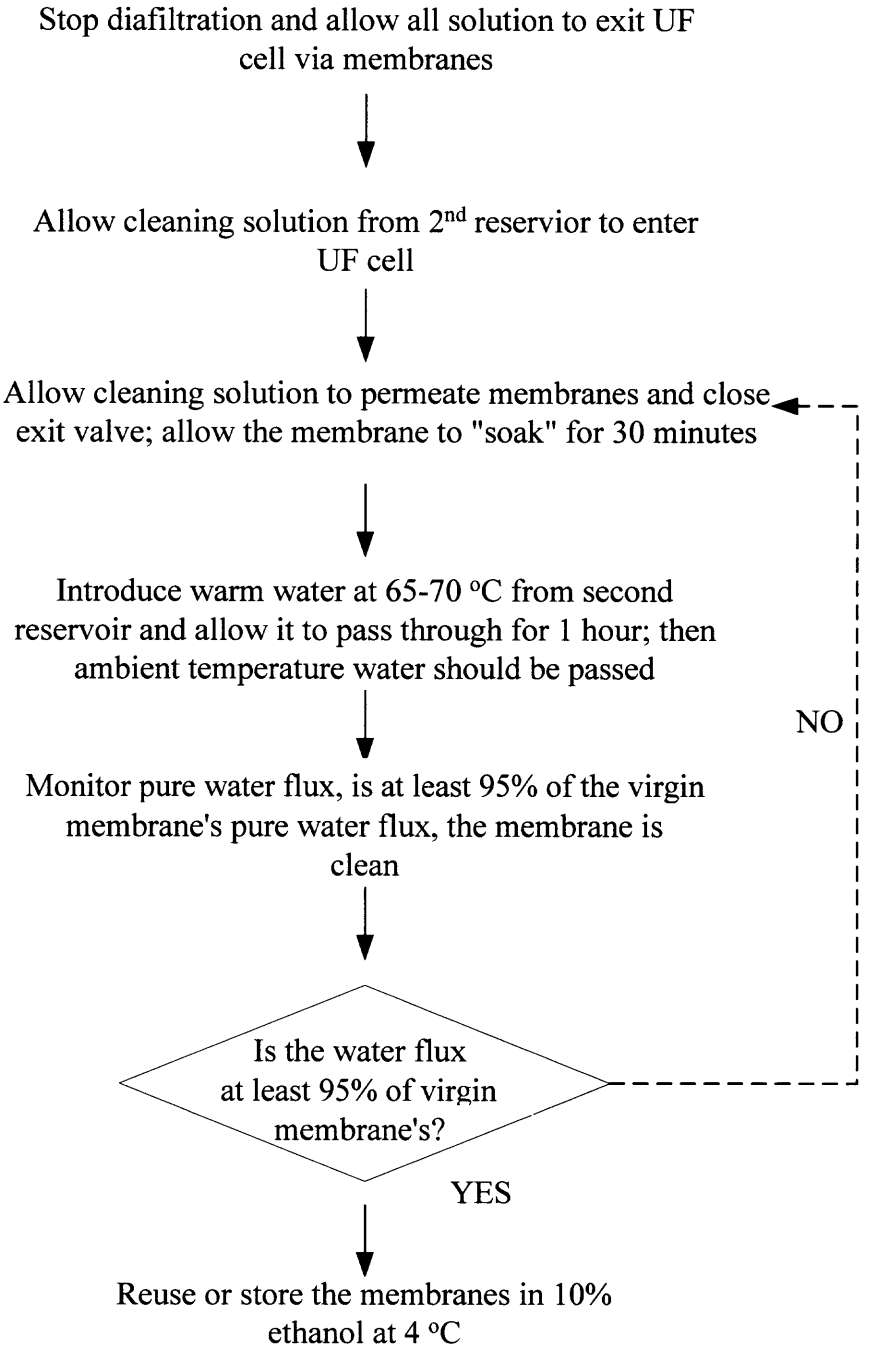

Figure 2.4 *In situ* cleaning protocol for YM30 regenerated cellulose membrane stack.

2.2.4.2 Polyethersulfone Membranes. After completion of the experiments, cleaning was conducted in two ways: *in situ* or off-line. Off-line cleaning procedures required disassembling the apparatus and briefly rinsing the membranes with tap water. Then, separately, each membrane was placed back in the ultrafiltration cell and 0.1 M NaOH solution was allowed to permeate through the membrane for 30 to 60 minutes.

The *in situ* cleaning protocol for the polyethersulfone Omega 100K membranes is shown in Figure 2.5. By following this procedure, water fluxes returned to their original level and ultrafiltration could be performed reproducibly, allowing cyclic processes to be performed without disassembling the ultrafiltration cell. This cleaning procedure was repeated if the desired pure water flux could not be obtained. However, maximum exposure of caustic solution to the membranes must be ≤ 60 minutes. If the membranes were soaked any longer, the membrane skin, according to the manufacturer, would be damaged.

2.2.5 Storage of the Membranes

Flat disk ultrafiltration membranes must be kept wet. YM30 and YM100 membranes were stored in 10% ethanol in water at 4°C in a glass dish. The membrane must be checked periodically to ensure that ethanol solution is still present in the dish. Each membrane was stored separately.

Omega 100K membranes were stored in a 0.05% sodium azide solution. These membranes were also stored separately in glass dishes at 4°C.

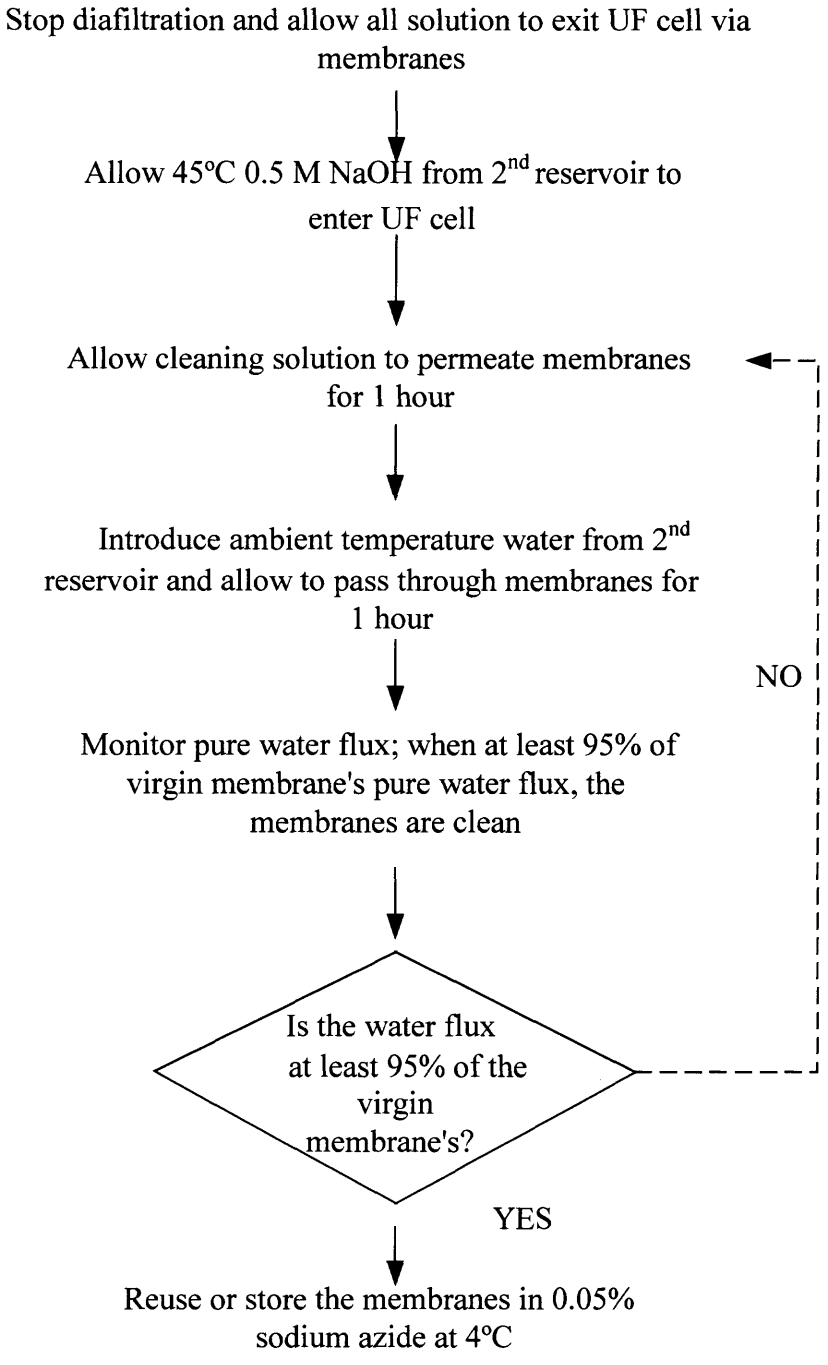

Figure 2.5 *In situ* cleaning protocol for Omega 100K polyethersulfone membrane stack.

2.2.6 Reuse of Membranes after Storage and Preparation for Ultrafiltration

Storage solution must be removed prior to reuse of membranes. YM30 and YM100 membranes were soaked separately in deionized water for one hour, changing the water at least three times. Omega 100K membranes were restored by passing 5.0 mL/cm^2 of deionized water through each membrane while it was in the stirred cell to ensure complete removal of the sodium azide solution. In order to ensure that the membrane was completely clean, the pure water or buffer flux was remeasured. If the pure water flux was at least 95% of the virgin membrane's pure water flux, then the membrane was to be reused. The pure water fluxes of membranes were measured at different pressures. Fluxes were plotted versus pressure. The slope obtained was the membrane permeance.

2.3 Measurement of Protein Concentrations

The concentrations of Hb, BSA, α-LA, and β-LG were determined by measuring the absorbance at a particular wavelength. The spectrum for Mb shows one peak at 280 nm and another peak at 410 nm. The spectrum for Hb shows peaks at 280 nm and 407 nm. BSA, α-LA, and β-LG have maximum absorbance at 280 nm, but negligible absorbance at 410 nm or 407 nm. Standard curves obtained at different wavelengths for various pure protein solutions are shown in Figures 2.6-2.12 and the calibration equations, as well as their corresponding linear ranges, are listed in Table 2.5.

The protein concentrations in a binary mixture were determined by the dual-wavelength method at 410 nm or 407 nm and 280 nm, corresponding to their maximum absorbances. Absorbance of the protein mixture was measured at 410 nm or 407 nm and 280 nm, respectively. The Mb concentration was determined directly from the absorbance at 410 nm. The Hb concentration was determined directly from the

absorbance at 407 nm. The other protein concentration in the binary mixture was then determined by the absorbance of the mixture at 280 nm subtracting the contribution from Mb or Hb. Samples whose protein concentrations were beyond the upper linear limits were diluted with the appropriate buffer before measurement.

Table 2.5 Standard Curves For Protein Solutions

Wavelength / Protein	280 nm	410 nm*, 407nm**
Mb	$C = 0.6699ABS$	$C = 0.1498ABS$
	Linear range: 0-1.0 mg/ml	Linear range: 0-0.4 mg/ml
α-LA	$C = 0.5269ABS$	–
	Linear range: 0-0.4 mg/ml	
β-LG	$C = 1.2593ABS$	–
	Linear range: 0-1.0 mg/ml	
Hb	$C = 0.7114ABS+3.0398$	$C = 0.1808ABS+1.0029$
	Linear range: 0-1.0 mg/ml	Linear range: 0-0.1 mg/ml
BSA*	$C = 1.6661ABS$	–
	Linear range: 0-1.0 mg/ml	

*Wavelength used for myoglobin
**Wavelength used for hemoglobin

The concentrations of BSA, α-LA, and β-LG in a binary mixture were obtained using the method of Sokol, Hána, and Albrecht (1961) by subtracting the concentration corresponding to 280 nm absorbances of Hb and Mb (calculated with their standard curves at 280 nm from their concentrations obtained at 410 nm and 407 nm, respectively) from the absorbance of the mixture (e.g., a mixture of Mb and β-LG and a mixture of Hb and BSA) at 280nm. An example calculation is shown in Appendix A.

This method is based on the assumption that the absorption coefficient of each protein in the mixture is constant. This assumption is a valid one, especially at low protein concentrations. All calibrations were performed in a buffer solution. Due to the very low ionic strength of the buffers used in all experiments, there was no precipitation of buffer salts or effect on absorbance. Therefore, regardless of the buffer used, all curves are valid.

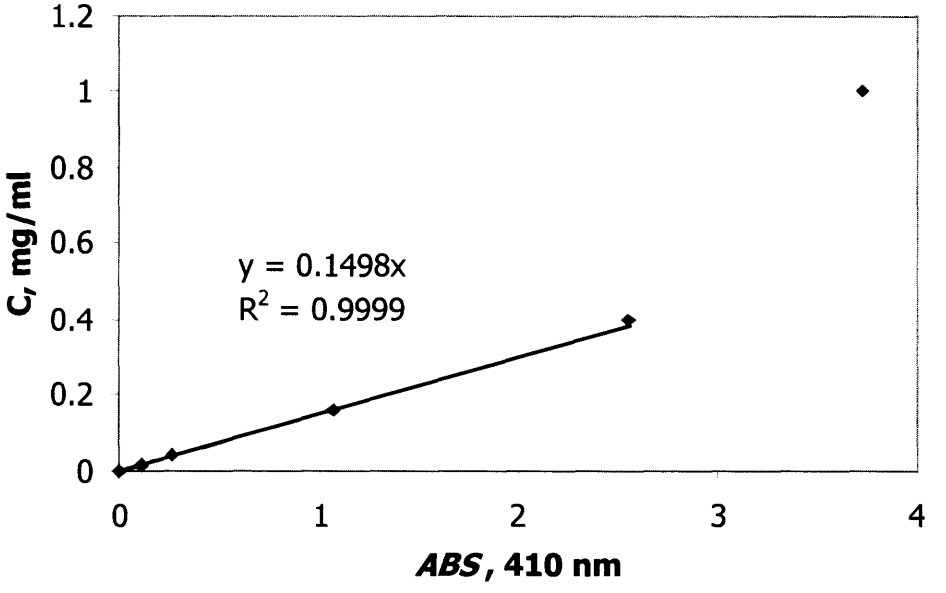

Figure 2.6 Standard curve for Mb at 410 nm.

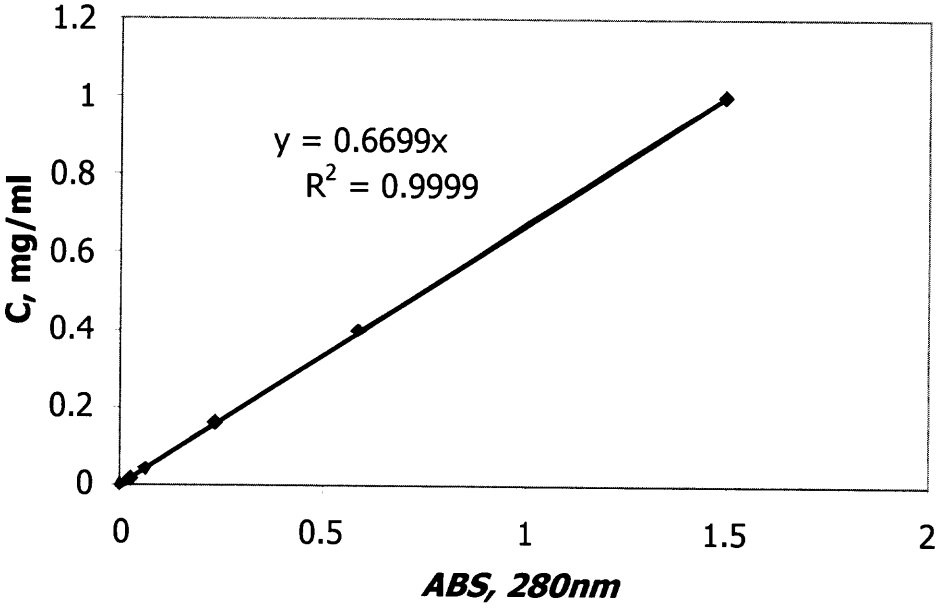

Figure 2.7 Standard curve for Mb at 280 nm.

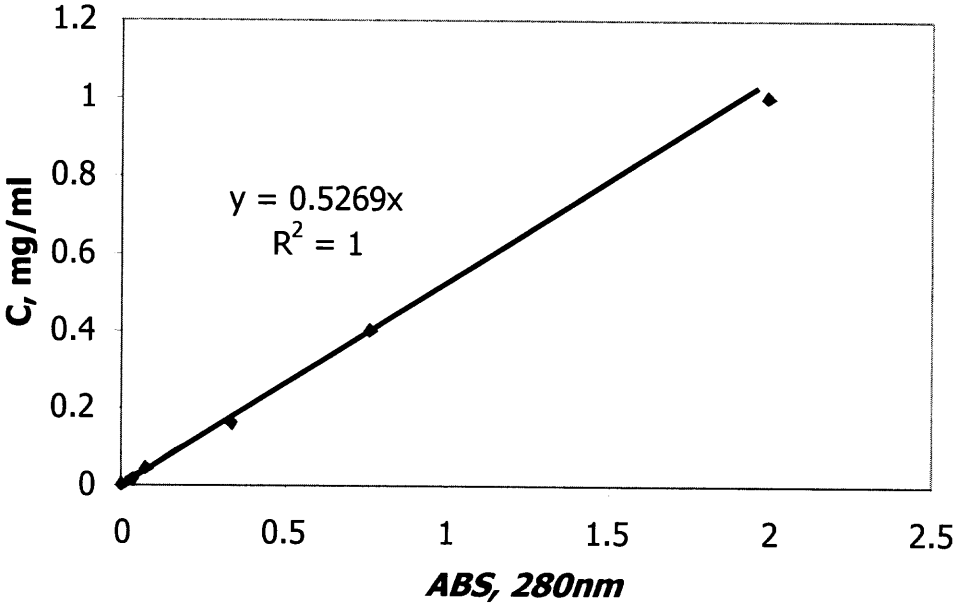

Figure 2.8 Standard curve for α-LA at 280 nm.

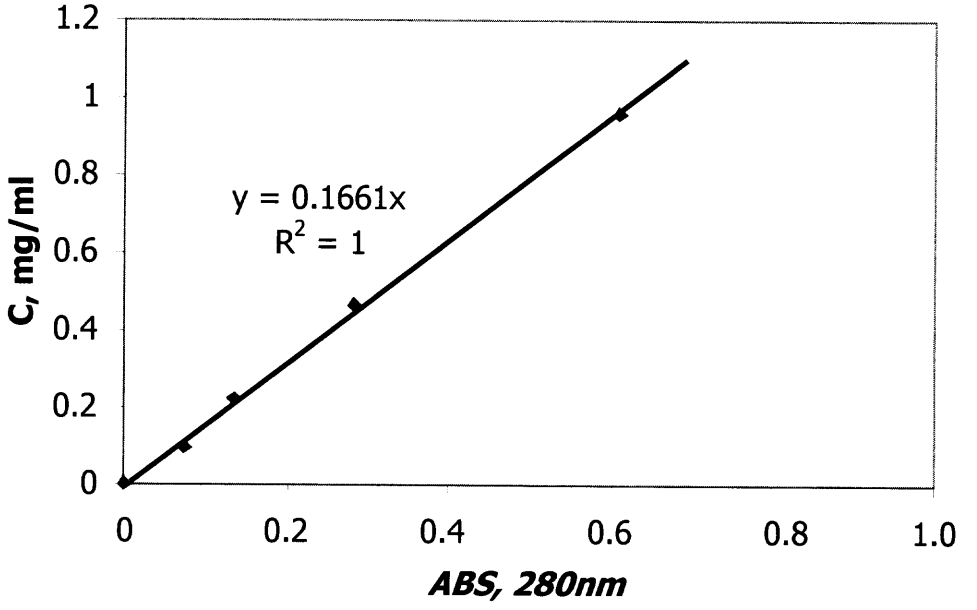

Figure 2.9 Standard curve for BSA at 280 nm.

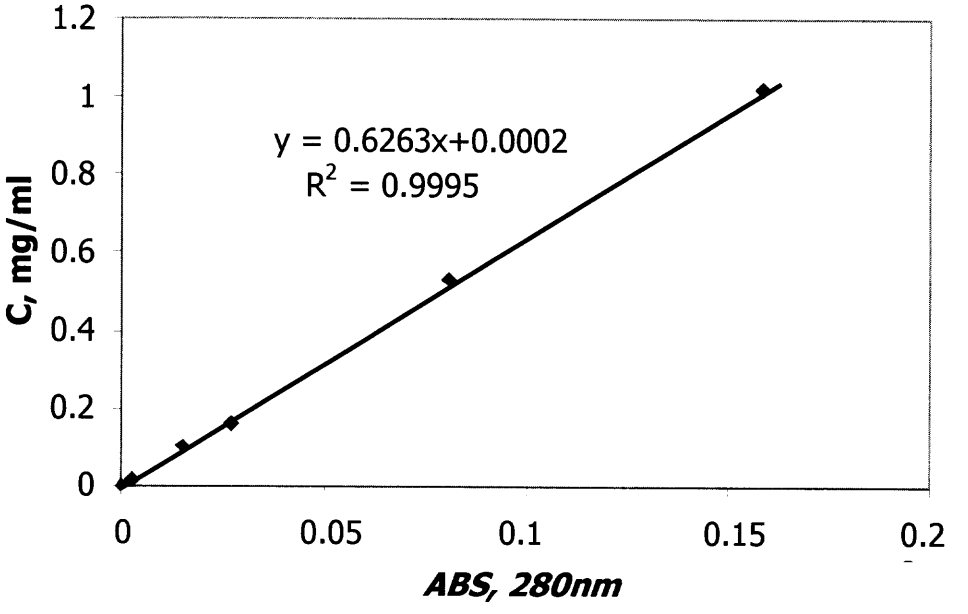

Figure 2.10 Standard curve for Hb at 280 nm.

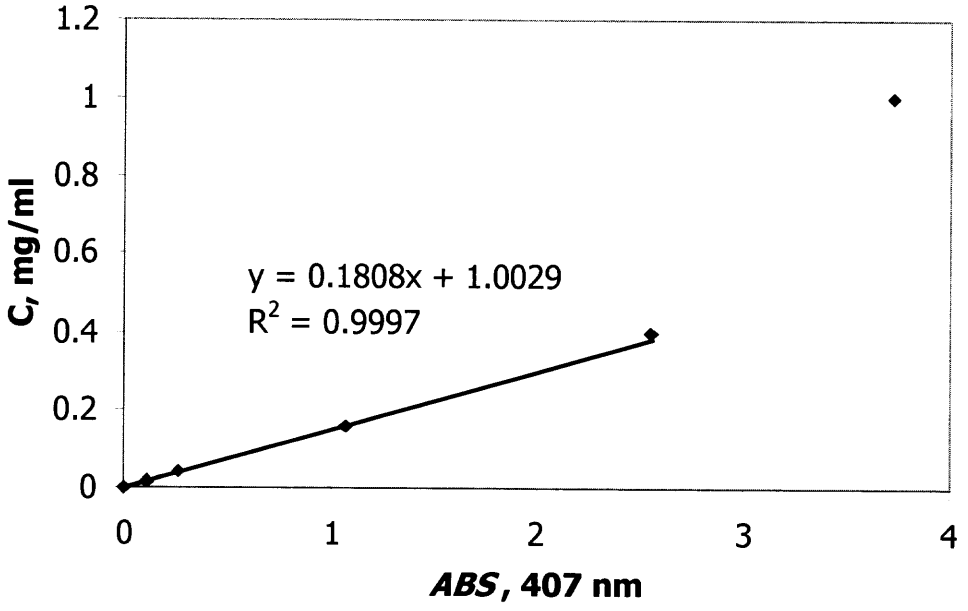

Figure 2.11 Standard curve for Hb at 407 nm.

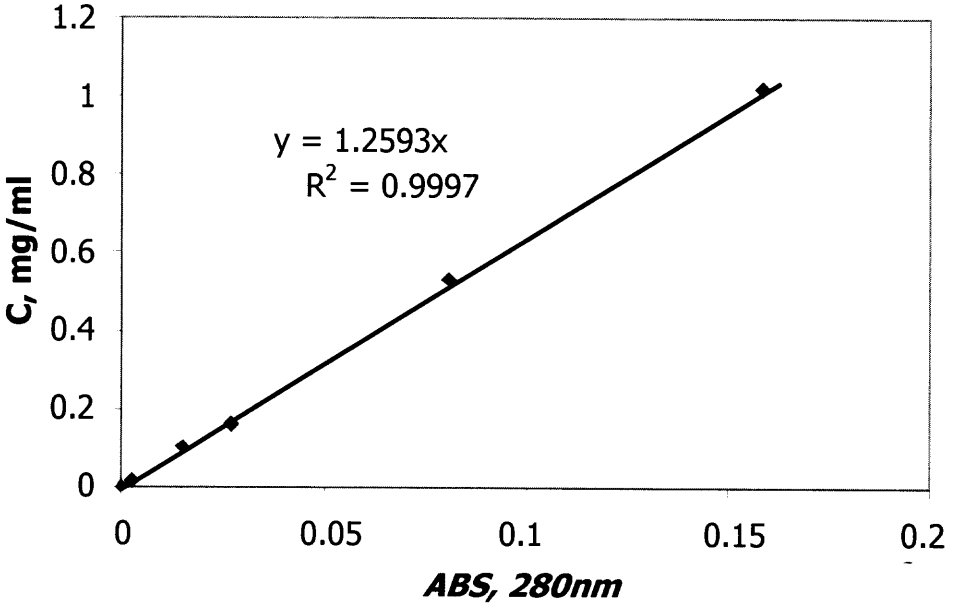

Figure 2.12 Standard curve for β-lactoglobulin at 280 nm.

2.4 Calculation Procedures

The solute rejection, R_1, for the first membrane as well as a single membrane for a solute is given by

$$R_1 = 1 - \frac{C_{p1}}{C_{f1}} \tag{2.1a}$$

where C_{p1} is the solute concentration on the permeate side of membrane 1 and C_{f1} is the solute concentration on the feed side of membrane 1 exposed to the feed solution. The concentrations of solutes in the retentate were changing over time due to the addition of fresh buffer and loss of solutes due to ultrafiltration; therefore a mass balance was used to calculate C_{f1} for every solute and for every data point. Rejection values can be calculated for a system of multiple membranes by assuming that the feed to the second membrane is the permeate from the previous membrane, etc.. The rejection for a two-membrane system can be calculated from rearranging equation 2.1a and assuming a rejection value valid for a single membrane system; the feed to the second membrane C_{f2} is C_{p1}, the permeate from the first membrane. Correspondingly, the feed to the third membrane, C_{f3}, is really C_{p2} which is the concentration of the permeate from membrane 2. Consequently

$$C_{p1} = (1 - R_1) C_{f1} \tag{2.1b}$$

$$C_{p2} = (1 - R_1) C_{p1} \tag{2.1c}$$

The overall rejections R_2, R_3 respectively for the systems of two membranes and three membranes in series are defined as

$$R_2 = 1 - \frac{C_{p2}}{C_{f1}} \tag{2.2}$$

$$R_3 = 1 - \frac{C_{p3}}{C_{f1}} \tag{2.3}$$

Rejection is related to the sieving coefficient and is defined in general as:

$$S = 1 - R = \frac{C_p}{C_f} \tag{2.4}$$

Where R is the solute rejection, C_p is the concentration in the permeate side of a single membrane or the bottom membrane in a multimembrane composite and C_f is the concentration on the feed side of the top membrane. More specifically, the observed sieving coefficient S_o and the actual sieving coefficient S_a are defined by the following equations

$$S_o = \frac{C_p}{C_f} \tag{2.5a}$$

$$S_a = \frac{C_p}{C_{wf}} \tag{2.5b}$$

Where C_{wf} is the concentration at the wall on the feed side of the membrane. Due to the effect of concentration polarization there is a build up of solute / protein on the feed side the membrane, $C_{wf} > C_f$; therefore $S_a < S_o$.

Selectivity, ψ, is used to evaluate the experimental data and is defined for two proteins, for example, Hb and BSA, as:

$$\Psi = \left(\frac{c_{f_{Hb}}}{c_{f_{BSA}}} \right) \Big/ \left(\frac{c_{p_{Hb}}}{c_{p_{BSA}}} \right) \tag{2.6}$$

The value of ψ allows quantitation of the preference of the membrane system for one species over another.

A mass balance (Equation 2.9) is used to calculate the changing concentration in the retentate at any time *t*, $C_r(t)$:

$$C_r(t) = C_f(t) = C_o - \left(\frac{V(t)}{V_o}\right) C_p(t) \qquad (2.7)$$

Where C_o is the initial concentration of solute in the feed solution, $C_p(t)$ is the concentration of solute in the permeate, V_o is the initial volume in the feed reservoir of the ultrafiltration cell, and $V(t)$ is the volume in the feed reservoir of the ultrafiltration cell at any time *t*. The total filtrate volume permeated through the membrane was calculated and then the total mass of solute permeated was calculated. From these values, in addition to the initial concentration of protein in the feed, C_o, the ratio of the total volume permeated at time *t*, $V(t)$, and the initial volume, V_o, and the concentration of permeated protein C_p, $C_r(t)$ was calculated. A mass balance (Equation 2.7) allowed the calculation of the changing solute concentration in the retentate $C_r(t)$ which, in turn, allowed the calculation of the time-dependent rejection of a solute by a single membrane or the overall rejection of a stack.

The yield of any solute is defined as:

$$\text{Yield} = \frac{C_{Tp} V_{Tp}}{C_f V_o} \qquad (2.8)$$

Where C_f is the initial concentration of solute in the feed, V_o is the initial volume in the feed reservoir of the ultrafiltration cell, C_{Tp} is the total permeate concentration of solute, and V_{Tp} is the total volume of the permeate. The yield was calculated at the end of ultrafiltration experiments.

Volume flux, J_v, is defined as the volumetric flow rate, Q, divided by the membrane area, a

$$J_v = Q/a \tag{2.9}$$

The volumetric flux of pure water or pure buffer was monitored as discussed in Section 2.2.4. The flux was also measured during ultrafiltration experiments to monitor system performance.

The permeance of the membrane, A, is defined as

$$A = \frac{J_v}{\Delta P} \tag{210}$$

where ΔP is equal to the difference between absolute feed pressure and atmospheric pressure. Fluxes were measured at different pressures. Fluxes were plotted versus feed gauge pressure. The slope of the line is the permeance.

CHAPTER 3

RESULTS AND DISCUSSION

The experimental results of investigations of multimembrane composites for protein separation by UF are presented in this chapter. First, pure water permeation values for the three different UF membranes employed are illustrated. Then different multimembrane arrangements and configurations using gaskets and screen supports are considered. Results from these studies led to the best configuration for the design and operation of the multimembrane composite. Single membrane UF experiments were performed next for Systems 1, 2, and 3 and their results are presented. These initial investigations were a tool to understand the separation characteristics of the binary mixtures; these results provided a way to compare the results for two- and three-membrane composite systems. All feed solutions were binary protein mixtures to facilitate the investigation of the fundamental separation characteristics. The protein mixtures whose separations have been studied are: Mb/β-LG (System 1), Mb/α-LA (System 2), and Hb/BSA (System 3).

Different operating conditions, such as pressure, pH, ionic strength etc. are useful in understanding the separation and flux behavior of the multimembrane stack. Next, experimental data are presented for 2- and 3- membrane composites investigating Systems 1, 2, and 3 under a variety of conditions. These data include optimized and non-optimized batch experiments for System 1, as well as pulse injection experiments. Results of optimized experiments on System 2 and System 3 are presented next. At the end of the chapter, results of cleaning experiments are presented for the two different

types of membranes (regenerated cellulose and polyethersulfone) used. These results also include those investigating the reproducibility of ultrafiltration data after cleaning the membrane composite *in situ*.

3.1 Pure Water Permeation of UF Membranes

Membrane water permeation was measured for new membranes as well as those thoroughly cleaned after ultrafiltration experiments. Water permeation flow rate of any system was measured under a given constant pressure and monitored to ensure that the value was constant. The permeance was calculated as the slope of water flux vs. pressure (Figures 3.1-3.6). For the three ultrafiltration membranes studied, the water flux of a cleaned membrane was around 95% of the original values after cleaning and remained at the same level after many repeated experiments and cleanings. Examples of pure water permeation flux values for the three membranes studied, comparing clean and dirty membranes, are shown in Table 3.1.

The cleaning experiments were performed according to the manufacturer's instructions. The regenerated cellulose membranes (YM30 and YM100) were cleaned by removing the membranes from the ultrafiltration cell and soaking them in cleaning solution (see Subsection 2.2.4.1). Polyethersulfone membranes were cleaned by allowing the cleaning solution to permeate through the membrane (see Subsection 2.2.4.2).

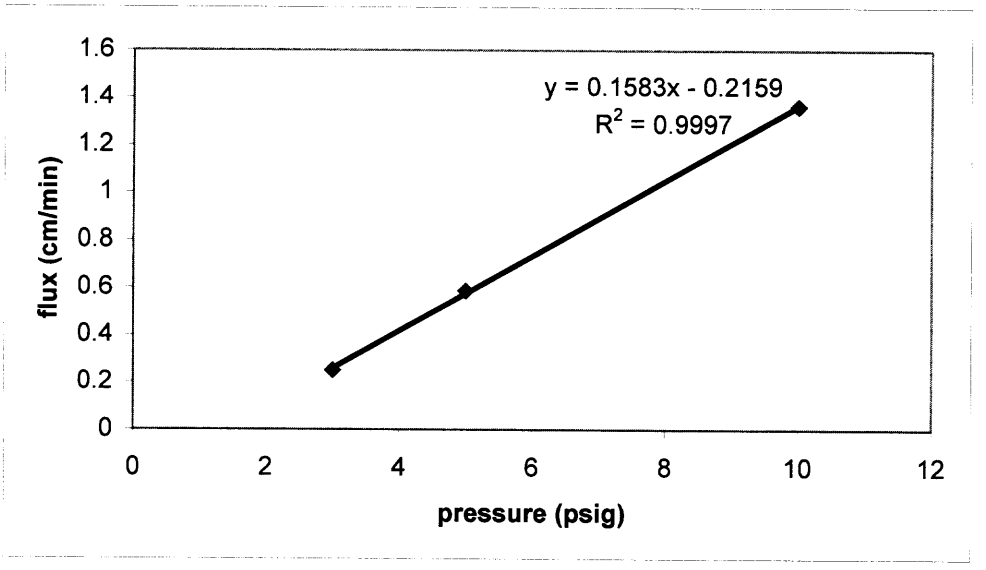

Figure 3.1 Pure water permeation data for a clean Ω100 membrane.

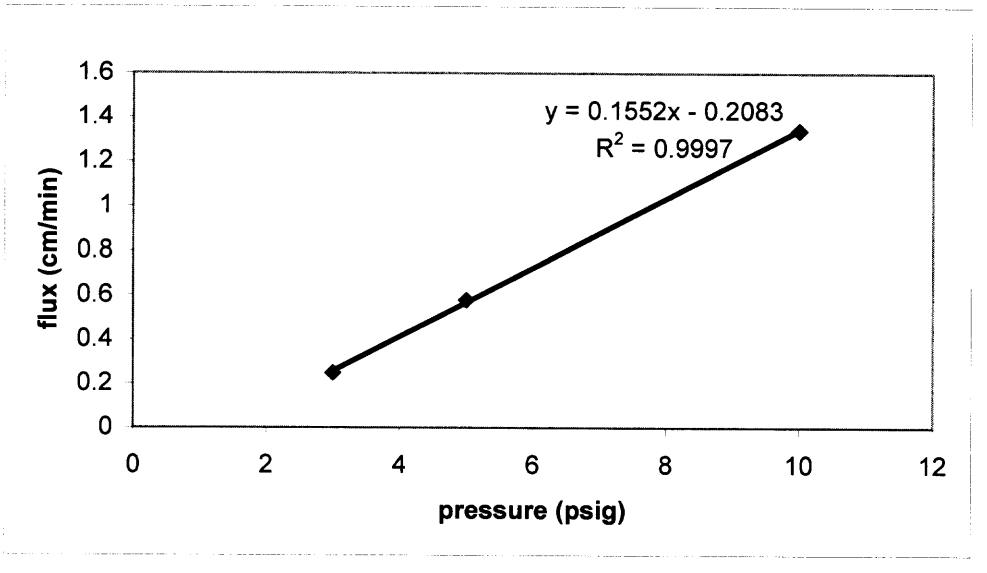

Figure 3.2 Pure water permeation data for a dirty Ω100 membrane.

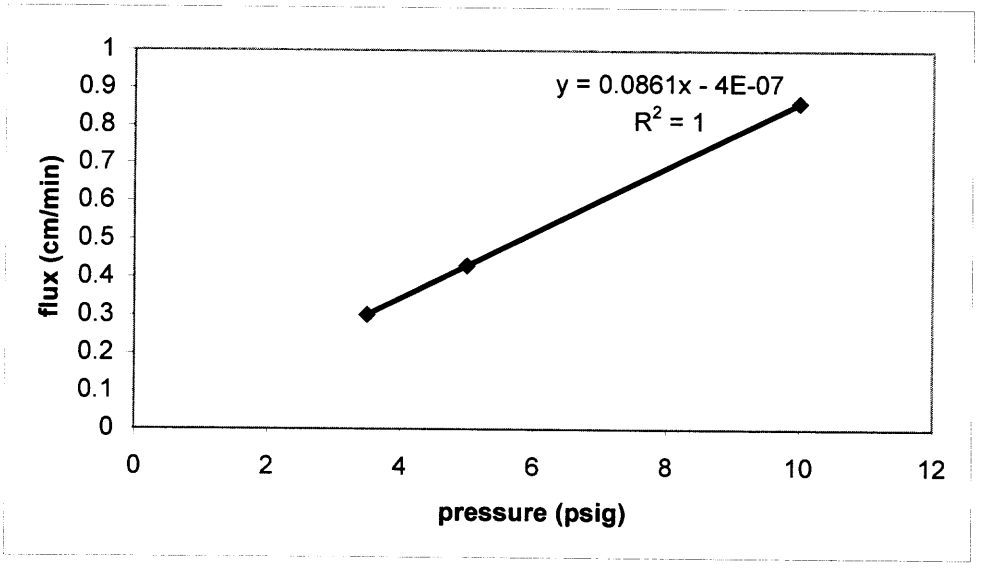

Figure 3.3 Pure water permeation data for a clean YM100 membrane.

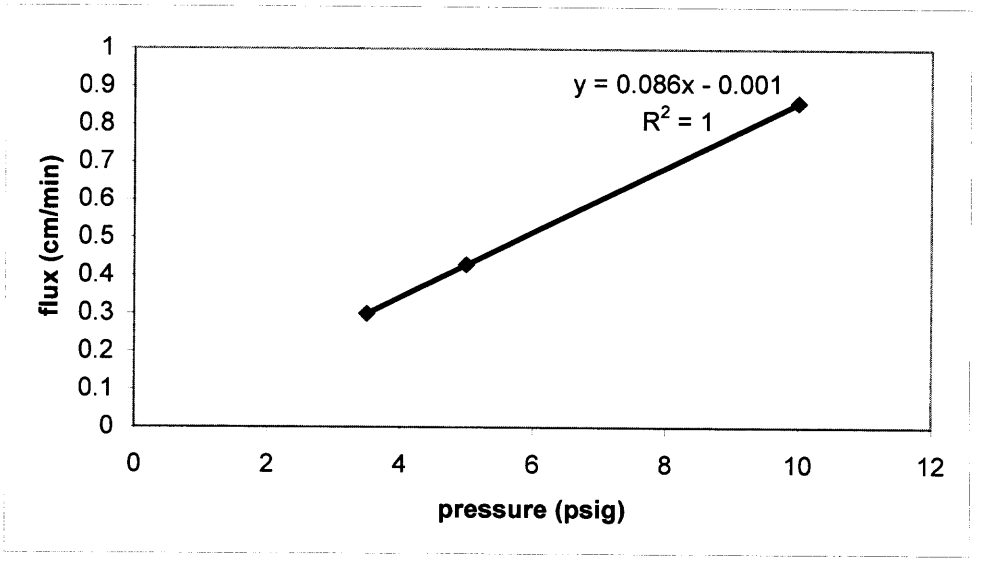

Figure 3.4 Pure water permeation for a dirty YM100 membrane.

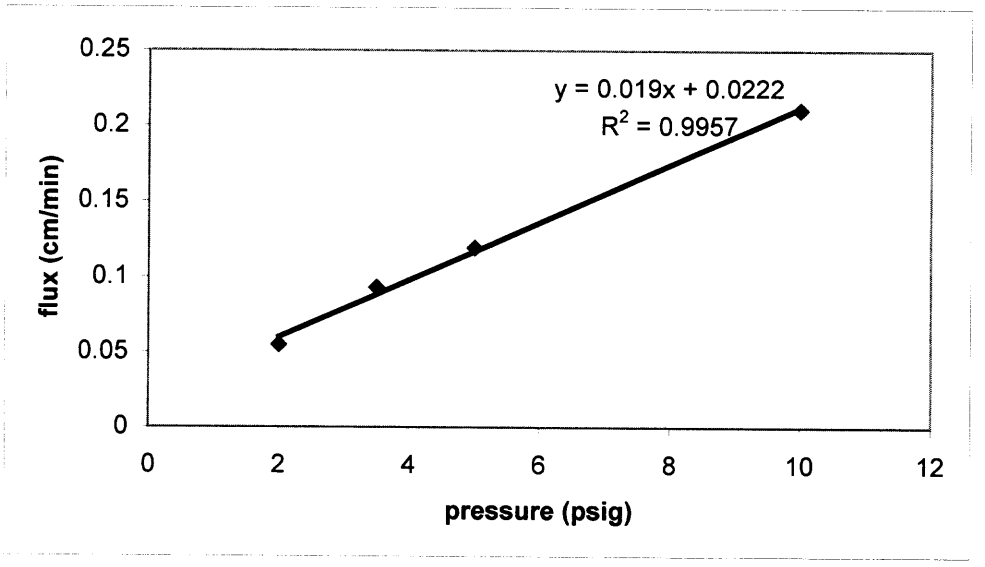

Figure 3.5 Pure water permeation for a clean YM30 membrane.

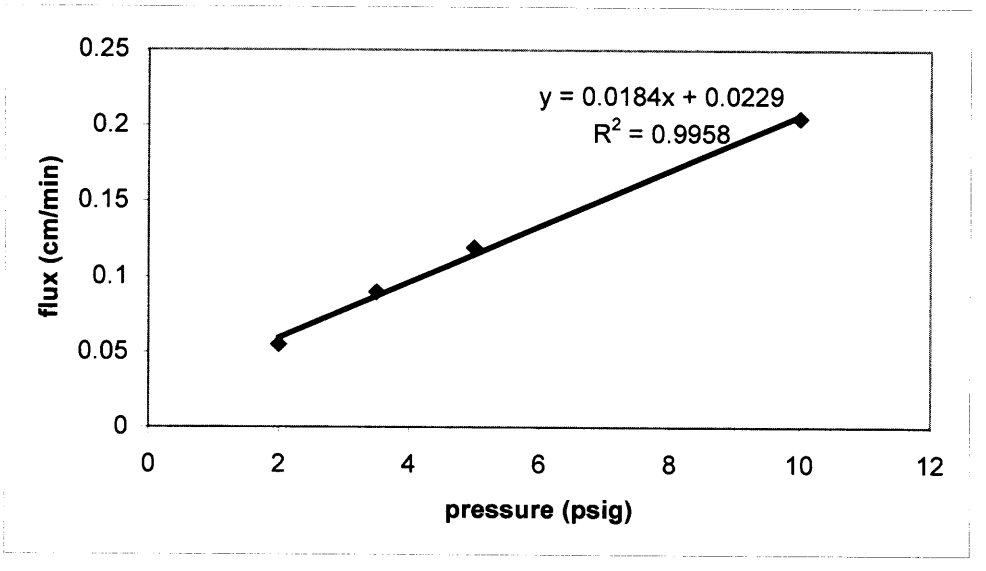

Figure 3.6 Pure water permeation data for a dirty YM30 membrane.

Table 3.1 Water Flux of Single UF Membranes and % Recovery of Flux

Membrane	New ($\times 10^3$ cm/min)	Cleaned ($\times 10^3$ cm/min)	% Recovery (%)
YM30	19.0	18.4	96.8
YM100	86.1	86.0	99.9
Ω100	158.3	155.2	98.0

3.2 Membrane Stack Configurations

A variety of experiments were initially performed to examine different configurations of the multimembrane stack. Different designs were investigated in order to determine the optimal configuration for rejection amplification without leakage. This leakage allowed the protein to escape permeation through the membrane and resulted in increased permeate concentration rather than increased rejection. The different configurations employed are described below. All experiments on different configurations were performed with YM30 regenerated cellulose membranes and the binary mixture of System 1 (1.0 mg/ml β-lactoglobulin and 0.2 mg/ml myoglobin; 20 mM Tris buffer; pH 7.3). The membranes in all experiments were placed skin side up, facing the feed.

3.2.1 Membranes Separated by Rubber Gaskets

The first experiment to investigate a membrane stack configuration employed a punched rubber gasket in between two membranes. The membranes were also sealed at the top with an o-ring. Figure 3.7 shows that when this punched rubber gasket arrangement was used, the concentration of both proteins actually increased in the permeate when the 2-membrane stack was studied. This indicated that there was leakage occurring around the

perimeter allowing the proteins to bypass the membranes. Therefore this arrangement was not effective for rejection amplification.

In order to prevent leakage, a bead of silicone was applied around the perimeter of the punch gasket. The membranes were also sealed at the top with an o-ring. Figure 3.8 shows that when this arrangement was used, again the concentration both proteins actually increased in the permeate when two membranes were studied. This meant that there was leakage occurring around the perimeter allowing the proteins to bypass permeating through the second membrane or both. This occurred in the presence of a gasket, despite the application of a bead of silicone, which indicated that the rubber gasket-based configuration was not suitable for the technique.

3.2.2 Membranes Separated by an O-Ring

For the data shown in Figure 3.9, an o-ring alone was used to separate the two membranes in the 2-membrane composite. The membranes were also sealed at the top with an o-ring. The results again showed that there was leakage occurring around the perimeter of the membranes due to incomplete sealing. This particular configuration, however, appeared to be more effective than the two experiments employing punched gasket between the membranes (Figure 3.7 and Figure 3.8). The 2-membrane composites appeared to yield a significantly higher rejection for Mb than that from a single membrane when the 2-membrane configuration was utilized. The leakage permeation of β-lactoglobulin was not as pronounced as in Figures 3.7 and 3.8. Also, the rejection of myoglobin (the more permeable protein) appears to be amplified, which was expected from the multi-membrane design.

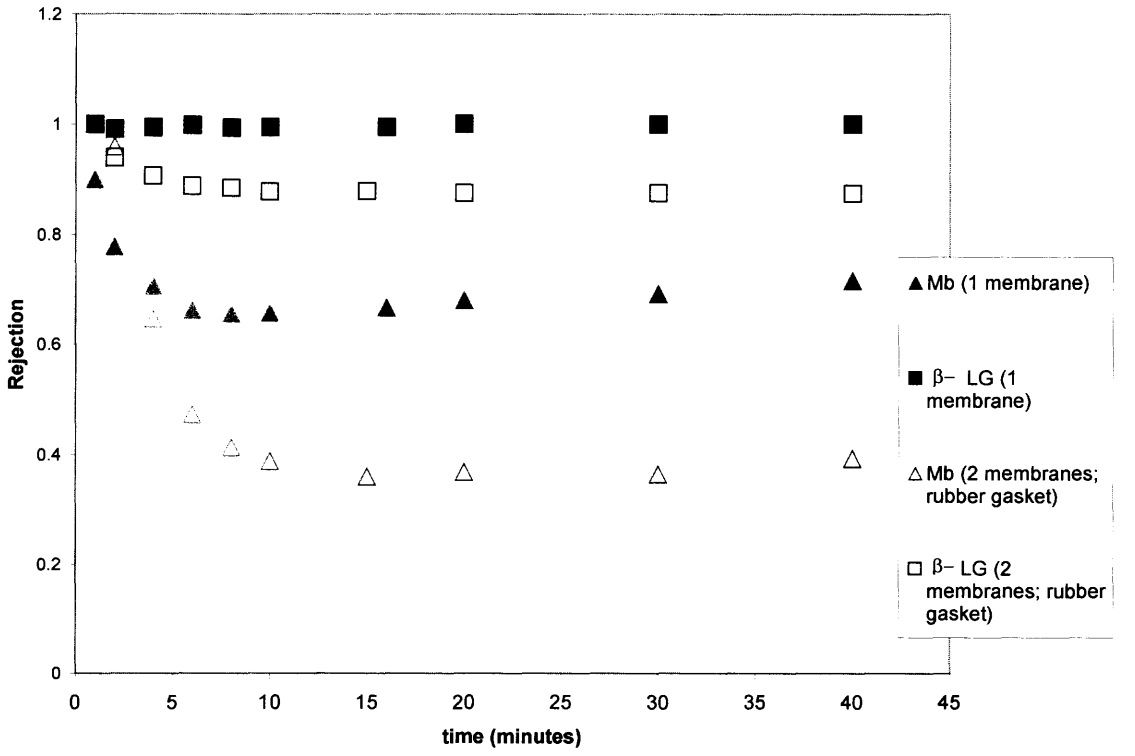

Figure 3.7 Rejection vs. time: comparing the performances of a single YM30 membrane and two YM30 membranes separated by a gasket (1.0 mg/ml β-lactoglobulin and 0.2 mg/ml myoglobin; 20 mM Tris buffer; pH 7.3).

3.2.3 Membranes Separated by an O-Ring and a Screen

Figure 3.10 shows the results for membranes separated by an o-ring and a polypropylene screen. The membranes were also sealed at the top with an o-ring. The results show that leakage was occurring due to the fact that there was an increase in the amount of β-lactoglobulin in the permeate in the 2-membrane case. This meant that the membranes were incompletely sealed around the perimeter allowing the protein to escape and eliminate the effect of any rejection amplification.

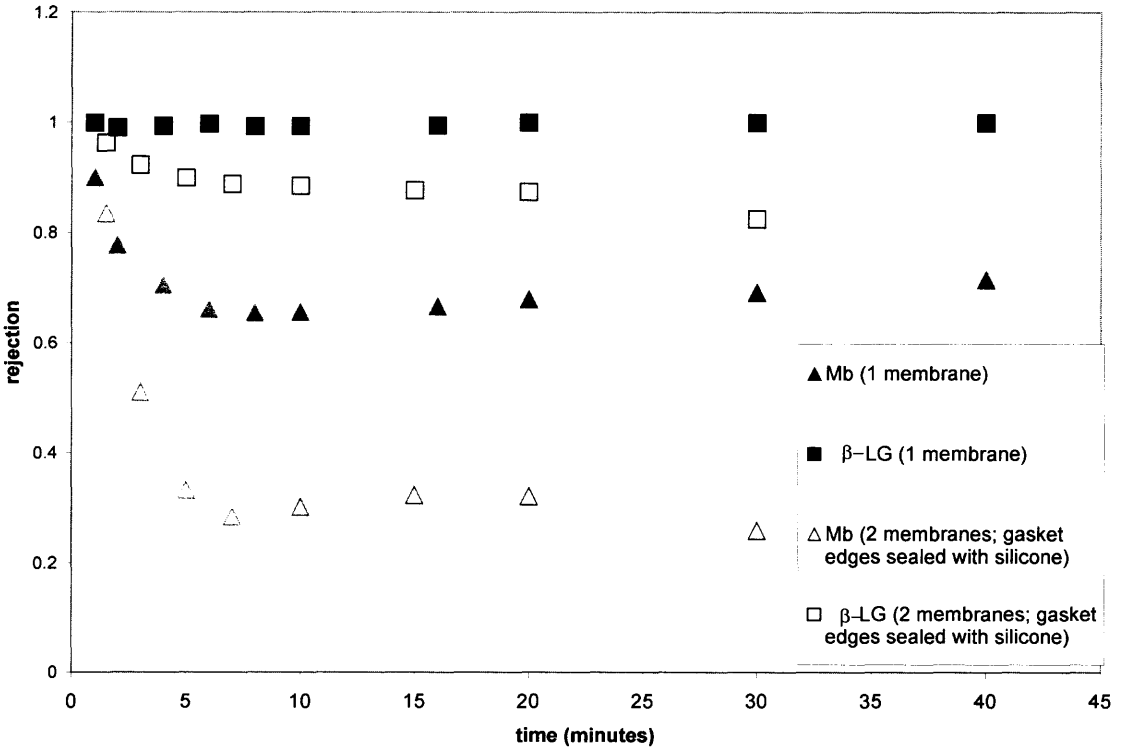

Figure 3.8 Rejection vs. time: comparing the performances of a single YM30 membrane and two YM30 membranes separated by a punched gasket with the edges sealed with silicone (1.0 mg/ml β-lactoglobulin and 0.2 mg/ml myoglobin; 20 mM Tris buffer; pH 7.3).

The increase in concentration of β-lactoglobulin in the permeate, when the 2-membrane configuration was utilized, was not as pronounced as in Figures 3-7 and 3-8. Also, the rejection of myoglobin (the more permeable protein) was amplified, which was what is expected with the multi-membrane design.

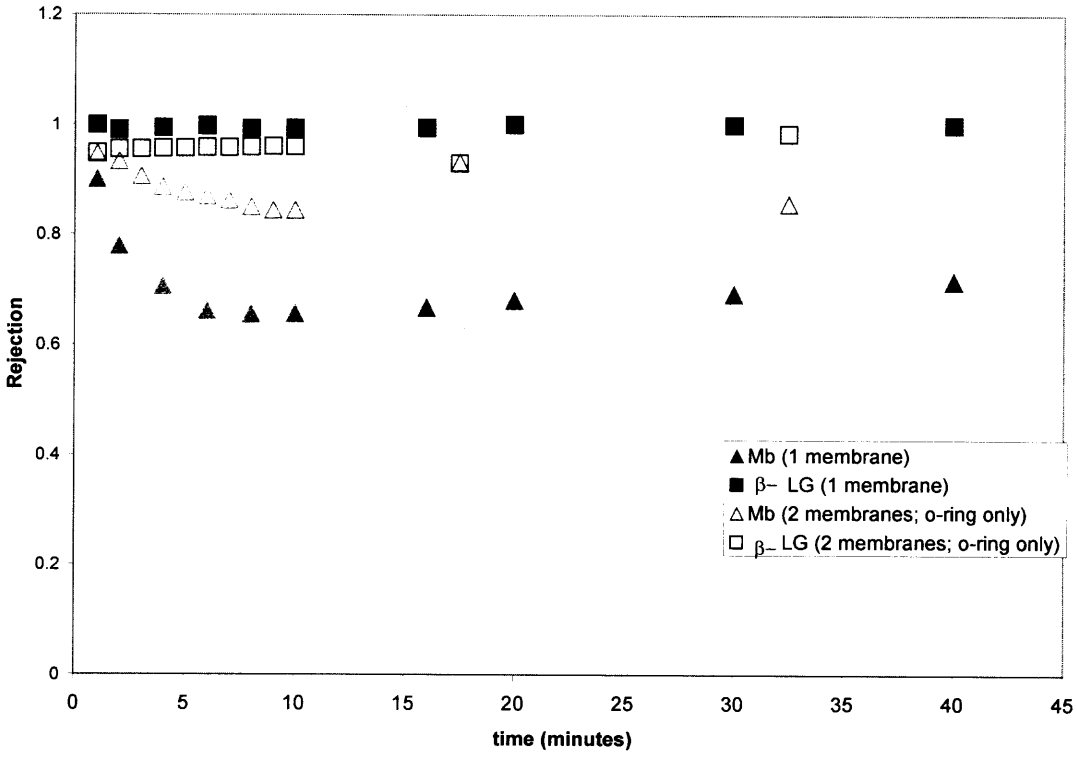

Figure 3.9 Rejection vs. time: comparing the performances of a single YM30 membrane and two YM30 membranes separated by an o-ring (1.0 mg/ml β-lactoglobulin and 0.2 mg/ml myoglobin; 20 mM Tris buffer; pH 7.3).

3.2.4 Membranes Sealed Together along the Outside Edge

Membranes were next sealed along the outside edge with silicone rubber without gaskets, o-rings, or polypropylene screens in-between. Filter paper was placed in-between the membranes and the sandwich was sealed together with silicone. The membranes were sealed from the top with an o-ring. Figure 3.11 shows the experimental results. This configuration was also ineffective and showed that there was more β-lactoglobulin in the permeate with the two membranes than was present from a single membrane system. It is apparent that leakage was occurring along the perimeter and the proteins were escaping permeation via the membranes. The performance of this particular configuration was

very poor. The rejection of both myoglobin and β-lactoglobulin decreased significantly. This can possibly be attributed to proteins escaping permeation through both membranes due to the poor sealing of the sandwich.

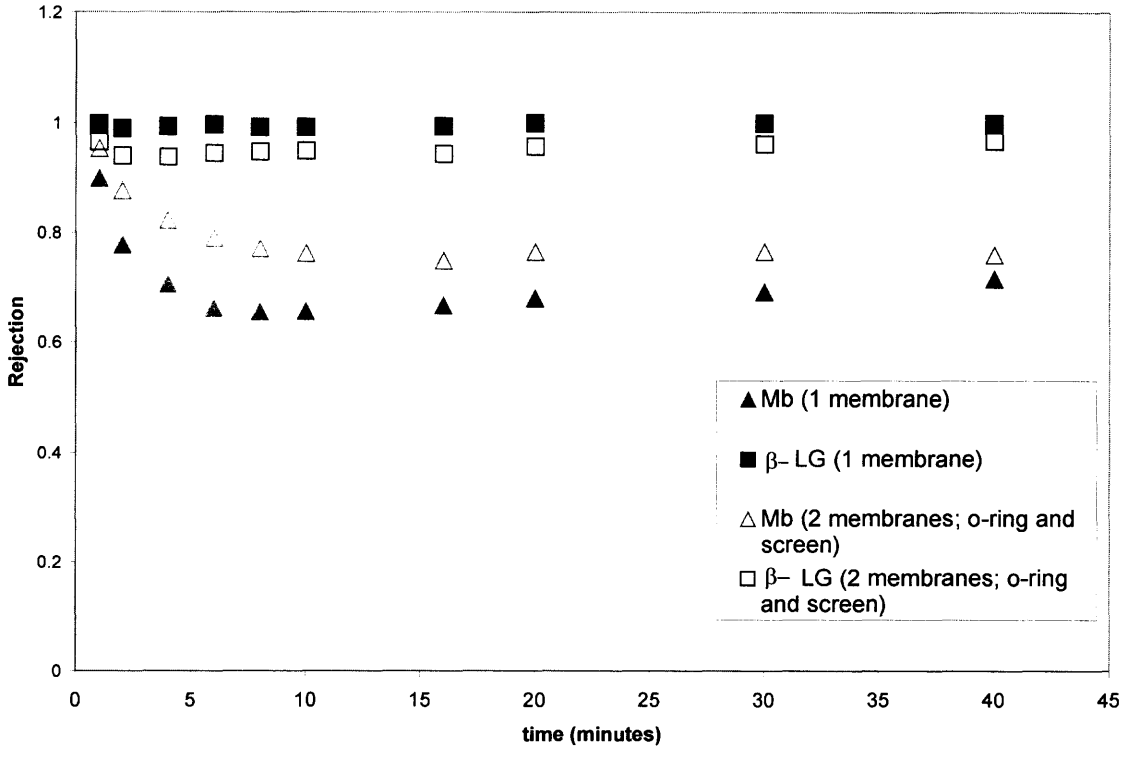

Figure 3.10 Rejection vs. time: comparing the performances of a single YM30 membrane and two YM30 membranes separated by a screen and an o-ring (1.0 mg/ml β-lactoglobulin and 0.2 mg/ml myoglobin; 20 mM Tris buffer; pH 7.3).

3.2.5 Membrane Sandwich

In the next configuration, membranes were placed in a sandwich fashion, directly on top of one another with no gaskets, o-rings, polypropylene screens, or filter paper in-between. The membranes were sealed from the top with an o-ring. Figure 3.12 shows the results comparing 1 and 2 membranes. The amplification of the rejection of β-lactoglobulin in

the permeate was now clearly visible in this configuration. When two membranes were used, the rejection of β-lactoglobulin was increased, which was not seen in any of the other configurations examined so far.

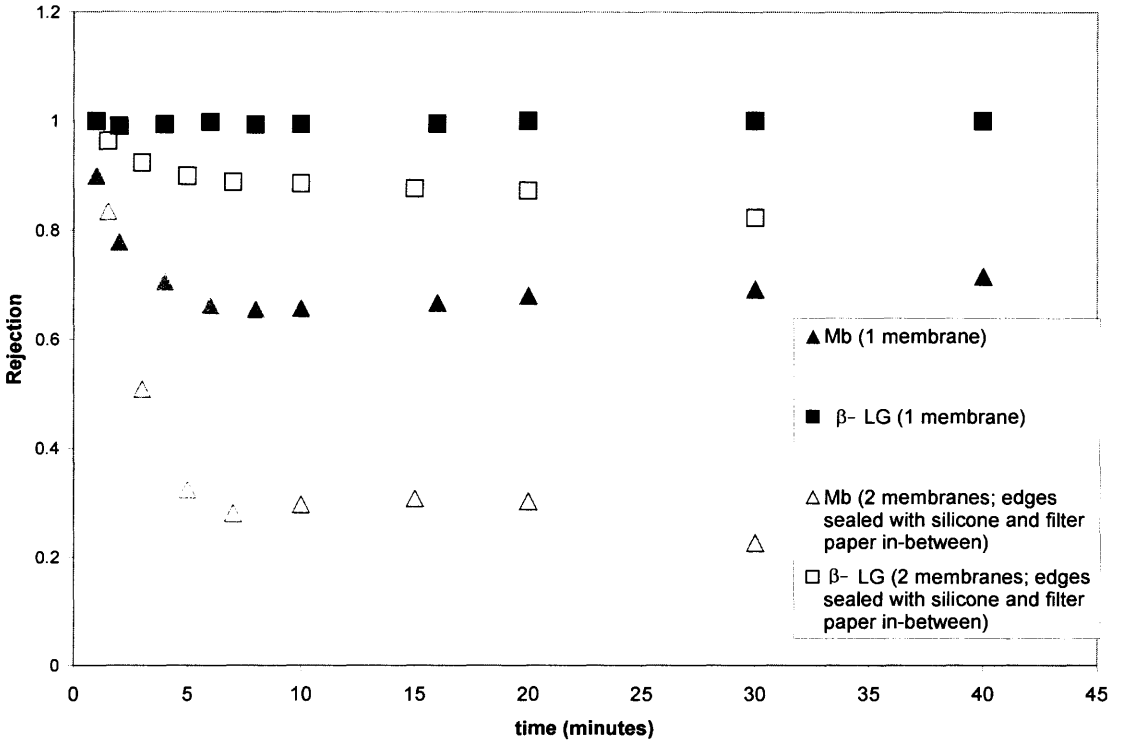

Figure 3.11 Rejection vs. time: comparing the performances of a single YM30 membrane and two YM30 membranes separated by a filter paper and sealed along the outside edge with silicone (1.0 mg/ml β-lactoglobulin and 0.2 mg/ml myoglobin; 20 mM Tris buffer; pH 7.3).

The results from these experiments yielded the optimal configuration for the multimembrane stack. Stacking the membranes in this fashion resulted in no protein leakage and did not allow proteins to escape membrane permeation. Operating in this

configuration allowed the achievement of rejection amplification. This configuration potentially created a membrane composite that increased the rejection with each additional membrane added.

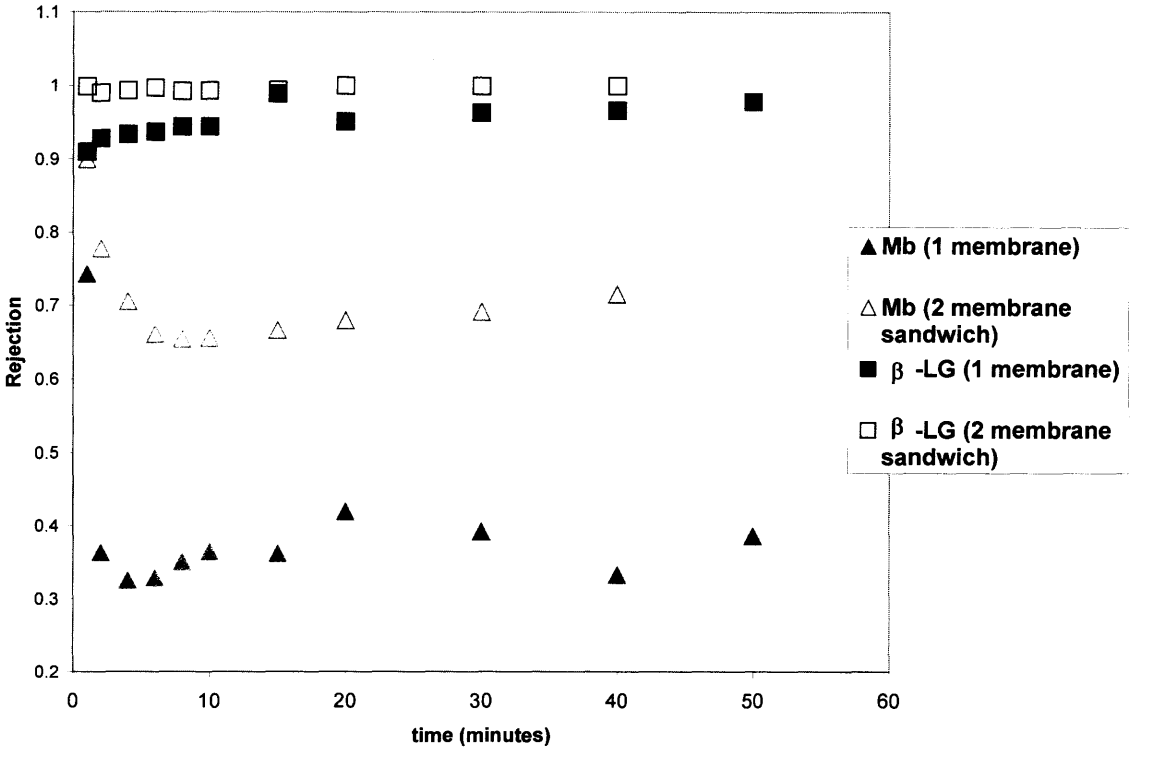

Figure 3.12 Rejection vs. time: comparing the performances of a single YM30 membrane and a 2-membrane sandwich (1.0 mg/ml β-lactoglobulin and 0.2 mg/ml myoglobin; 20 mM Tris buffer; pH 7.3).

3.3 Single Membrane Studies

3.3.1 System 1

System 1, consisting of β-lactoglobulin and myoglobin (molecular weight ratio 2.05), was studied in great detail and most of the preliminary investigations were performed on this system. The majority of the data collected, therefore, was based on System 1. All experiments utilized YM30 regenerated cellulose ultrafiltration membranes.

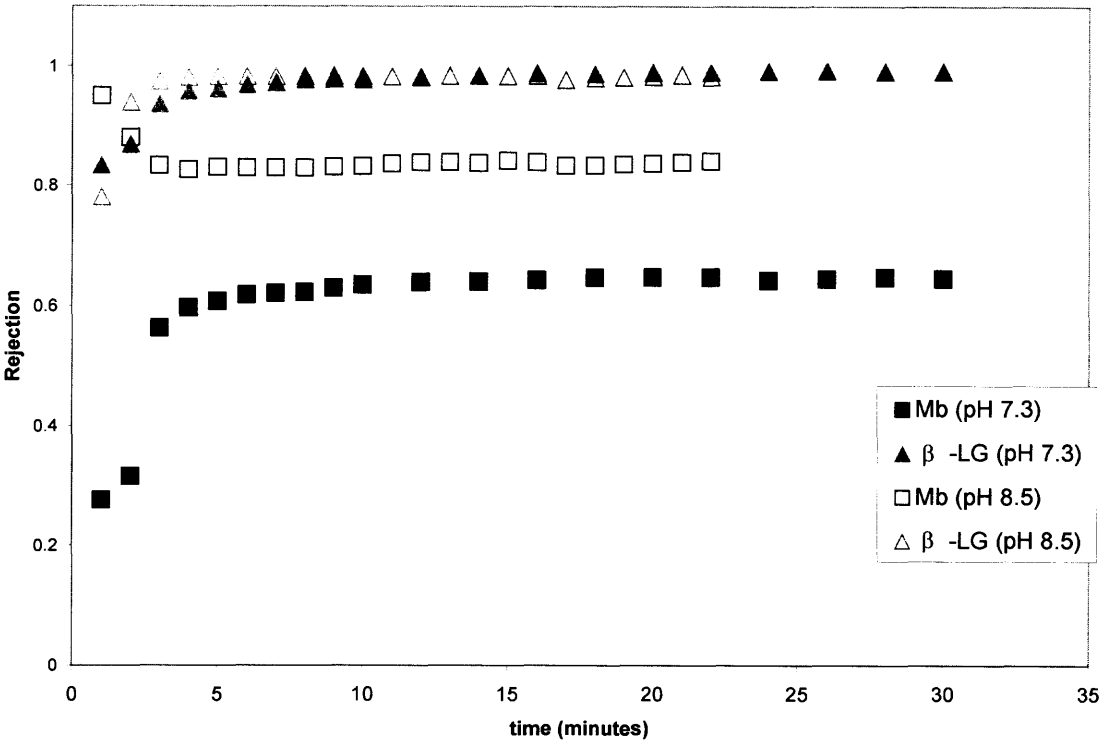

Figure 3.13 Rejection vs. time: comparing the performances of a single YM30 membrane at two different buffer pHs (1.0 mg/ml β-lactoglobulin and 0.2 mg/ml myoglobin; 20 mM Tris buffer; pH 7.3 and pH 8.5).

3.3.1.1 Different pH-Based Operating Conditions. Initial experiments were performed on System 1 to better investigate the optimal physicochemical operating conditions for the multimembrane stack. First, single membrane studies of System 1

comparing different pH conditions and their effects on the rejection coefficient and selectivity were carried out. Figure 3.13 compares the results of System 1 operating at two pH values, 8.5 and 7.3. The pI of myoglobin is 7.3; therefore, when operating at buffer conditions of pH 7.3, myoglobin did not have any net charge while β-lactoglobulin had a net charge. The pI of β-lactoglobulin is 5.3, and therefore it is negatively charged at pH 7.3. When the buffer conditions were pH 8.5, both proteins were negatively charged. There is a slight negative charge on the YM30, which aids in the rejection of the negatively charged proteins.

Figure 3.13 shows that the rejection coefficient of myoglobin at pH 8.5 was approximately 0.83 and at pH 7.3 the rejection coefficient of myoglobin was 0.62. This increased transmission of myoglobin is due to the lack of any net charge on the myoglobin molecule at pH 7.3 (pI of myoglobin). The rejection for β-lactoglobulin was similar at both pH 8.5 and pH 7.3 experiments due to the presence of a net negative charge in both cases.

The selectivity data for myoglobin over β-lactoglobulin is shown in Figure 3.14. After the first five minutes of ultrafiltration equilibration, the selectivity difference between the two operating conditions is apparent. At pH 8.5, the selectivity was between 9 and 10. At pH 7.3, the selectivity increase was apparent and went as high as 49. This increased selectivity was due to the increased transmission of myoglobin at this pH. It is also important to note that when operating at pH=pI, the operating flux is at a minimum (Swaminathan, Chaudhuri, and Sirkar 1981; Sirkar and Prasad 1986). The flux loss when operating at pH=pI was 8.3% compared to 0% loss with respect to initial values when operating at pH 8.5 (pH≠pI).

3.3.1.2 Different Operating Pressures. Initial investigations into different operating pressures are important in understanding the conditions that each membrane was exposed to in a multimembrane stack. For example, if there are two membranes in a stack operating at a total pressure of 10 psig, each membrane is exposed to approximately 5 psig; similarly, for three membranes in a stack operating at a total pressure of 10 psig, each membrane is exposed to approximately 3.3 psig.

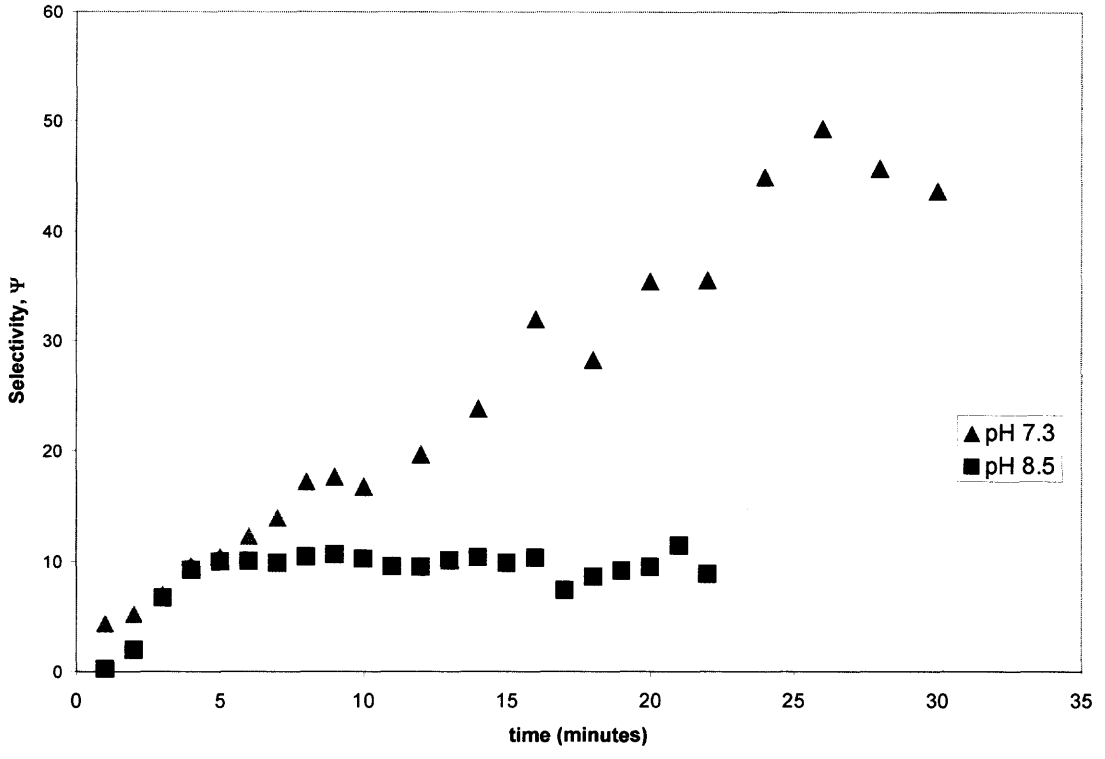

Figure 3.14 Selectivity vs. time: comparing the performances of a single YM30 membrane at two different buffers pHs (1.0 mg/ml β-lactoglobulin and 0.2 mg/ml myoglobin; 20 mM Tris buffer; pH 7.3 and pH 8.5).

Experiments were performed on System 1 with an initial feed concentration of 1.0 mg/ml β-lactoglobulin and 0.2 mg/ml myoglobin (20 mM Tris buffer; pH 7.3) at four different pressures: 2.0, 3.5 psig, 5 psig, and 10 psig. The solute rejection results from

these experiments are shown in Figure 3.15. When the pressure was increased, the rejection coefficient was decreased. This is due to the increased driving force resulting in an increased wall concentration of the protein, which leads to increased transmission of the protein. This occurred because the experiments were operating in the pressure dependent region of the ultrafiltration curve. If the conditions were in the pressure independent region of the ultrafiltration curve due to the formation of a gel layer on the membrane, the wall concentration would have been constant due to a balance between convection toward the membrane and diffusion back into the bulk.

In the beginning of ultrafiltration, there is a decrease in rejection (Figure 3.15). This pattern is seen in most of the ultrafiltration experiments performed. Water or buffer elutes through the membrane, polypropylene support screen, base of ultrafiltration cell, and exit tubing before the proteins. Therefore the permeate concentration is therefore diluted, which translates into a higher value of rejection. With time, protein concentrations stabilize / increase in the absence of dilution.

Figure 3.16 shows the flux data for 2.0, 3.5, 5.0, and 10 psig runs for the same system (1.0 mg/ml β-lactoglobulin and 0.2 mg/ml myoglobin; 20 mM Tris buffer; pH 7.3). As expected, when the pressure increased, the flux increased proportionally. Also, it is important to note that there was no significant flux decline and the flux was maintained at a steady level throughout the experiment.

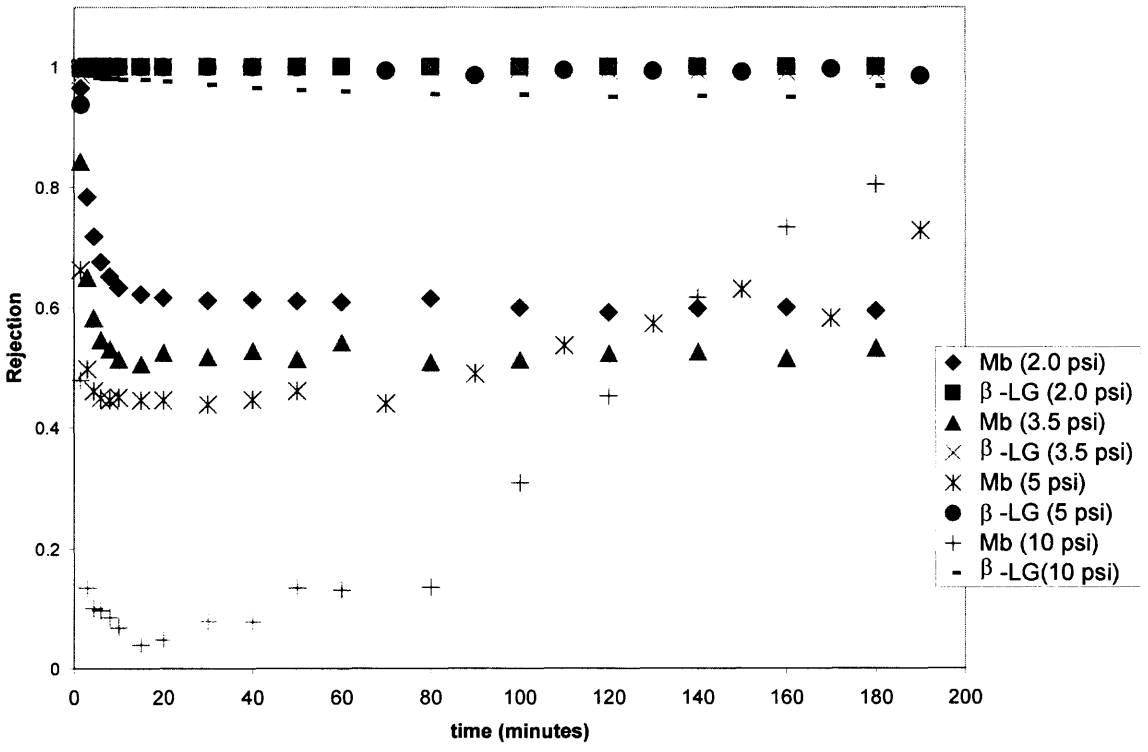

Figure 3.15 Experimental rejection behaviors for 1 membrane system (YM30) at four different pressures. Batch ultrafiltration of System 1 (1.0 mg/ml β-lactoglobulin and 0.2 mg/ml myoglobin, pH 7.3; 2.0 3.5, 5.0, and 10.0 psig).

3.3.2 System 2

System 2, consisting of α-lactalbumin and myoglobin (molecular weight ratio 1.22), was investigated as a follow-up study to System 1. Here, YM30 regenerated cellulose membranes were used in all experiments with a feed concentration of 0.2 mg/ml α-lactalbumin and 0.2 mg/ml myoglobin in pH 4.35 citric acid buffer. Due to the small molecular weight ratio, buffer optimized conditions were chosen for the experiments in order to exploit the charge interactions and achieve separation.

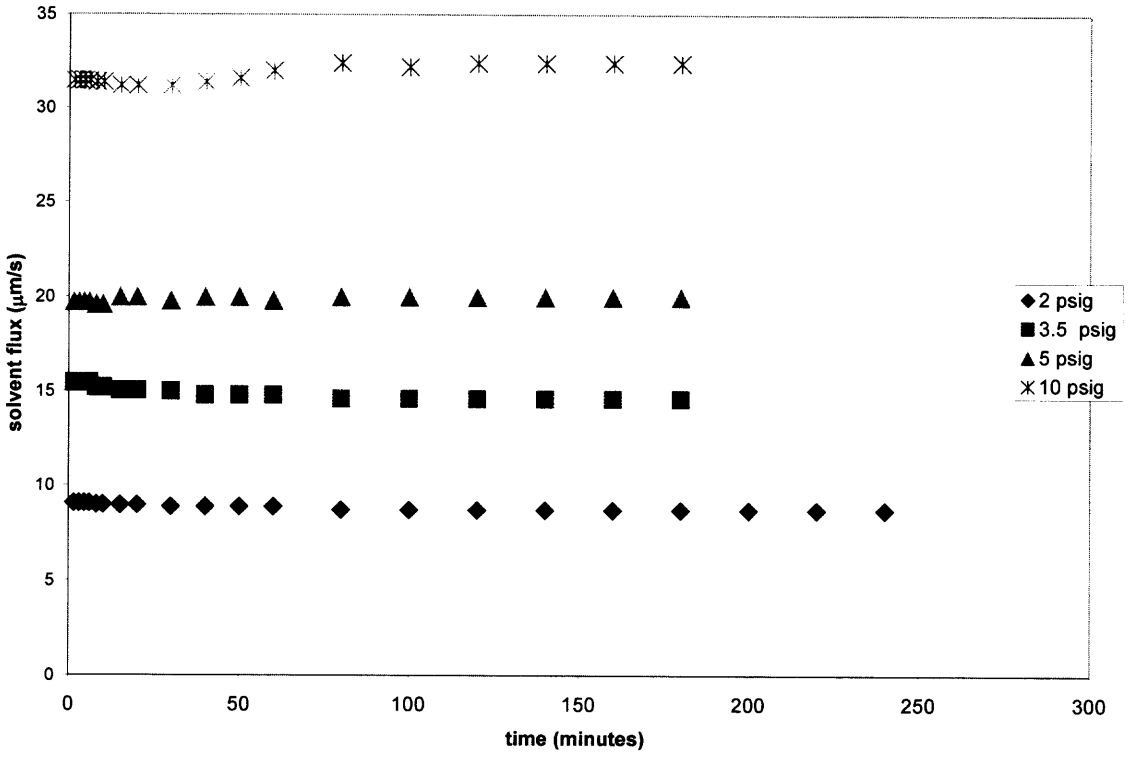

Figure 3.16 Experimental solvent fluxes for 1 membrane system (YM30) at four different pressures. Batch ultrafiltration of System 1 (1.0 mg/ml β-lactoglobulin and 0.2 mg/ml myoglobin, pH 7.3; 2.0, 3.5, 5.0, and 10.0 psig).

The citric acid buffer was used at pH 4.35. The pI for α-lactalbumin ranges between 4.2-4.5 and citric acid buffer was chosen because it is an effective buffer at these pHs. At pH 4.35, α-lactalbumin carries a zero net charge while myoglobin (whose pI is 7.3) has a net positive charge. It was observed that myoglobin has a low solubility at pH 4.35 and therefore partially precipitated out of solution, regardless of the salt concentration. Prefiltering was utilized to remove the insoluble myoglobin and the feed concentration was monitored. Due to the high cost of myoglobin, lower initial feed concentrations of myoglobin (the more highly rejected protein) were utilized.

3.3.2.1 Different Operating Pressures. Figure 3.17 illustrates the rejection profiles for system 2 under various pressure conditions. At low pressures, where diffusion dominated over convection, there is less of an effect of pore plugging. This can be seen in the data for α-lactalbumin (the more permeable protein) at 2.0 and 3.5 psig. At 5.0 and 10 psig, the effect of pore plugging can be seen as the rejection quickly moved toward 1.0. Myoglobin (the more highly rejected protein) also showed the effects of fouling / concentration polarization at the higher pressures. At 5.0 and 10.0 psig, there was an initial decrease in rejection meaning that myoglobin permeated through the membrane and then plugged the pores that resulted in the rejection shifting towards 1.0. The effect of fouling / concentration polarization was also seen when the solvent flux data were analyzed.

Figure 3.18 shows the solvent flux data at 2.0, 3.5, 5.0, and 10.0 psig. As the pressure was increased, the effects of fouling / concentration polarization were prevalent. This was apparent from the flux decline that was seen at higher operating pressures. Due to increased pore plugging and increased wall concentration of protein, the solvent flux experienced a large decline, which was apparent at the higher pressures. The percentage flux declines were as follows: 8.0 % at 2.0 psig, 57.8% at 3.5 psig, 81.1% at 5.0 psig, and 74.7% at 10 psig. The flux declines seen with this system are because both proteins are similar in size and at higher pressures, where convection was dominant, pore plugging was occurring. When lower pressures were used, diffusion was dominant which minimized the effects of fouling / concentration polarization. Also, there is a slight negative charge on the membrane and at pH 4.35, myoglobin carries a net positive charge

which contributes to gel layer formation. Therefore, a lower operating pressure is necessary for the system.

3.3.3 System 3

System 3, consisting of bovine serum albumin (BSA) and hemoglobin (molecular weight ratio 1.03) was investigated as a follow-up study to System 1. Here, Omega 100K polyethersulfone membranes were used in all experiments and a feed concentration of 1.0 mg/ml bovine serum albumin and 0.2 mg/ml hemoglobin in pH 6.8 sodium phosphate buffer. Due to the small molecular weight ratio, buffer optimized conditions were chosen for the experiments in order to exploit the charge interactions and achieve separation. Initial investigations using Omega 100K membranes were conducted by operating at the pI of hemoglobin, pH 6.8. This meant that there was no net charge on hemoglobin while bovine serum albumin had a net negative charge.

3.3.3.1 Ionic Strength. Different ionic strengths were investigated to determine the selectivity of hemoglobin over BSA. Figure 3.19 compares the experimental data for batch ultrafiltration of 1.0 mg/ml bovine serum albumin and 0.2 mg/ml hemoglobin at 2.3 mM and 20 mM ionic strength. Both experiments were performed using pH 6.8 sodium phosphate buffer. Due to the lack of selectivity (ranging from 1 to 2) at 20 mM buffer concentration, a lower ionic strength, 2.3 mM, was explored to achieve improved separation of this system. When the ionic strength was lowered from 20 mM to 2.3 mM, the selectivity increased substantially ranging from approximately 5 to 45. This occurred because at lower ionic strength, the negative charges on BSA are less shielded due to the low salt concentration of the buffer. By

operating at low ionic strength, the physicochemical properties of the system are fully exploited allowing higher selectivities.

3.3.3.2 Different Operating Pressures. The rejection profiles are shown in Figure 3.20 for System 3 at three different pressures; 1.5, 3.0, and 4.5 psig. As described in section 3.3.2.2, the rejection of hemoglobin tends towards 1.0 faster at higher pressures due to increased flux and decrease of hemoglobin retentate concentration due to batch operation. The rejection of bovine serum albumin is substantial in all cases due to the conditions of the experiments (i.e., low ionic strength, operating at pH=pI of hemoglobin). All experiments were performed using Omega 100K polyethersulfone membranes.

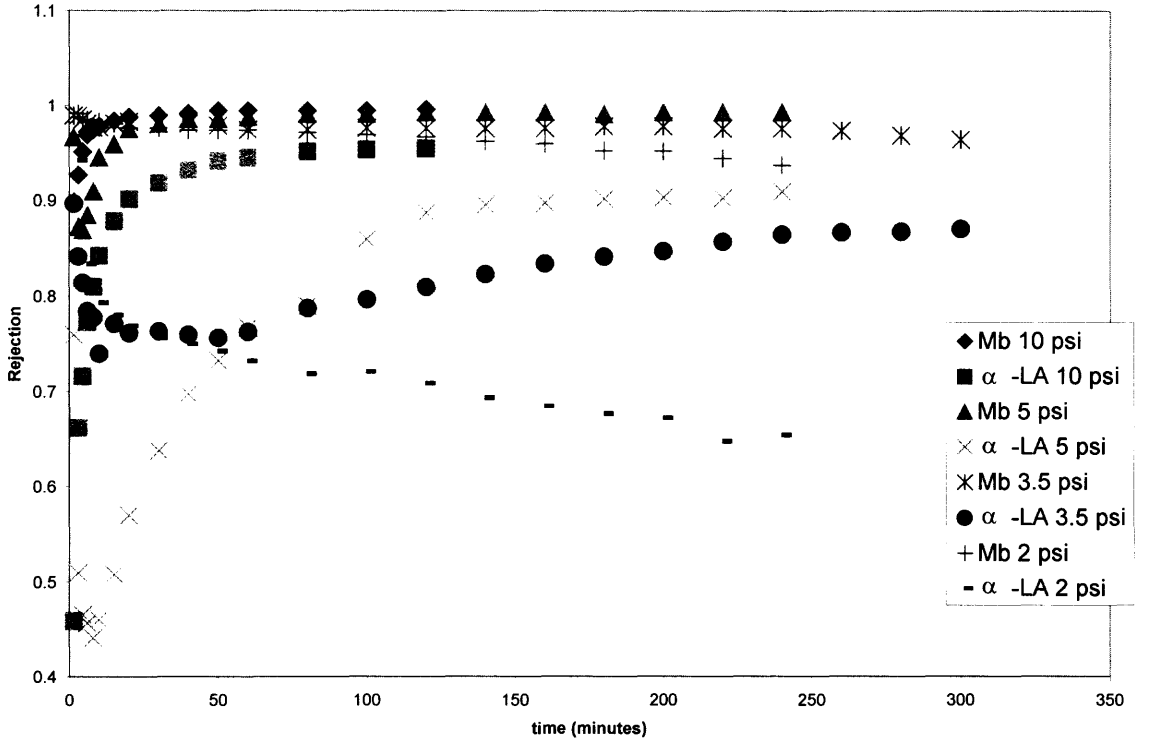

Figure 3.17 Experimental rejection behaviors for 1 membrane (YM30) at four different pressures. Batch ultrafiltration of System 2 (0.2 mg/ml α-lactalbumin and 0.2 mg/ml myoglobin, pH 4.35 20 mM citric acid buffer; 2.0 3.5, 5.0, and 10.0 psig).

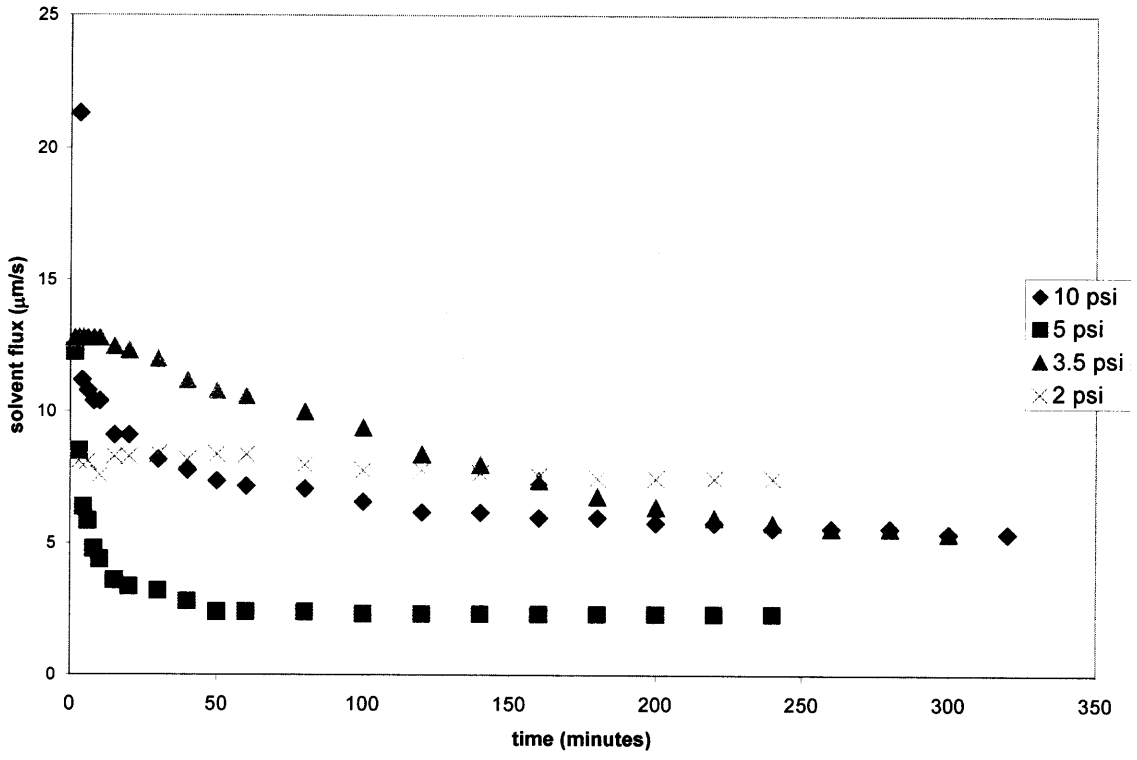

Figure 3.18 Experimental solvent fluxes for 1 membrane system (YM30) at four different pressures. Batch ultrafiltration of System 2 (0.2 mg/ml α-lactalbumin and 0.2 mg/ml myoglobin, pH 4.35; 2.0 3.5, 5.0, and 10.0 psig).

Data comparing flux measurements at three different pressures are shown in Figure 3.21. It is important to take note that lower pressures are being investigated due to the effects of fouling (mentioned in Subsection 3.3.2.2) that occur when operating at higher pressures for a binary mixture whose proteins are so close in molecular weight. The flux measurements provided in Figure 3.21 show that after 10 minutes all fluxes reached steady levels. The flux loss encountered at 4.5 psig was 19.28%, at 3.0 psig was 1.0%, and at 1.5 psig was 5.8 %. At 4.5 psig, there is more of an effect of fouling / concentration polarization (as seen by the higher percentage flux loss) due to pore plugging and increased wall concentration of the protein.

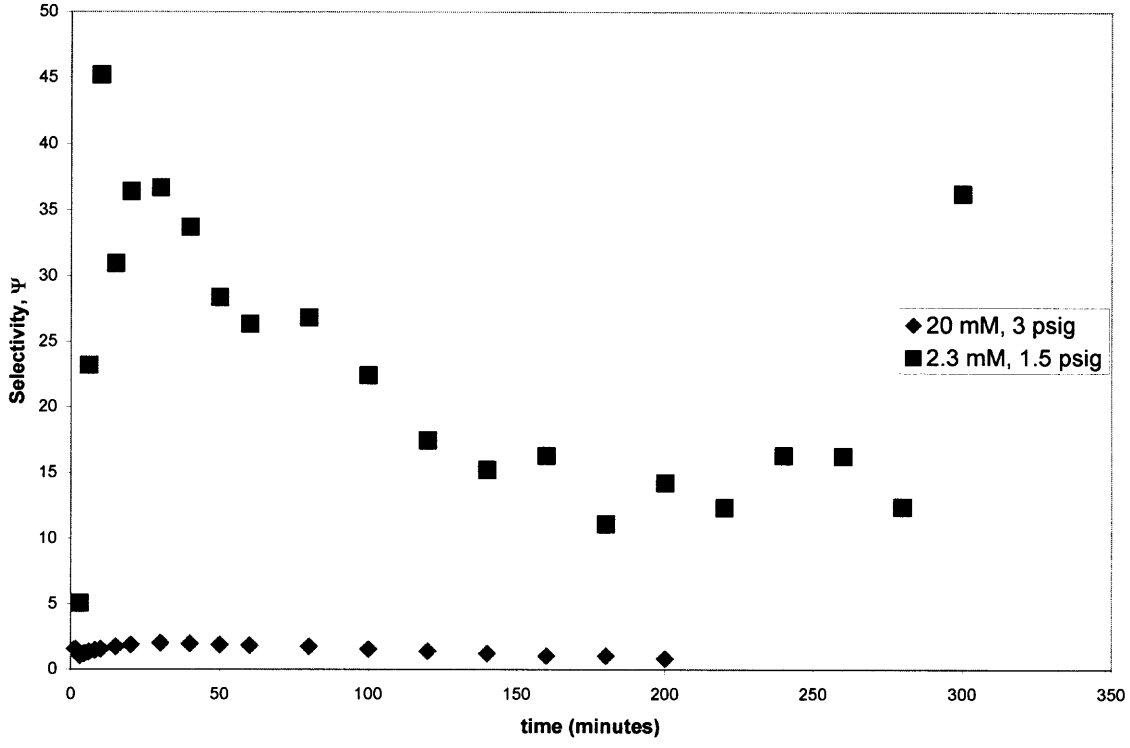

Figure 3.19 Selectivity vs. time comparing two different ionic strengths for batch ultrafiltration of System 3 (1.0 mg/ml bovine serum albumin and 0.2 mg/ml hemoglobin, pH 6.8, 2.3 mM and 20 mM sodium phosphate buffer; Omega 100K membranes).

In this Section 3.3, single membrane experimental results have been presented for the preliminary investigation of the experimental results using the multimembrane composite. Comparison of single membrane experimental data with those from multimembrane composites will be discussed in the following section.

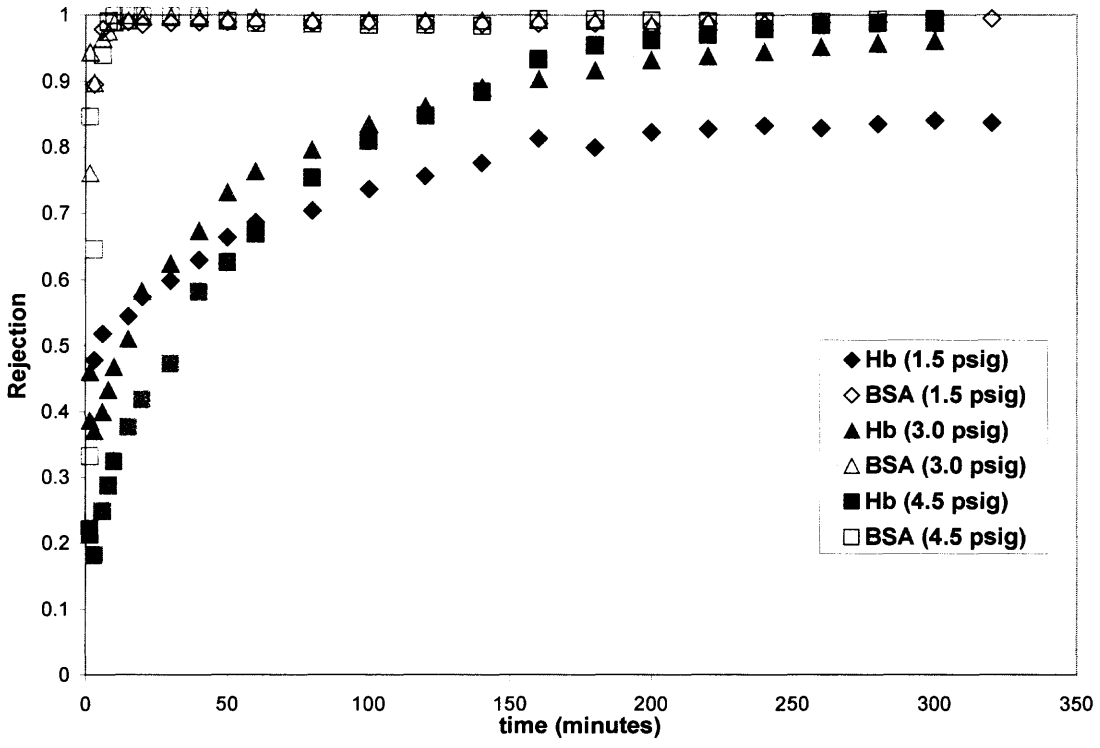

Figure 3.20 Experimental rejection behaviors for 1 membrane system (Ω100K) at three different pressures. Batch ultrafiltration of System 3 (1.0 mg/ml bovine serum albumin and 0.2 mg/ml hemoglobin, pH 6.8, 2.3 mM sodium phosphate buffer; Omega 100K membranes, 1.5, 3, and 4.5 psig).

3.4 Multimembrane Composite Studies

In this Section, experimental results from multimembrane composites will be presented and discussed. Here, all experiments were performed using the sandwich configuration described earlier in Section 3.2.5. The membranes were stacked together, skin side up, without gaskets, o-rings, screens, or filter paper. By utilizing this design, the rejection behaviors displayed in single membrane studies were potentially amplified. Experiments were performed on System 1, System 2, and System 3.

3.4.1 System 1

System 1 consisted of a binary mixture of 1.0 mg/ml β-lactoglobulin and 0.2 mg/ml myoglobin. This was the first system studied. Therefore, most of the experimental data were collected with this system. Multimembrane experiments were performed under non-optimized conditions (pH≠pI) and optimized conditions (pH=pI) vis-à-vis the more permeable protein. Pulse experiments were also investigated using this system. Experimental results involving higher pressures, extended duration, continuous feed flow, different feed concentrations, and cyclic patterns will be discussed in this section as well. All experiments were performed using YM30 regenerated cellulose membranes.

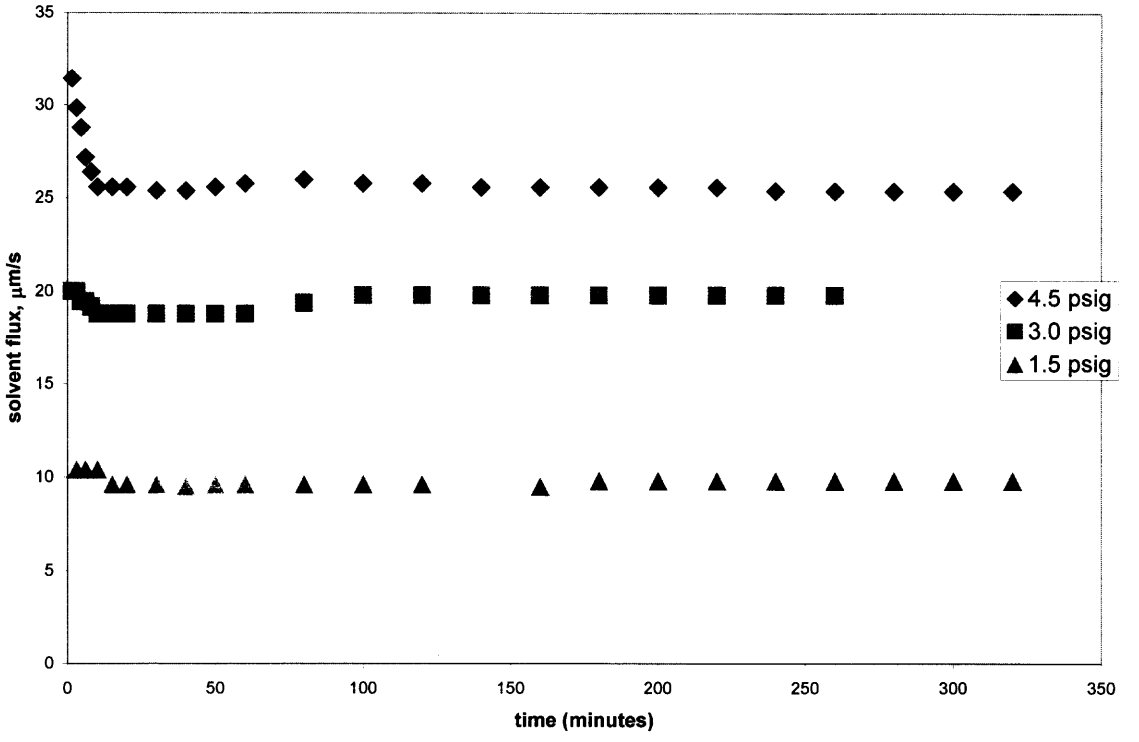

Figure 3.21 Experimental fluxes for 1 membrane in System 3 at three different pressures. Batch ultrafiltration of System 3 (1.0 mg/ml BSA and 0.2 mg/ml hemoglobin, pH 6.8, 2.3 mM sodium phosphate buffer; 1.5, 3.0, and 4.5 psig).

When the membranes were analyzed after completion of ultrafiltration prior to cleaning, it was found that very little protein had been adsorbed on the membranes. Less than 1.0 μg/ml of the more permeable protein (myoglobin) was found in all cases. The more rejected protein concentration was also very low, ranging from 14 μg/ml for the top membrane to less than 1 μg/ml for the bottom membrane. This was seen under all experimental conditions.

3.4.1.1 Non-optimized Batch Ultrafiltration. The separation of myoglobin and β-lactoglobulin at pH 6.0 was performed at 10 psig. A buffer of 20 mM citric acid at pH 6.0 was used. At pH 6.0, both myoglobin and β-lactoglobulin have a net charge. Myoglobin, with a pI of 7.3, has a positive net charge at pH 6.0 and β-lactoglobulin, pI of 5.3, has a negative net charge. Therefore, by operating at pH.6.0, both proteins carry a net charge and their physicochemical property differences are not exploited.

Figure 3.22 shows the permeate concentration profiles of β-lactoglobulin (the more highly rejected protein) comparing one, two, and three membranes. With the addition of each additional membrane, the concentration of β-lactoglobulin in the permeate stream was reduced, ultimately resulting in a pure myoglobin product (the more permeable protein). With the three-membrane composite, after 15 minutes, the concentration of β-lactoglobulin in the permeate was zero. A completely purified myoglobin fraction was obtained.

Figure 3.23 shows the permeate concentration profiles of myoglobin (the more permeable protein) comparing one, two, and three membranes. The concentration of myoglobin in the permeate stream was reduced with each membrane added due to the

flux loss encountered. Also the single membrane rejection was amplified, as seen with β-lactoglobulin, smaller permeate concentrations as the membrane number was increased.

Table 3.2 illustrates the % yield for these experiments. Longer operation time would have led to increased % yield.

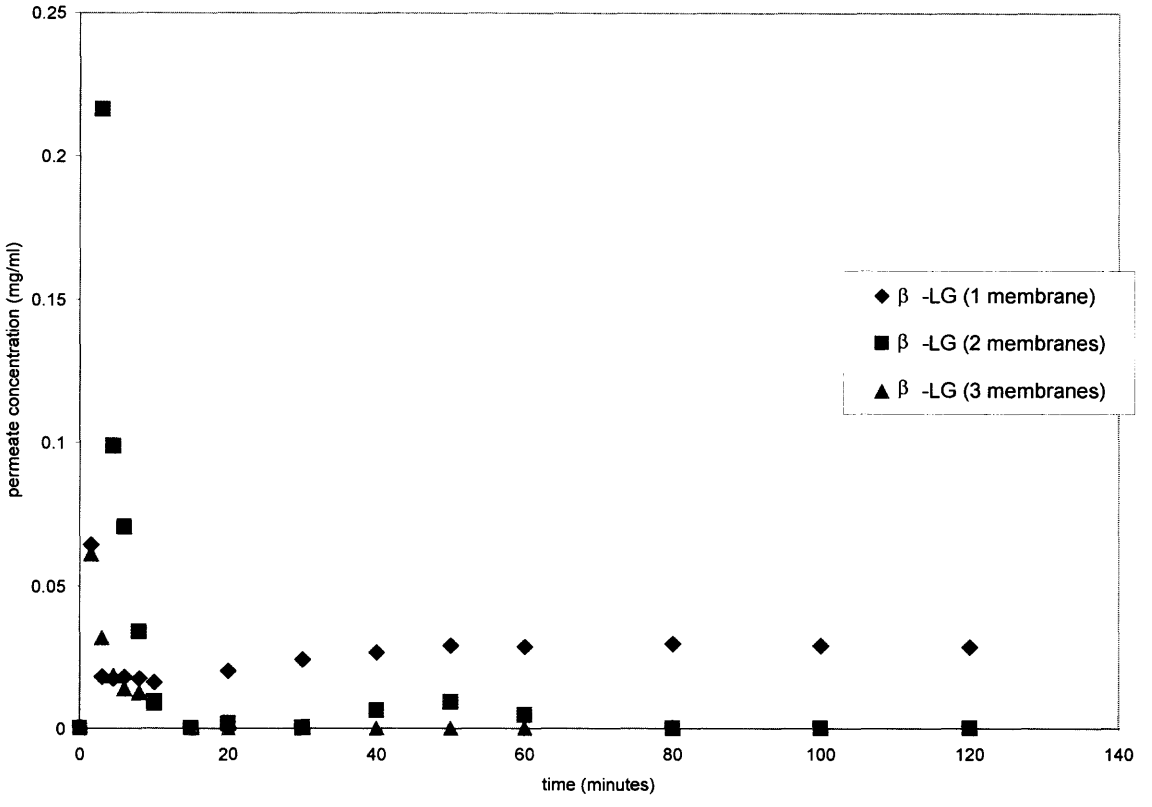

Figure 3.22 Nonoptimized batch ultrafiltration of System 1: 1.0 mg/ml β-lactoglobulin and 0.2 mg/ml myoglobin, pH 6.0, 20 mM citric acid buffer, 10 psig (only more highly rejected protein, β-LG, shown).

The results from these nonoptimized experiments show that when operating at an arbitrary pH, one may still achieve complete purification of the more permeable protein containing stream with this technique. Therefore modifications of the feed stream and buffers may be avoided which is attractive to ongoing processes.

Table 3.2 Comparison of % Yield For a Given Operating Time For Different Numbers of Membranes. Batch Ultrafiltration of System 1 (1.0 mg/ml β-Lactoglobulin and 0.2 mg/ml Myoglobin, pH 6.0, 20 mM Citric Acid Buffer)

	Myoglobin Yield (%)	Time (minutes)
One membrane (10 psig)	90.92	120
Two membranes (10 psig)	57.02	120
Three membranes (10 psig)	49.80	120

3.4.1.2 Optimized Batch Ultrafiltration. The separation of myoglobin and β-lactoglobulin at pH 7.3 was performed at 10 psig. 20 mM Tris buffer at pH 7.3 was used. Myoglobin, whose pI is 7.3, had no net charge at pH 7.3 and β-lactoglobulin, whose pI is 5.3, had a net negative charge. Also, the YM30 regenerated cellulose membrane carries a slight negative charge. Therefore, by operating at pH.7.3, the physicochemical properties of the proteins and the membrane were utilized. However, due to the high selectivity at 20 mM ionic strength, lower ionic strength experiments were not conducted.

Figure 3.24 shows the permeate concentration profile of β-lactoglobulin (the more highly rejected protein) comparing one, two, and three membranes. With the addition of each additional membrane, the concentration of β-lactoglobulin in the permeate stream was reduced, ultimately resulting in a pure myoglobin product (the more permeable protein). With the three-membrane composite, after the first few minutes, the concentration of β-lactoglobulin in the permeate was zero, therefore complete purification of the more permeable protein was achieved.

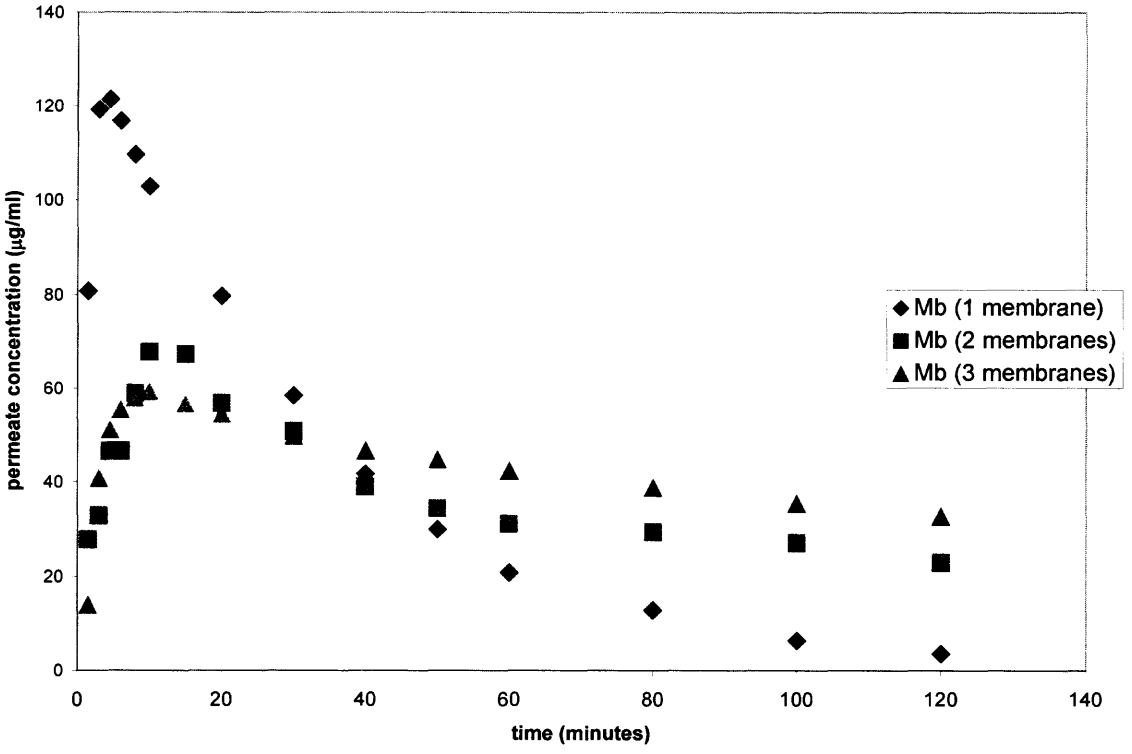

Figure 3.23 Nonoptimized batch ultrafiltration of System 1: 1.0 mg/ml β-lactoglobulin and 0.2 mg/ml myoglobin, pH 6.0, 20 mM citric acid buffer, 10 psig (only more permeable protein, Mb, shown).

Figure 3.25 shows the permeate concentration profiles of myoglobin (the more permeable protein) comparing one, two, and three membranes. With the addition of each additional membrane, myoglobin rejection was increased; therefore the myoglobin concentration in the permeate was reduced. Further, when the total pressure was 10 psig, the flux was reduced by half for a 2-membrane composite and to one third for a 3-membrane composite. Therefore, when utilizing a 2-membrane composite, myoglobin will take a longer time to fully permeate and when a three-membrane composite is used, myoglobin will take an even longer time to fully permeate.

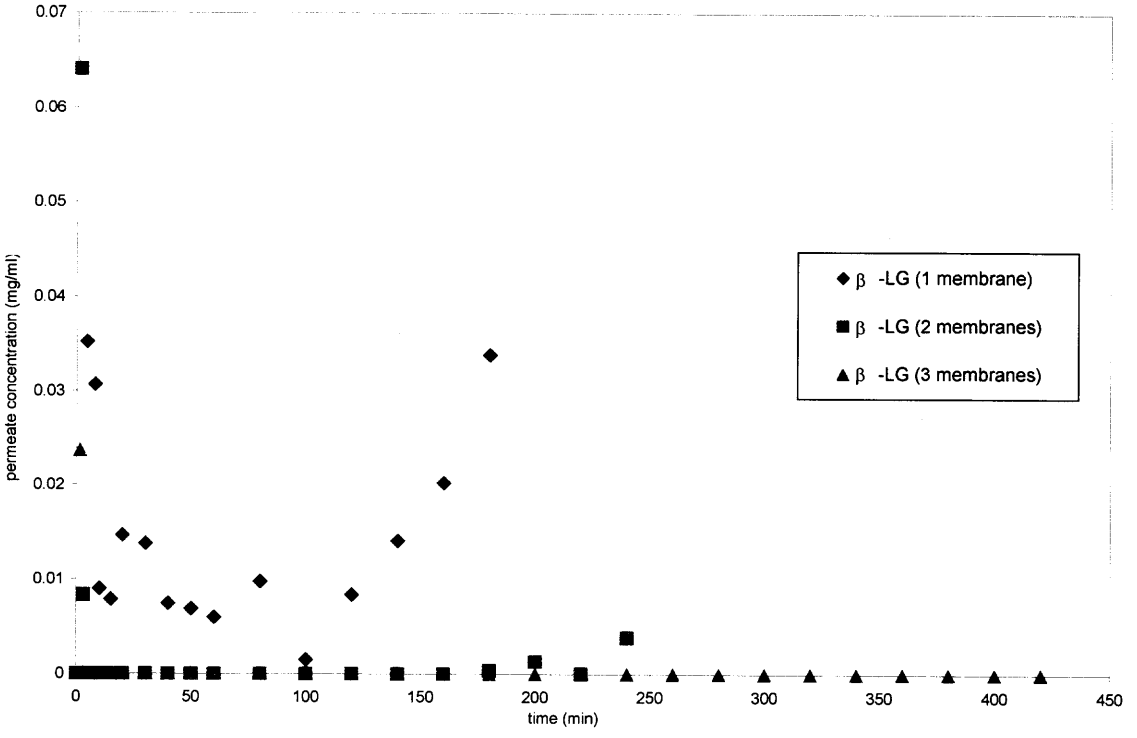

Figure 3.24 Optimized batch ultrafiltration of System 1: 1.0 mg/ml β-lactoglobulin and 0.2 mg/ml myoglobin, pH 7.3, 20 mM tris buffer, 10 psig (only more highly rejected protein, β-LG, shown).

Figure 3.26 shows the selectivity of a single membrane and a 2-membrane composite versus time. The selectivity for the 3-membrane composite is undefined due to complete rejection of β-lactoglobulin and therefore, is not shown. The selectivity increases almost an order of magnitude when a 2-membrane composite is utilized.

The % yield values of myoglobin versus the process time are shown in Table 3.3. The myoglobin yield achieved with three membranes can be increased even further using a longer operating time. The number of diavolumes needed for the three membrane processes are shown in Table 3.3. It is important to note that the 2- membrane composite and the 3-membrane composite require about 1.2-1.7 times the diavolumes required for a

single membrane. This is a minimal amount of buffer volume compared to other purification processes. For example, in HPTFF processes, the number of diavolumes ranged from 80-179 (van Reis, Gadam, Frautschy, Orlando, Goodrich, Saksena, Kuriyel, Simpson, Pearl, and Zydney 1997).

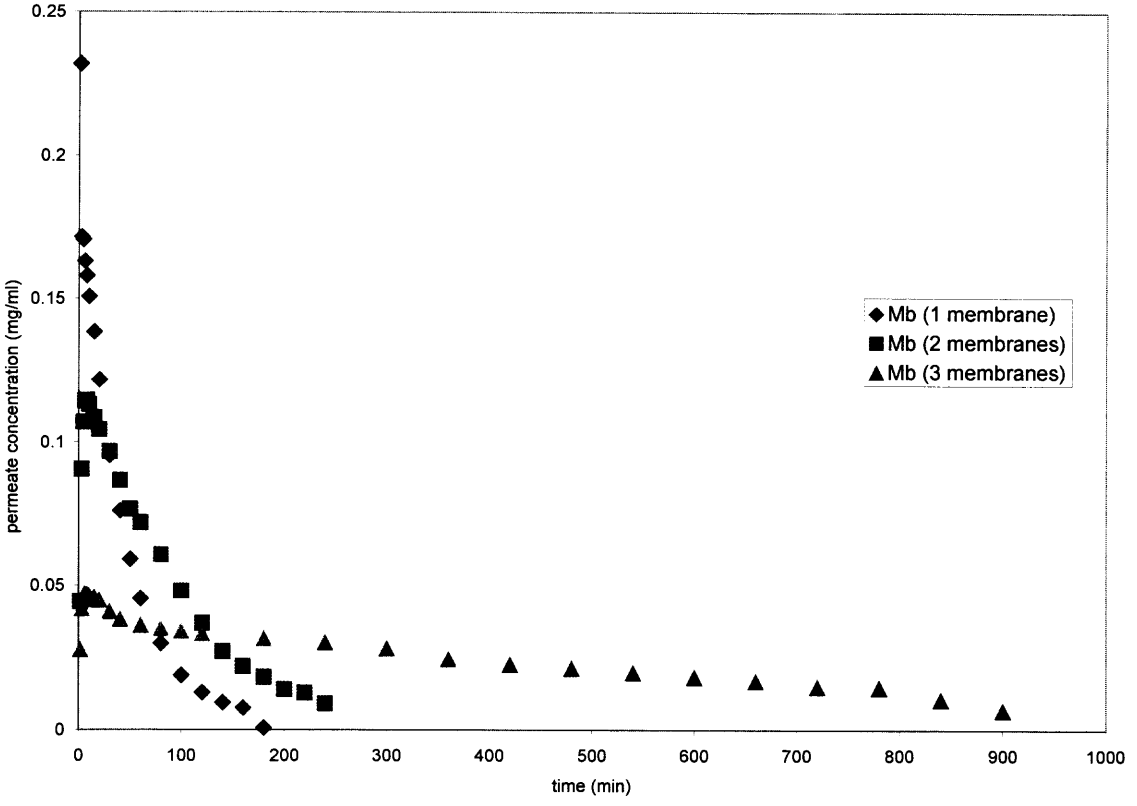

Figure 3.25 Optimized batch ultrafiltration of System 1: 1.0 mg/ml β-lactoglobulin and 0.2 mg/ml myoglobin, pH 7.3, 20 mM tris buffer, 10 psig (only more permeable protein, myoglobin, shown).

Table 3.3 Comparison of % Yield and Number of Diavolumes For a Given Operating Time With the Number of Membranes. Batch Ultrafiltration of System 1 (1.0 mg/ml β-Lactoglobulin and 0.2 mg/ml Myoglobin, pH 7.3, 20 mM Tris Buffer)

	Myoglobin Yield (%)	Number of Diavolumes	Time (minutes)
One membrane (10 psig)	100.00	3.24	100
Two membranes (10 psig)	98.23	4.62	240
Three membranes (10 psig)	80.25	5.36	900

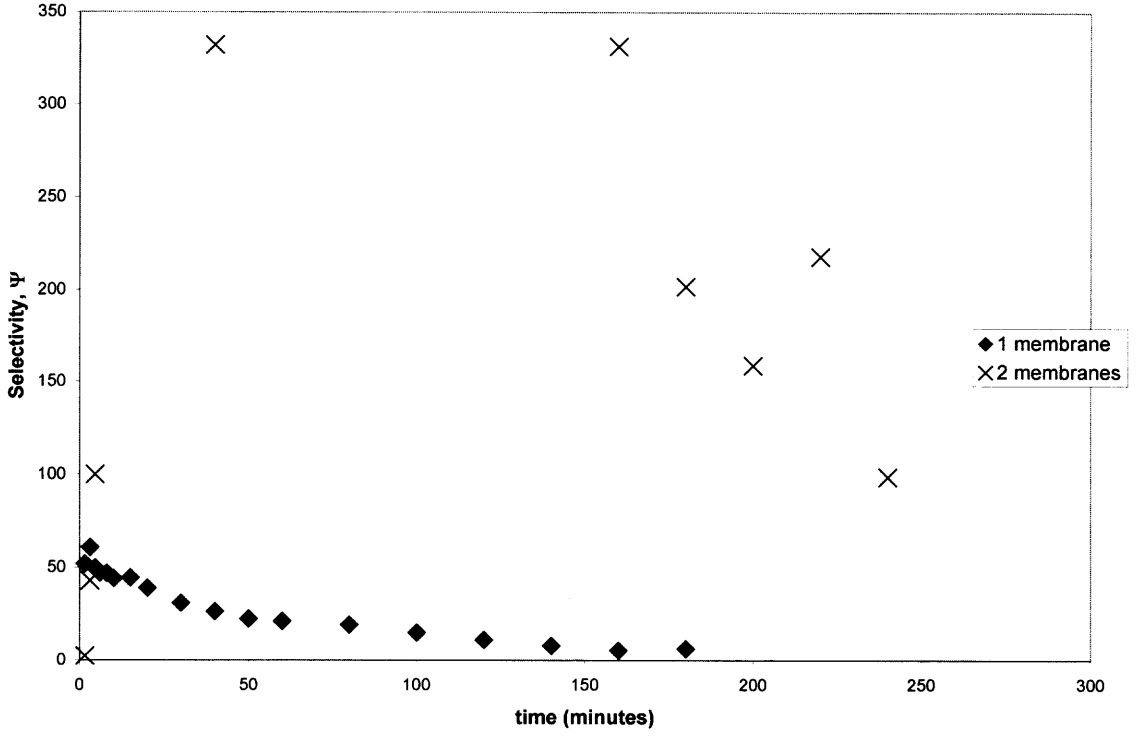

Figure 3.26 Selectivities of System 1 comparing a single membrane and a 2-membrane composite (1.0 mg/ml β-lactoglobulin and 0.2 mg/ml myoglobin, pH 7.3, 20 mM tris buffer, 10 psig).

3.4.1.3 Extended Term Operation under Optimized Conditions. Figure 3.27 illustrates the results for an extended term experiment, which lasted 15 hours. The 3-membrane composite was used at a total operating pressure of 10 psig. After the first 30 minutes, the flux remained constant throughout the whole 15 hours. Also, the rejection of β-lactoglobulin remained at 1.0 (except for the first three minutes), which showed that there was no breakthrough of the rejected protein. This indicates that the 3-membrane composite could be utilized for long periods of time, while still achieving purification.

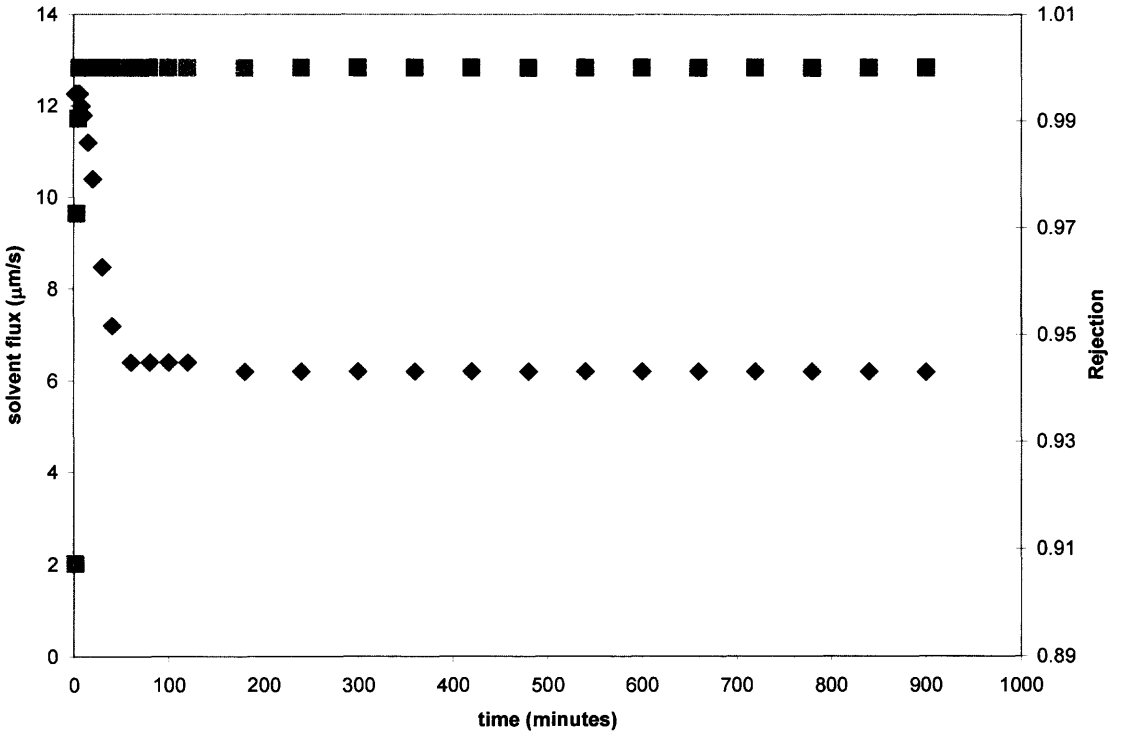

Figure 3.27 Batch ultrafiltration: extended term solvent flux measurements (♦) and rejection (■) of β-lactoglobulin (1.0 mg/ml β-lactoglobulin and 0.2 mg/ml myoglobin, pH 7.3, 20 mM tris buffer, 10 psig, 3 membranes).

3.4.1.4 Optimized Pulse Injection Ultrafiltration. In the pulse injection experiments, a pulse of a concentrated solution was introduced after 15 minutes of buffer-only ultrafiltration. The concentrated pulse was then immediately mixed with the buffer and resulted in final solute concentrations of 1 mg/ml β-LG and 0.2 mg/ml Mb. The buffer was optimized at pH 7.3; the operating pressure was 10 psig. 20 mM Tris buffer was used. Myoglobin (pI 7.3), had no net charge at pH 7.3 and β-lactoglobulin (pI is 5.3), was negatively charged. Also, the YM30 regenerated cellulose membrane carried a slight negative charge. Therefore, by operating at pH.7.3, the physicochemical properties were utilized for high selectivity. Initially, a 50 ml pulse injection was used. However, the injection time was too long, which resulted in an unknown initial feed concentration. Next, a 15 ml pulse was used. This injection time was also too long and resulted in an unknown initial feed concentration. Finally, a smaller pulse volume of 5 ml was chosen and employed for the experiments.

The results for a 5 ml pulse are shown in Figure 3.28. As the number of membranes was increased, the permeate concentration of the unwanted protein decreased. It is shown that using three membranes led to complete rejection of β-lactoglobulin, resulting in a pure permeate. Myoglobin profiles are similar to those shown in Figure 3.25 due to same operating conditions.

Pulse experiments are useful when there is a small amount of valuable sample available. Also buffer conditions are controlled independently of the feed solution, which allows one to operate at optimized conditions by just adjusting the buffer.

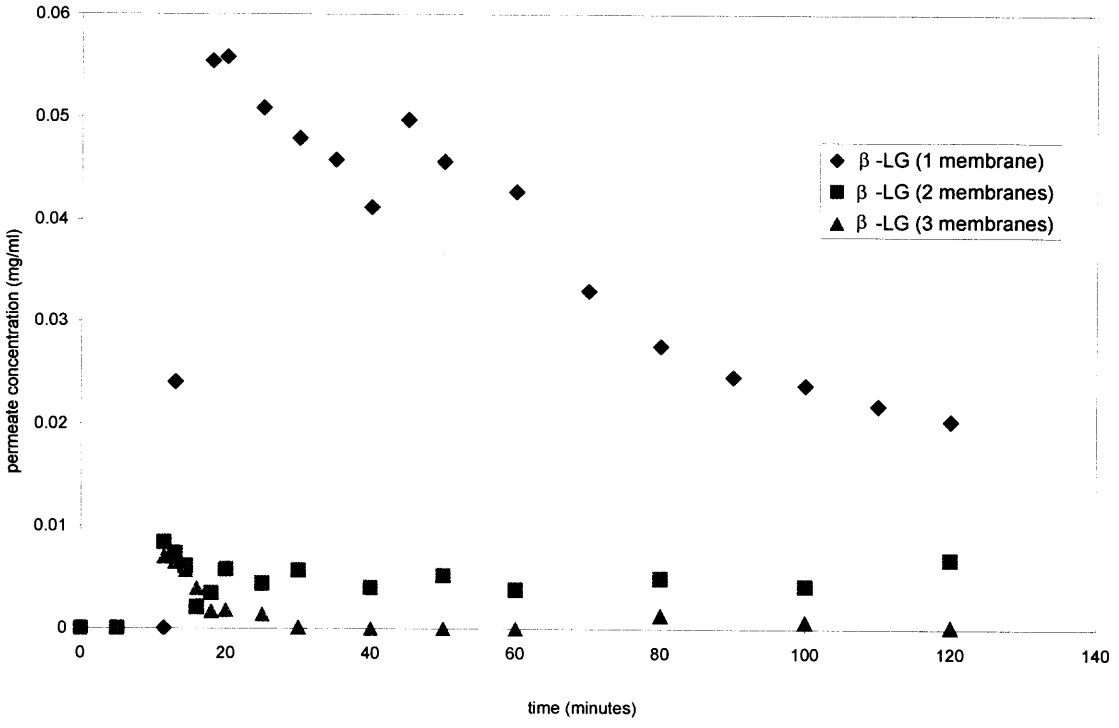

Figure 3.28 Optimized pulse injection ultrafiltration: 1.0 mg/ml β-lactoglobulin and 0.2 mg/ml myoglobin, 5 ml pulse, pH 7.3, 20 mM Tris buffer, 10 psig (only more highly rejected protein, β-LG, shown).

3.4.1.5 Continuous Feed Flow Ultrafiltration. Continuous feed flow-based ultrafiltration experimental results spanning 300 minutes are shown in Figure 3.29. Three membranes were used at a total operating pressure of 10 psig. In these experiments, feed solution (1.0 mg/ml β-lactoglobulin and 0.2 mg/ml myoglobin in pH 7.3, 20 mM Tris buffer) was used as the diluent into the stirred cell instead of pure buffer. The results from these experiments show that although the concentration in the retentate was increasing, unlike batch ultrafiltration experiments in diafiltration mode, the rejection of β-lactoglobulin remained constant at 1.0. Also, unlike batch ultrafiltration experiments in the diafiltration mode where the concentration of myoglobin in the retentate was being

depleted, the rejection of myoglobin remained constant (after initial unsteadiness) at approximately 0.7.

The flux data shown in Figure 3.29 show a slight decline, 30.1%. This was caused by the increased wall concentration due to the increasing concentration in the retentate of both proteins. Even though the wall concentration was increasing, there was no breakthrough of β-lactoglobulin in the permeate. This meant that the multimembrane composite may potentially withstand increasing concentration and still maintain the objective of complete rejection, without breakthrough.

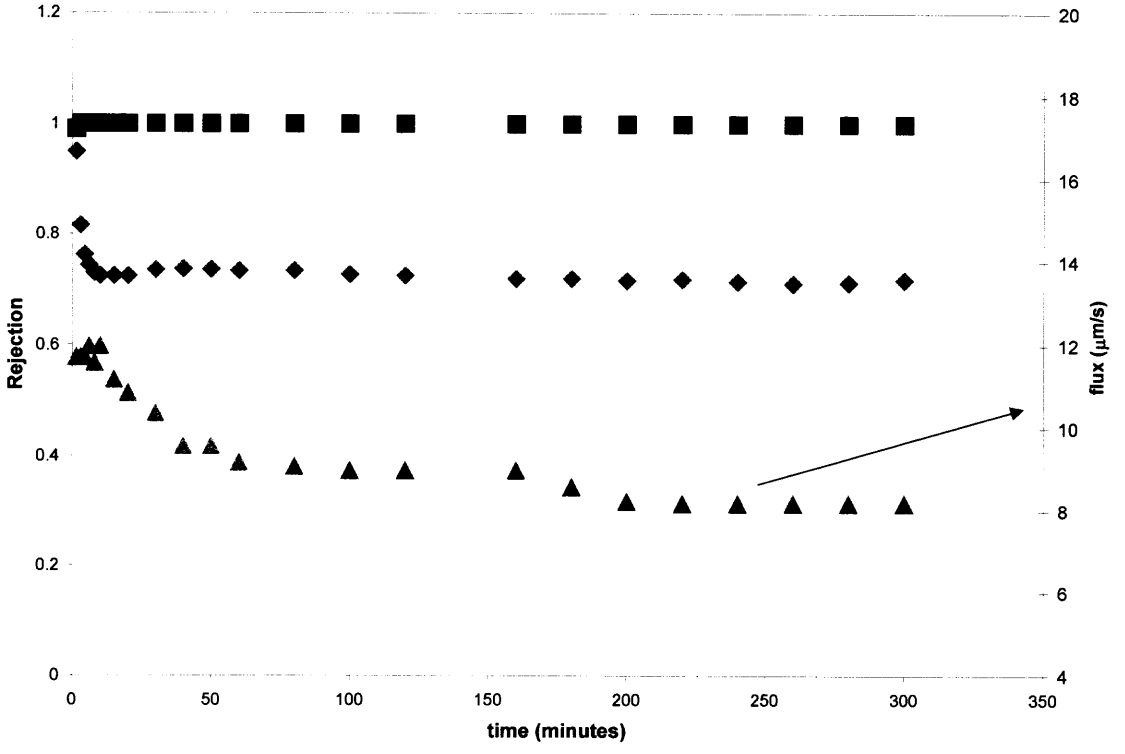

Figure 3.29 Continuous feed flow ultrafiltration studies: flux (▲), rejection of β-lactoglobulin (■), and rejection of myoglobin (◆) (1.0 mg/ml β-lactoglobulin and 0.2 mg/ml myoglobin, pH 7.3, 20 mM tris buffer, 10 psig, 3 membranes).

3.4.1.6 Higher Pressure Ultrafiltration. Higher pressure ultrafiltration was performed to increase the flux that is reduced with the addition of each membrane in the multimembrane composite. In this experiment, the operating pressure was 30 psig. A 3-membrane composite was utilized. Therefore, each membrane was exposed to approximately 10 psig.

Figure 3.30 shows the permeate concentration profiles for the higher pressure experiment. There was complete purification of myoglobin from the mixture in the permeate at this higher pressure, with the rejection of β-lactoglobulin remaining constant at 1.0 due to the zero concentration of β-lactoglobulin in the permeate. The flux profiles for this experiment compared to 10 psig (described in section 3.4.1.2) are shown in Figure 3.31. As the pressure was tripled, the flux was increased by a factor of three. The flux loss when operating at the higher pressure of 30 psig was approximately the same (~32%) as when operating at 10 psig. This meant that the effect of fouling / concentration polarization was negligible. The % yield of myoglobin at 30 psig was 84.00% in 180 minutes. This was comparable to the % yield of myoglobin for a 3-membrane composite at 10 psig, 80.25% in 900 minutes (shown in Table 3.3). The number of diavolumes was 3.98, which was much less than that for the 3-membrane composite at 10 psig (shown in Table 3.3). Therefore, large buffer volumes can be avoided.

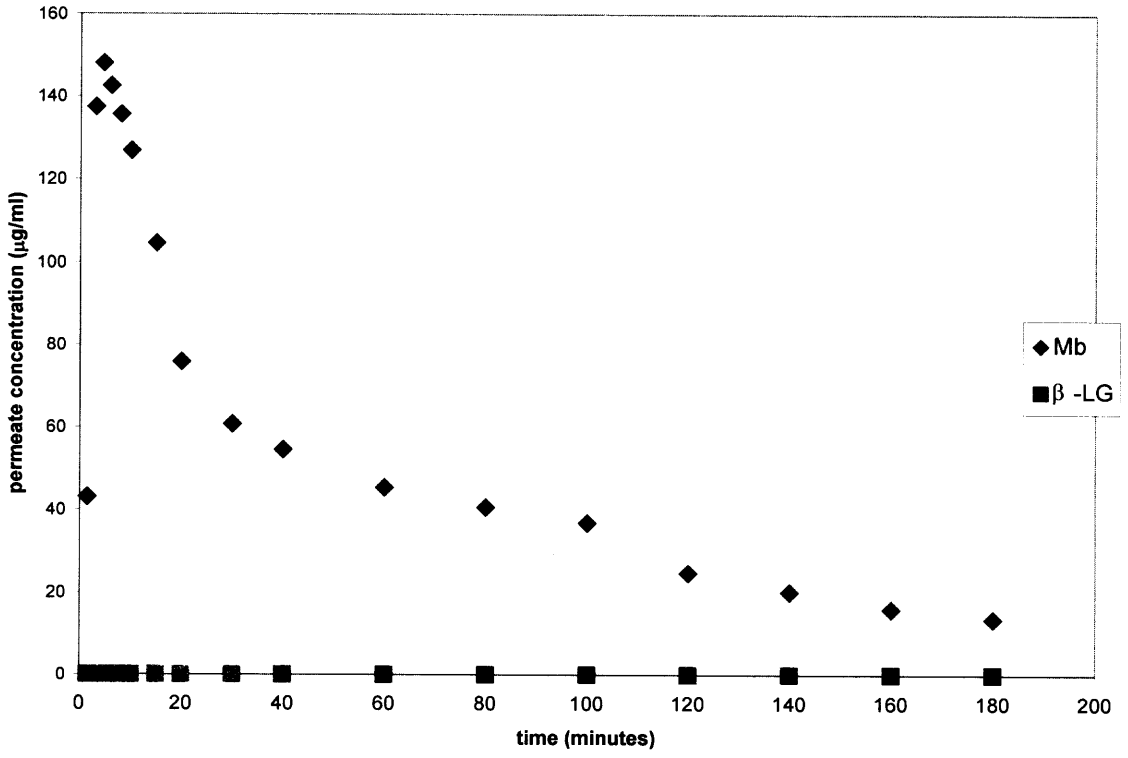

Figure 3.30 Optimized batch ultrafiltration at higher pressure: 1.0 mg/ml β-lactoglobulin and 0.2 mg/ml myoglobin, pH 7.3, 20 mM tris buffer, 30 psig.

3.4.1.7 Different Feed Concentrations. Optimized ultrafiltration was performed with different feed concentrations. In these experiments, the feed concentrations were 0.5 mg/ml β-lactoglobulin and 0.5 mg/ml myoglobin. The data from one membrane were compared with those from a 2-membrane and a 3-membrane composite. The total operating pressure for all experiments was 10 psig.

The results for the permeate concentration profile of β-lactoglobulin are shown in Figure 3.32. Both the 2-membrane and the 3-membrane composite achieved complete rejection. There was less of an effect of concentration polarization, i.e., a smaller wall concentration, due to the lower concentration of β-lactoglobulin in the feed solution. The

2-membrane composite achieved complete rejection (zero permeate concentration) of β-LG unlike earlier observations (Subsection 3.4.1.2) where a 3-membrane composite was needed to achieve complete rejection. The permeate concentration profile of β-LG for one membrane was not steady; this could have been due to variable conditions caused by concentration polarization and / or fouling due to the high concentration of feed.

Figure 3.33 illustrates the concentration profiles of myoglobin for the three cases; they follow the same trend observed earlier with different concentrations as shown in Figure 3.25.

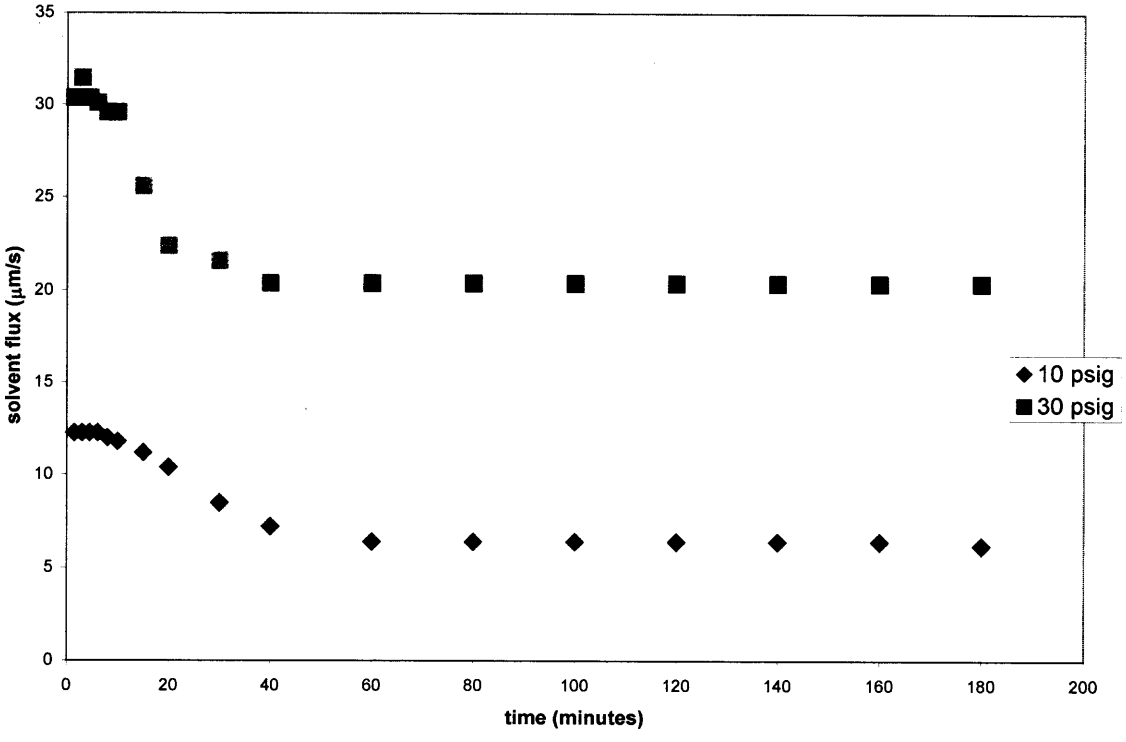

Figure 3.31 Batch ultrafiltration flux measurements at two different pressures for System 1 (1.0 mg/ml β-lactoglobulin and 0.2 mg/ml myoglobin, pH 7.3, 20 mM tris buffer, 3 membranes).

3.4.1.8 Cyclic Experiments. A cyclic experiment was performed to show that the membrane composite can be cleaned in situ and the ultrafiltration behavior of the proteins observed with fresh membranes can be reproduced with the cleaned membranes. Ultrafiltration was performed with 3 membranes at 30 psig, the *in situ* cleaning procedure was implemented, and then ultrafiltration was repeated. The results are shown in Figure 3.34. This means that the membrane composite can be restored to its original performance level without disassembling the apparatus. They can also be used repeatedly, which is cost effective.

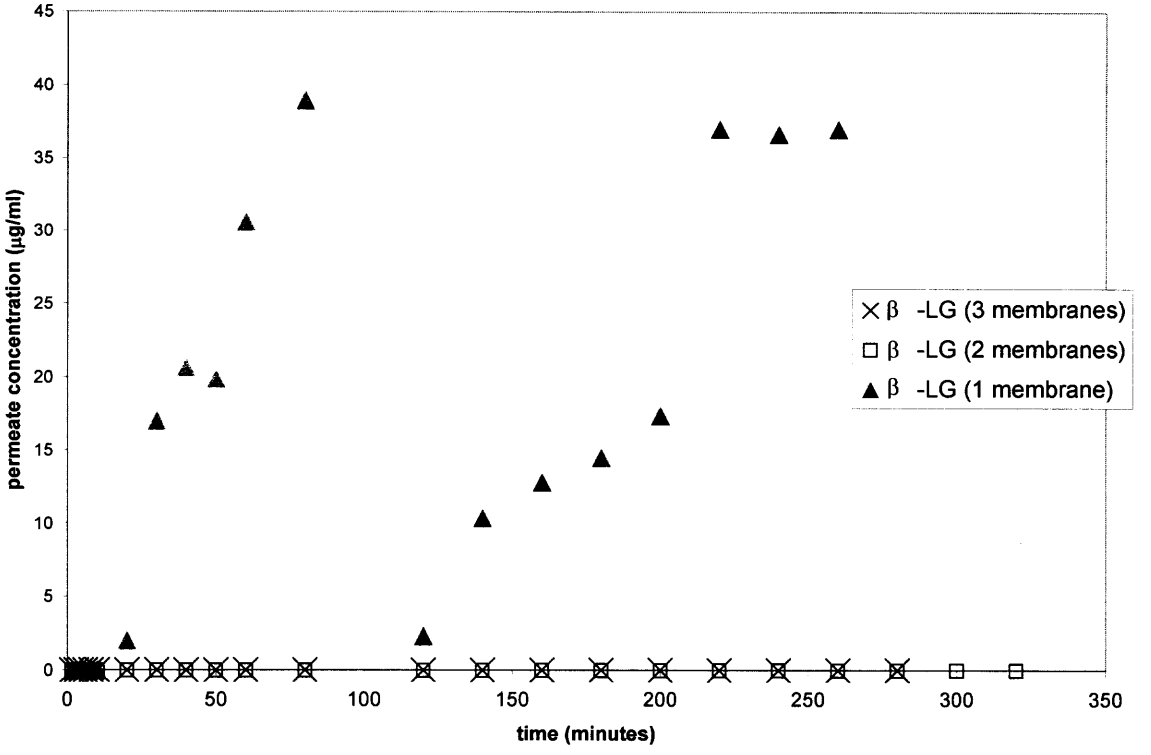

Figure 3.32 Optimized batch ultrafiltration of System 1: 0.5 mg/ml β-lactoglobulin and 0.5 mg/ml myoglobin, pH 7.3, 20 mM tris buffer, 10 psig (only more highly rejected protein, β-LG, shown).

3.4.2 System 2

System 2 consisted of a binary mixture of 0.2 mg/ml α-lactalbumin and 0.2 mg/ml myoglobin (molecular weight ratio 1.22). This was the second system studied and was considered a follow-up to system 1 utilizing the same membrane with smaller molecular weight ratio between the two proteins. The goal of studying this system was to illustrate an application to another binary system that demonstrated rejection amplification with a multimembrane composite. Multimembrane experiments performed under optimized conditions (pH=pI) and higher pressure experiments, will be discussed in this section. All experiments were performed using YM30 regenerated cellulose membranes.

3.4.2.1 Optimized Batch Ultrafiltration. The separation of α-lactalbumin and myoglobin at pH 4.35 was performed at 10 psig (Figures 3.35 and 3.36). 20 mM citric acid buffer at pH 4.35 was used. α-lactalbumin, whose pI is 4.35, had no net charge at pH 4.35 and myoglobin, whose pI is 7.3, was positively charged. Also, the YM30 regenerated cellulose membrane carries a very slight negative charge (according to manufacturer). Therefore, by operating at a pH of 4.35, the physicochemical properties were considered optimized. Because high selectivity was achieved at 20 mM ionic strength, lower ionic strength experiments were not conducted.

Figure 3.35 shows the permeate concentration profile of myoglobin, the more highly rejected protein. As the number of membranes was increased, the concentration of myoglobin in the permeate stream was decreased. With the 3-membrane composite, after 6 minutes, the concentration of myoglobin in the permeate was zero; the rejection was equal to 1.0. Therefore when the 3-membrane composite was utilized, sufficient rejection amplification was observed.

Figure 3.36 shows the permeate concentration profile of α-lactalbumin, the more permeable protein. As expected due to the flux decline encountered with the addition of each membrane, the concentration of α-lactalbumin in the permeate was less. Also, due to the rejection amplification expected with this protein as well, the concentration profile in the permeate was significantly decreased. The % yields for all α-LA for one membrane, a 2-membrane composite and a 3- membrane composite were respectively: 22.67, 31.44, and 13.57. Longer operation time would have led to improved yield.

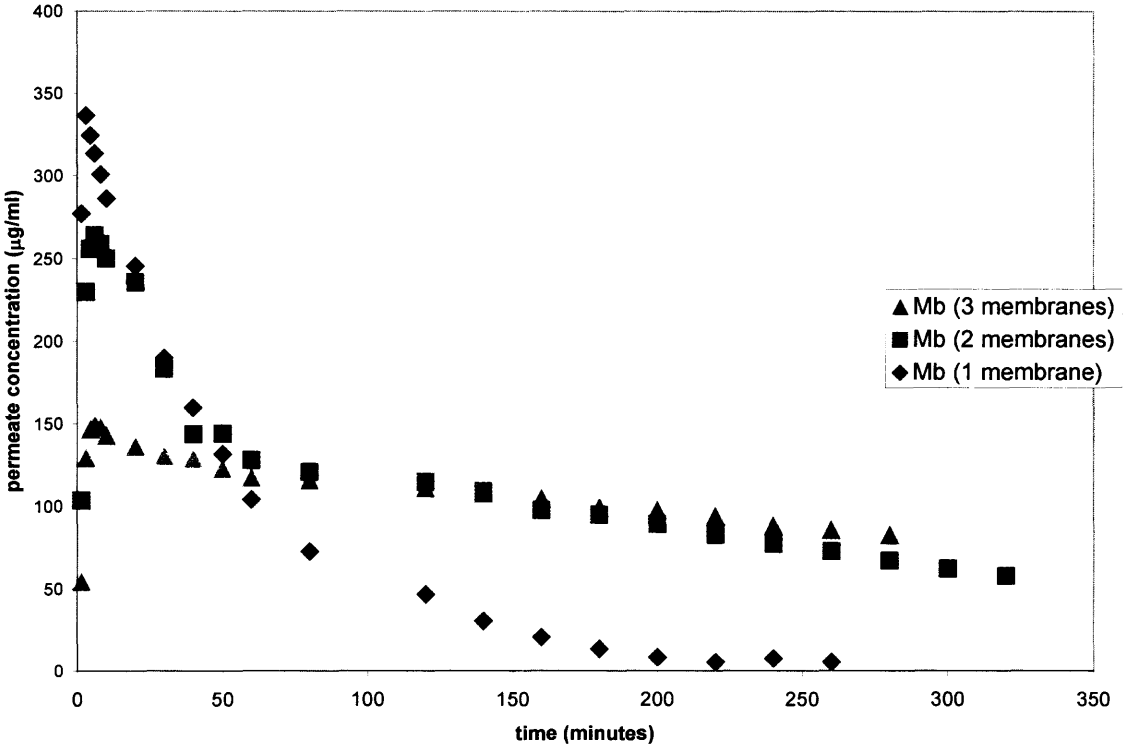

Figure 3.33 Optimized batch ultrafiltration of System 1: 0.5 mg/ml β-lactoglobulin and 0.5 mg/ml myoglobin, pH 7.3, 20 mM tris buffer, 10 psig (only more permeable protein, myoglobin, shown).

Figure 3.37 shows the selectivity of a single membrane and a 2-membrane composite versus time. The selectivity for the 3-membrane composite is undefined due to complete rejection of myoglobin and therefore, is not shown. The increase in selectivity was significant when the 2-membrane composite was used compared to the single membrane selectivity data.

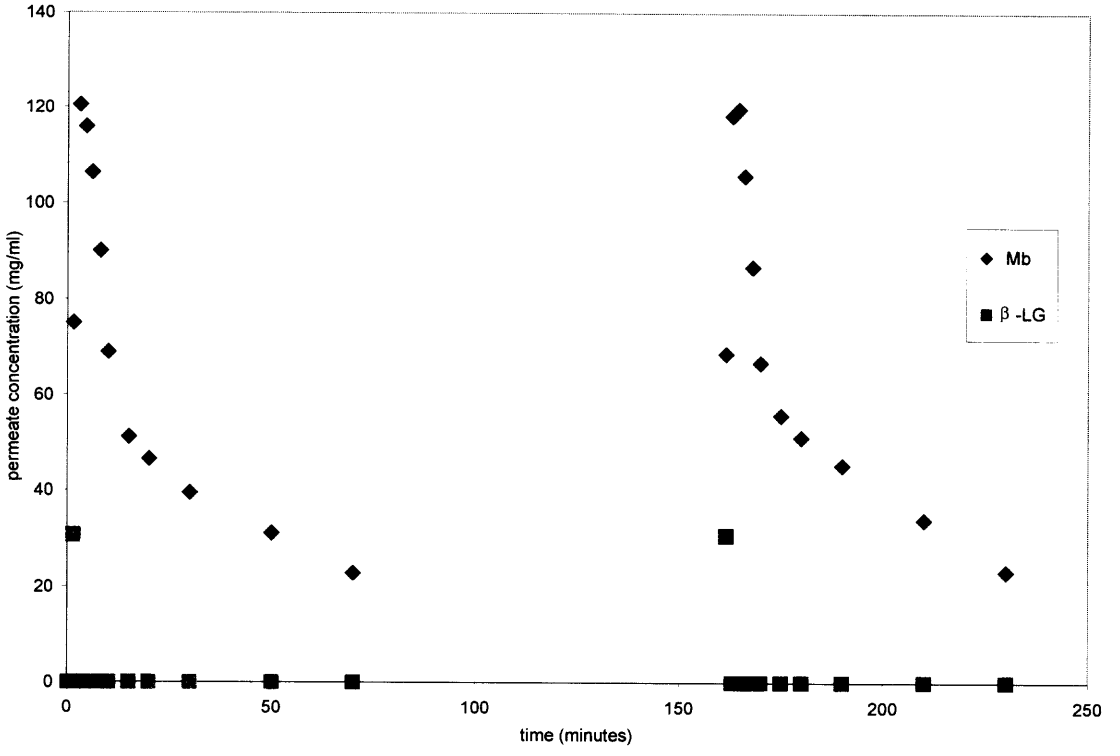

Figure 3.34 Permeate concentration profiles comparing batch ultrafiltration before and after cleaning *in situ* (1.0 ml β-lactoglobulin and 0.2 mg/ml myoglobin, pH 7.3, 20 mM tris buffer, 30 psig, 3 membranes).

3.4.2.2 Higher Pressure Ultrafiltration. Higher pressure ultrafiltration was carried out to compensate for the flux that was lost with the addition of each membrane in the multimembrane composite. In this experiment, the operating pressure was 30 psig. A 3-

membrane composite was utilized. Therefore, each membrane was exposed to approximately a 10 psig pressure differential.

The results for the higher pressure experiment were poor. Flux decline was very pronounced (Figure 3.38). At 30 psig, the flux loss was 76.0 % and never reached a steady level. This is due to a high amount of fouling at this higher pressure because of the similar size molecular weights of the proteins. From these results, it was concluded that operation of this system at higher pressures to overcome the flux loss was not practical (unlike System1). Therefore, it is necessary to investigate each system in detail before expecting each of them to perform like System 1.

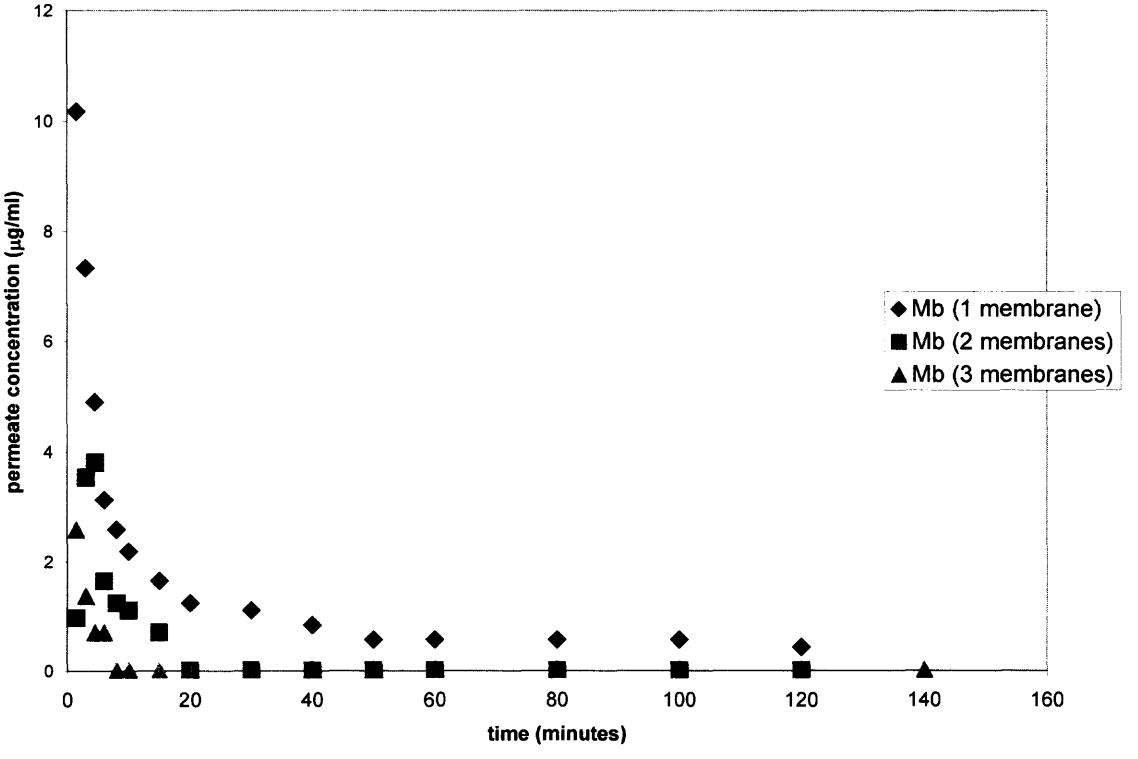

Figure 3.35 Optimized batch ultrafiltration of System 2: 0.2 mg/ml α-lactalbumin and 0.2 mg/ml myoglobin, pH 4.35, 20 mM citric acid buffer, 10 psig (only more highly rejected protein, Mb, shown).

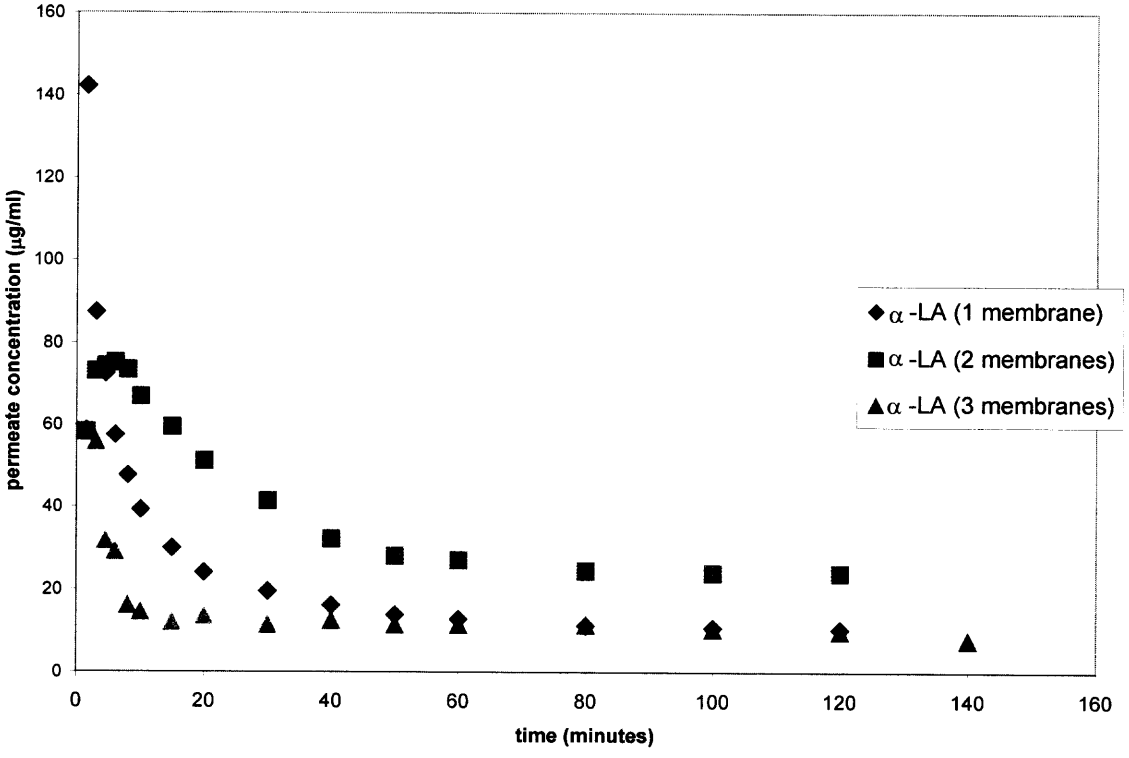

Figure 3.36 Optimized batch ultrafiltration of System 2: 0.2 mg/ml α-lactalbumin and 0.2 mg/ml myoglobin, pH 4.35, 20 mM citric acid buffer, 10 psig (only more permeable protein, α-LA, shown).

3.4.3 System 3

System 3, consisting of a binary mixture of bovine serum albumin and hemoglobin (molecular weight ratio 1.03), was explored to investigate larger molecular weight cutoff membranes, larger molecular weight / size proteins, as well as a system having a lower molecular weight ratio (1.03). For this, Omega 100K polyethersulfone membranes and YM100 regenerated cellulose membranes were investigated; in all experiments, feed concentrations of 1.0 mg/ml bovine serum albumin and 0.2 mg/ml hemoglobin in sodium phosphate buffer pH 6.8 were utilized. Due to the smaller molecular weight ratio, buffer

optimized conditions were chosen for the experiments to exploit the charge interactions and achieve better separation. Initial investigations using the Omega 100K membrane (first presented in Section 3.3.3) were successfully conducted by operating at the pI of hemoglobin, pH 6.8 and at a low ionic strength of 2.3 mM; therefore those conditions were adopted as the operating conditions for the multimembrane stack.

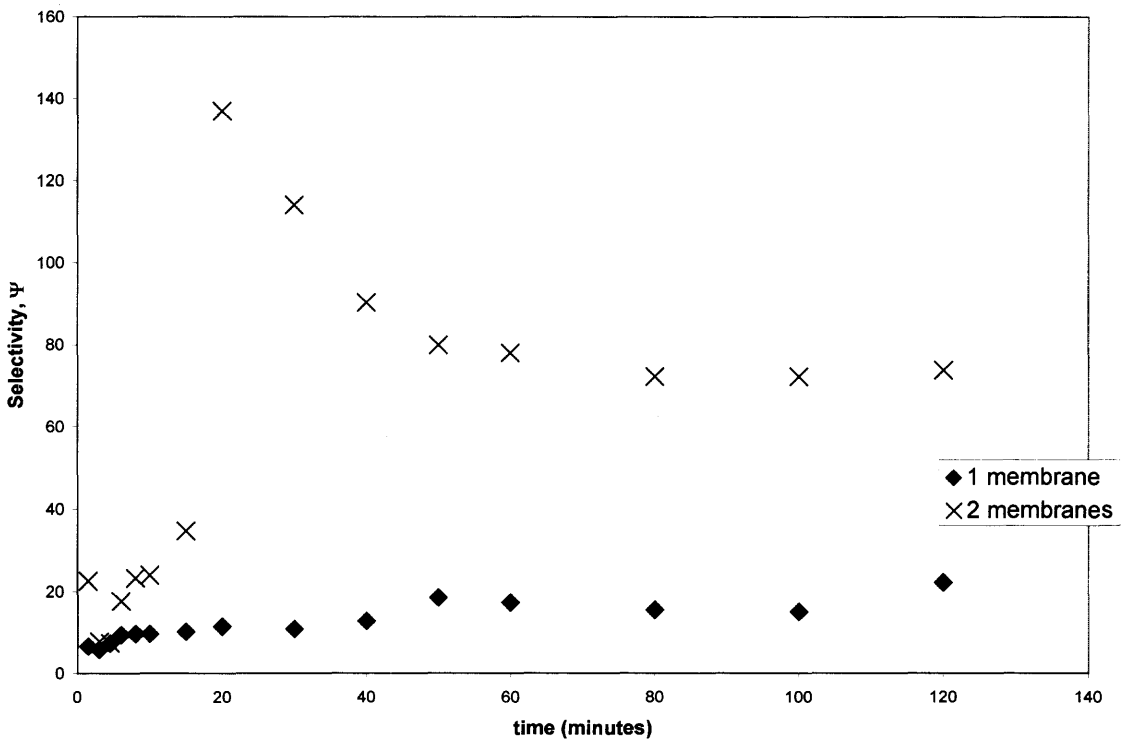

Figure 3.37 Selectivities of System 2 comparing a single membrane and a 2-membrane composite (0.2 mg/ml α-lactalbumin and 0.2 mg/ml myoglobin, pH 4.35, 20 mM citric acid buffer, 10 psig).

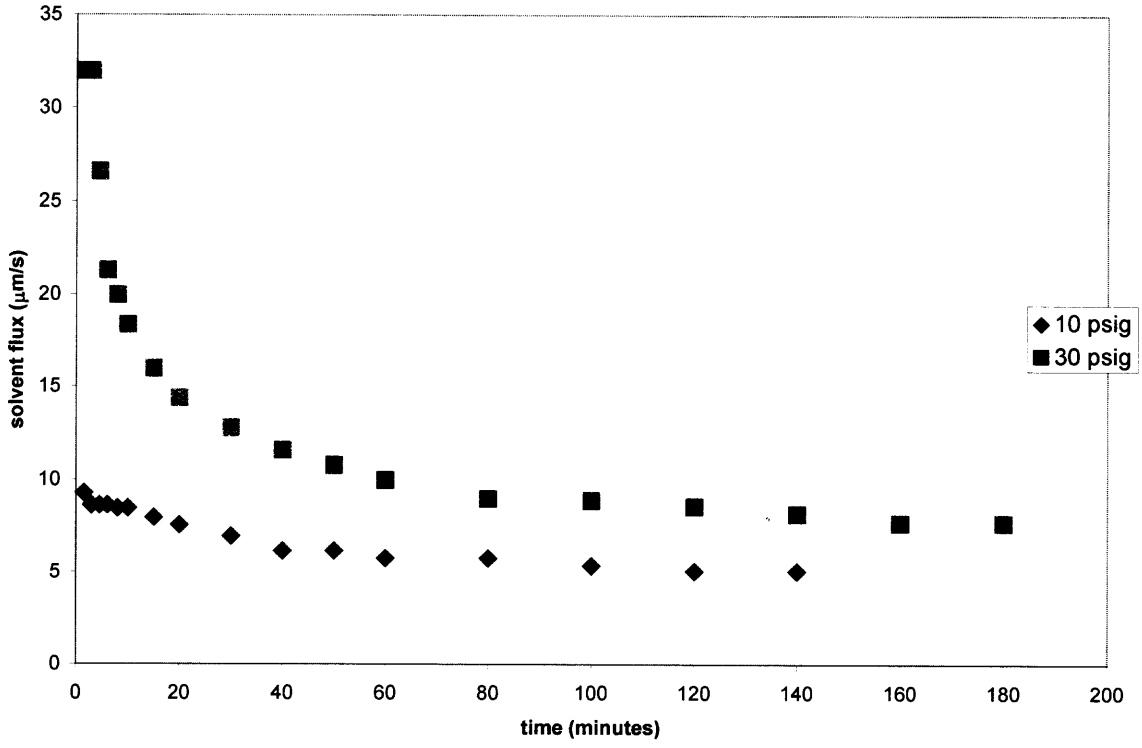

Figure 3.38 Batch ultrafiltration flux measurements at two different pressures for System 2: (0.2 mg/ml α-lactalbumin and 0.2 mg/ml myoglobin, pH 4.35, 20 mM citric acid buffer, 3 membranes).

3.4.3.1 Optimized Batch Ultrafiltration with Omega 100K Membrane. Theseparation of hemoglobin and bovine serum albumin under the operating buffer conditions of 2.3 mM, pH 6.8 was performed at 1.5, 3, and 4.5 psig using an Omega 100K polyethersulfone membrane. The time-dependent permeate concentration profiles of the more permeable protein, hemoglobin, are shown in Figure 3.39 for each additional membrane that was added. Figure 3.40 shows the corresponding data for BSA. It is shown that when 3 membranes were stacked together, it was possible to achieve essentially complete rejection of bovine serum albumin from the feed mixture, resulting in a permeate that contained hemoglobin only. These results, for this particular system,

show that when low ionic strength and pH=pI of the protein of interest were maintained, complete fractionation was achieved with this technique and this particular membrane. The bovine serum albumin concentration in the permeate was zero after 10 minutes. Amplification of a single membrane's rejection by a multimembrane composite was successful with the larger molecular weight cutoff membranes. The % yields of hemoglobin obtained in these experiments are shown in Table 3.4. Longer time for the 3-membrane system would have led to almost complete hemoglobin recovery.

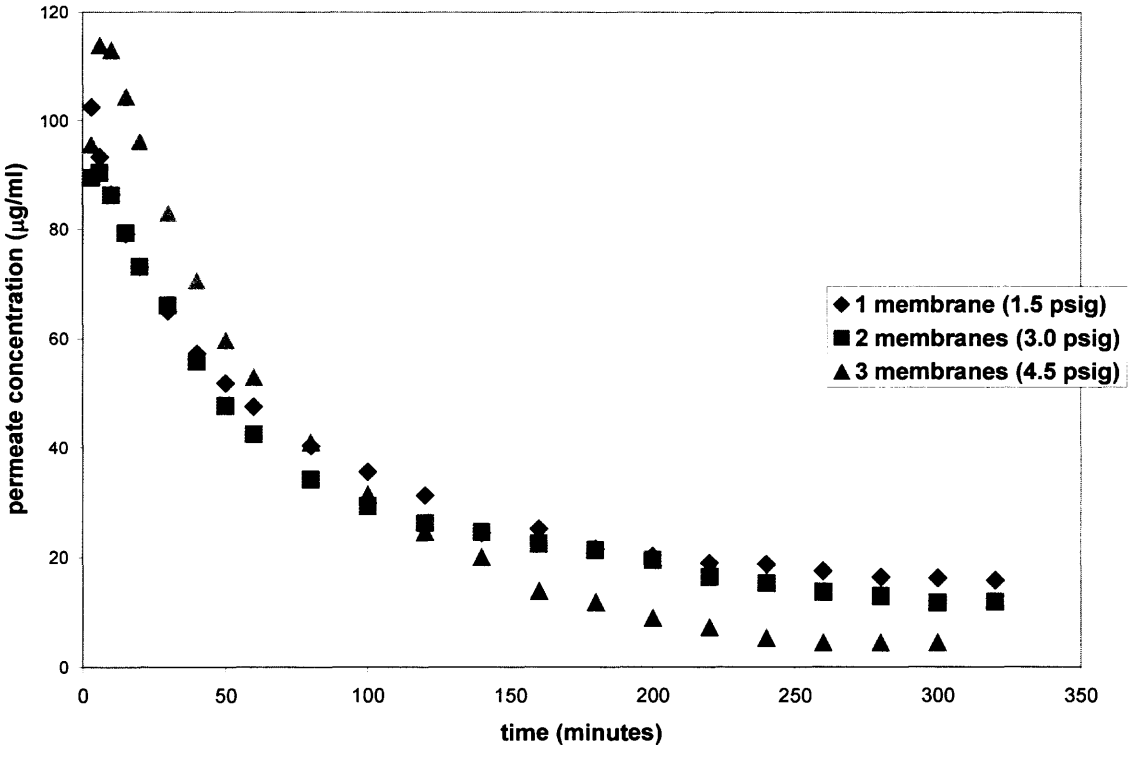

Figure 3.39 Optimized batch ultrafiltration of System 3: 1.0 mg/ml bovine serum albumin and 0.2 mg/ml hemoglobin, pH 6.8, 2.3 mM sodium phosphate buffer; Omega 100K membranes, 1.5, 3, and 4.5 psig (only permeated protein, hemoglobin, shown).

Table 3.4 shows the number of diavolumes needed versus process time. The 2-membrane composite and the 3-membrane composite require about 1.3-1.4 times the diavolumes required for a single membrane for a similar yield of hemoglobin. This is a minimal amount of buffer volume compared to other purification processes (i.e. HPTFF).

Table 3.4 Comparison of % Yield For a Given Operating Time With the Number of Membranes. Batch Ultrafiltration of System 3 (1.0 mg/ml Bovine Serum Albumin and 0.2 mg/ml Hemoglobin, pH 6.8, 2.3mM Sodium Phosphate Buffer)

	Hemoglobin Yield (%)	Number of Diavolumes	Time (minutes)
One membrane (1.5 psig)	55.44	3.16	300
Two membranes (3.0 psig)	50.92	3.41	300
Three membranes (4.5 psig)	60.60	4.45	300

By operating at increasing pressure with each additional membrane, the flux loss was also recovered. The flux profiles observed during the above described conditions are shown in Figure 3.41. This figure illustrates that the system operated at steady flux, (disregarding the first 10-15 minutes due to system equilibration). It is also important to note that when operating at 4.5 psig, there is increased evidence of flux decline due to increased concentration polarization. However, one can still overcome the overall loss of flux that was encountered with a 3-membrane composite by raising the pressure. After 5 hours of operation, it is also important to note that there was no breakthrough of the unwanted protein (BSA).

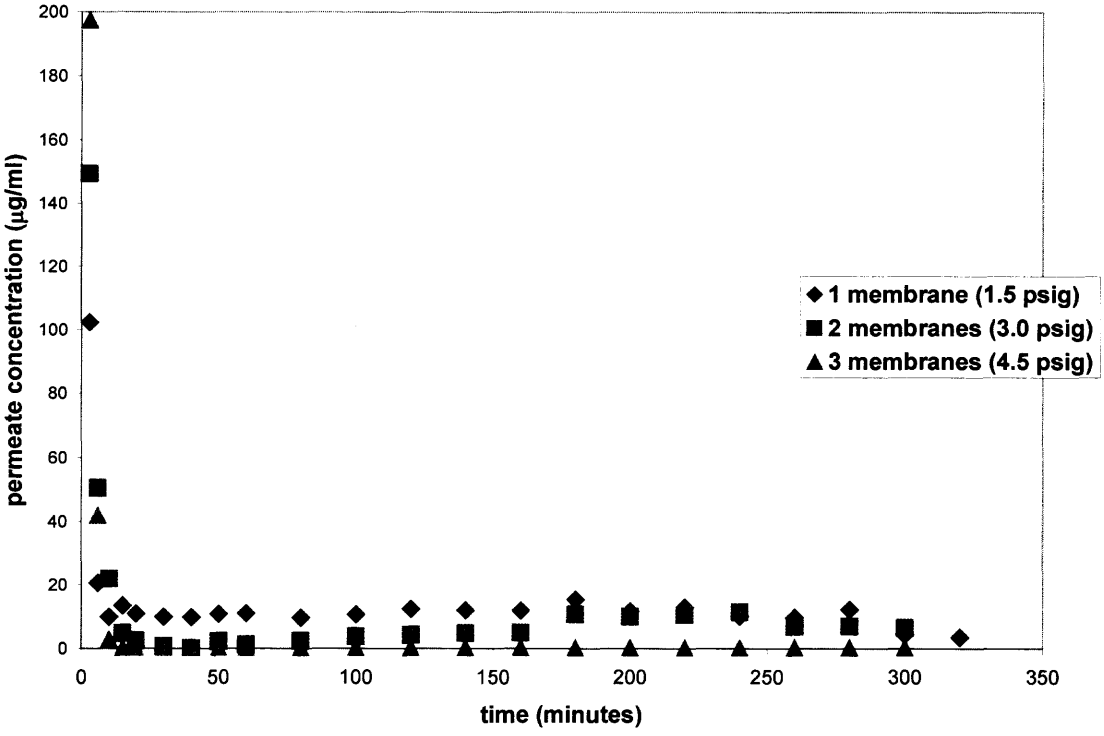

Figure 3.40 Optimized batch ultrafiltration of System 3: 1.0 mg/ml bovine serum albumin and 0.2 mg/ml hemoglobin, pH 6.8, 2.3 mM sodium phosphate buffer; Omega 100K membranes, 1.5, 3, and 4.5 psig (only more highly rejected protein, bovine serum albumin, shown).

Figure 3.42 shows the selectivities for a single membrane and a 2-membrane composite. When a 2-membrane composite was utilized, the selectivities increased significantly. Due to complete rejection of BSA with the 3-membrane composite, the values for selectivity were undefined. There is a significant increase in selectivity when the 2-membrane composite was utilized.

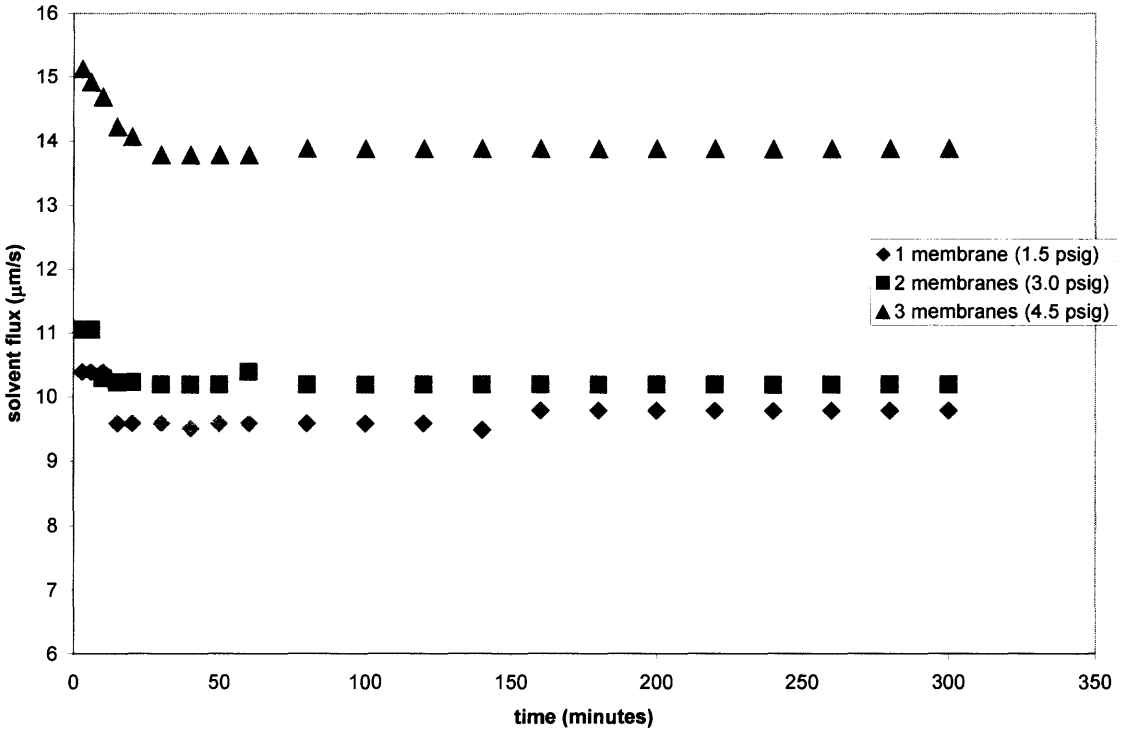

Figure 3.41 Batch ultrafiltration: solvent flux measurements of 1, 2- and 3-membrane composites at three different pressures (1.0 mg/ml bovine serum albumin and 0.2 mg/ml hemoglobin, pH 6.8, 2.3 mM sodium phosphate buffer; Omega 100K membranes, 1.5, 3, and 4.5 psig).

When the membranes were analyzed after completion of ultrafiltration prior to cleaning, a significant amount of protein was seen on the Omega 100K membranes. The more rejected protein (bovine serum albumin) concentration was, ranging from as high as 582 μg/ml for the top membrane to 333 μg/ml for the bottom membrane. Less than 25.0 μg/ml of the more permeable protein (hemoglobin) was found in all cases.

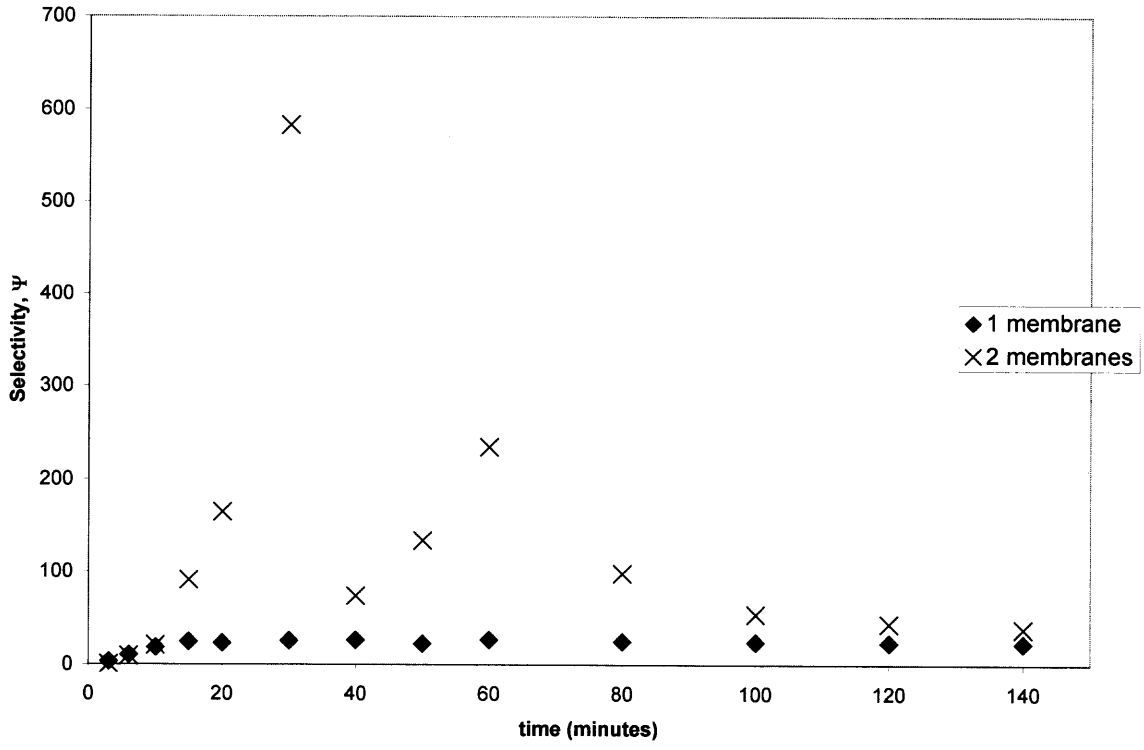

Figure 3.42 Selectivities of Omega 100K ultrafiltration membranes comparing a single membrane and a 2-membrane composite (1.0 mg/ml bovine serum albumin and 0.2 mg/ml hemoglobin, pH 6.8, 2.3 mM sodium phosphate buffer; 1.5 psig and 3.0 psig).

3.4.3.2 Different Feed Concentrations. Optimized ultrafiltration was performed with different feed concentrations. In these experiments, the feed concentrations were 0.5 mg/ml BSA and 0.5 mg/ml hemoglobin. The data from one membrane were compared with those from a 2-membrane and a 3-membrane composite. The total operating pressures for 1 membrane, a 2-membrane composite, and a 3-membrane composite were respectively, 1.5, 3.0, and 4.5 psig. Optimized conditions were utilized, pH 6.8 sodium phosphate buffer at 2.3 mM ionic strength. Figure 3.43 shows the concentration profiles of hemoglobin for the three membrane arrangements.

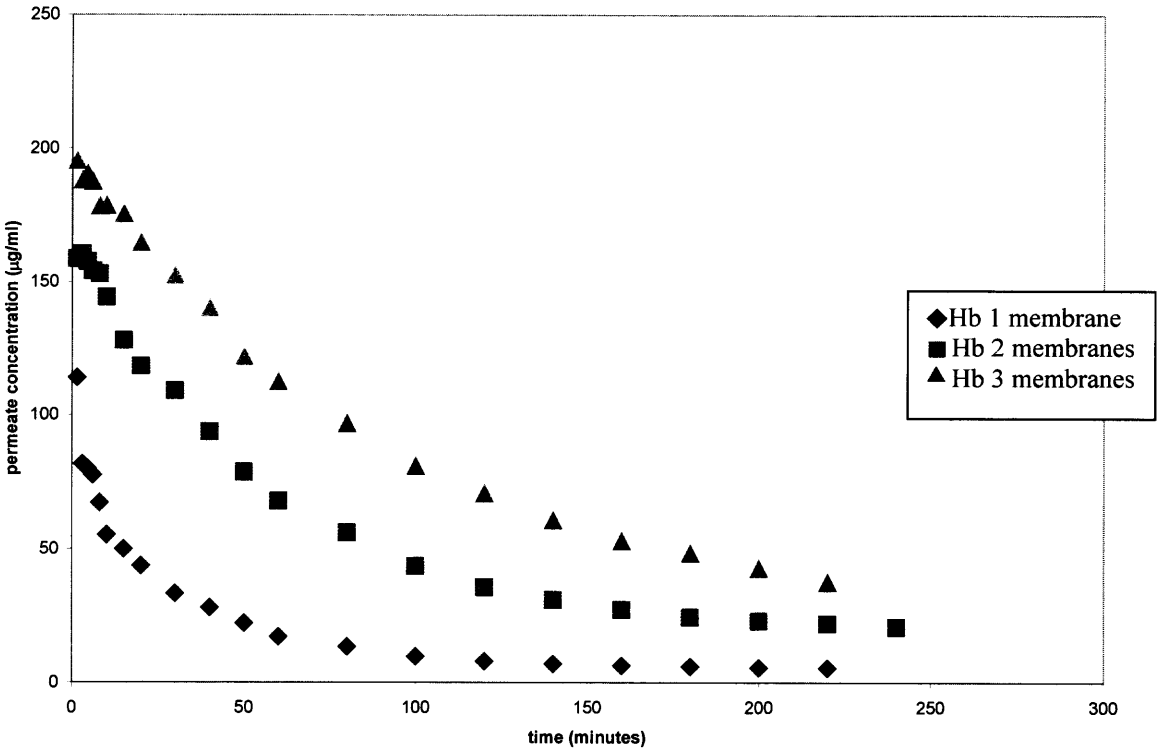

Figure 3.43 Optimized batch ultrafiltration: 0.5 mg/ml bovine serum albumin and 0.5 mg/ml hemoglobin, pH 6.8, 2.3 mM sodium phosphate buffer; Omega 100K membranes, 1.5, 3, and 4.5 psig (only permeated protein, hemoglobin, shown).

Figure 3.43 illustrates the effect of concentration polarization due to the increased feed concentration of the more permeable protein, hemoglobin (compare Figure 3.39). It is important to note that in the experiments performed on System 3, the pressure was increased with the addition of membranes in the multimembrane stack (as discussed in Subsection 3.4.3.1). Therefore, when the pressure was increased along with the increased wall concentration, the transport was enhanced. Due to the low fluxes, compared to the System 1 experiments at the same feed concentrations discussed in Subection 3.4.1.7, the diffusional contribution is greater.

The permeate concentration profiles of BSA are shown in Figure 3.44. When a 3-membrane composite was utilized, complete rejection was observed. However, the experimental results show a higher concentration of BSA in the permeate than observed under the feed conditions described in Subsection 3.4.3.1. This can perhaps be attributed to a lower degree of fouling due to the increased transport of hemoglobin, resulting in higher transport of BSA. Further due to the small pressure difference of 1.5 psig between the experiments, a small error in measurement was likely to have been amplified.

3.4.3.3 Regenerated Cellulose Membranes. When using the YM100 regenerated cellulose membranes, low selectivity was observed regardless of the buffer conditions or operating pressures. Figure 3.45 shows the selectivity for one and two membranes under two different buffer conditions. Selectivities ranged from 0-2 when operating at 20 mM ionic strength buffer and was not amplified when the membrane number was increased. At lower ionic strengths (2.3 mM), selectivities were somewhat higher (0-14) but sufficient selectivity enhancement was not observed when a 2-membrane composite was investigated. These data reveal that selectivites above 15 (as seen in Figure 3.42) must be attained in single membrane systems in order to have rejection amplification in multimembrane composite-based UF systems. Additional studies with different protein systems are needed to confirm such a requirement.

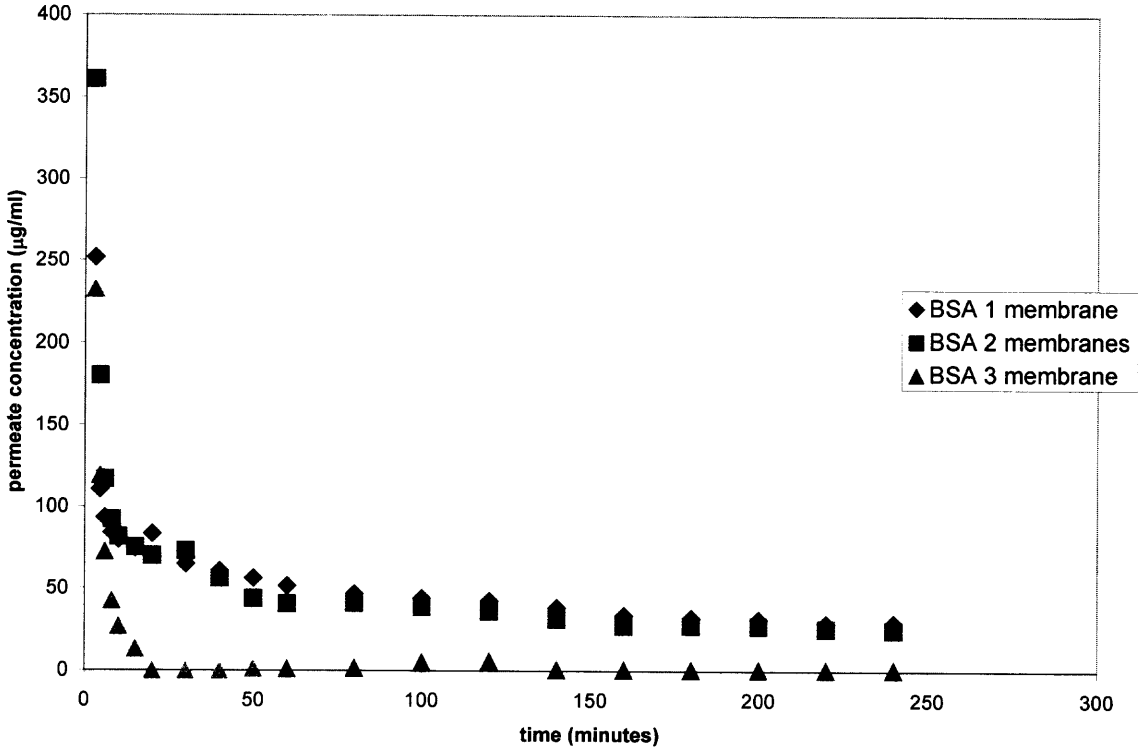

Figure 3.44 Optimized batch ultrafiltration: 0.5 mg/ml bovine serum albumin and 0.5 mg/ml hemoglobin, pH 6.8, 2.3 mM sodium phosphate buffer; Omega 100K membranes, 1.5, 3, and 4.5 psig (only rejected protein, BSA, shown).

Burns and Zydney (2000) conducted an extensive study of buffer effects on the zeta potential of ultrafiltration membranes. Due to a diffuse double layer of ions present near the surface of the membrane, ionic strength and membrane charge are important variables in separation. Operating at low ionic strength creates a more diffuse double layer due to the lack of ions present to adsorb on the membrane surface. Therefore, at low ionic strengths there is more repulsion from the negatively charged BSA and the negatively charged membrane surface. Burns and Zydney (2000) presented limited data for the Omega 100K membrane and showed that at pH 6.8, the apparent zeta potential

was at a minimum with a value of approximately –17.0 (mV). Regenerated cellulose-based YM100 membrane was found to have a zeta potential of around –4.5 mV (Kim, Fane, Nystrom, Pihlajamaki, Bowen and Mukhtar 1996) at pH 6.8, which therefore provides an explanation for increased rejection of BSA by the Omega 100K membrane. This explains the increased selectivity obtained with this binary system at 2.3 mM (Subsection 3.4.3.1) using the polyethersulfone membrane. Therefore, when purifying mixtures of similar molecular weight, membrane selection and membrane charge are important considerations.

When the membranes were analyzed after completion of ultrafiltration prior to cleaning, it was found that very little protein had been absorbed on the membranes. Less than 7.0 μg/ml of the more permeable protein (hemoglobin) was found in all cases. The more rejected protein (bovine serum albumin) concentration was also very low, ranging from 33 μg/ml for the top membrane to less than 25 μg/ml for the bottom membrane.

This is due to the nature of the membrane material. Regenerated cellulose membranes (YM series) are very hydrophilic which results in low protein adsorption (Amicon 1995). This can be illustrated by the low contact angle of 31° for the YM100 membrane (Jucker and Clark 1994). When membranes have more hydrophobic groups, there is an interaction between the hydrophobic regions on the membrane and the hydrophobic region present on the proteins (Cheryan 1998).

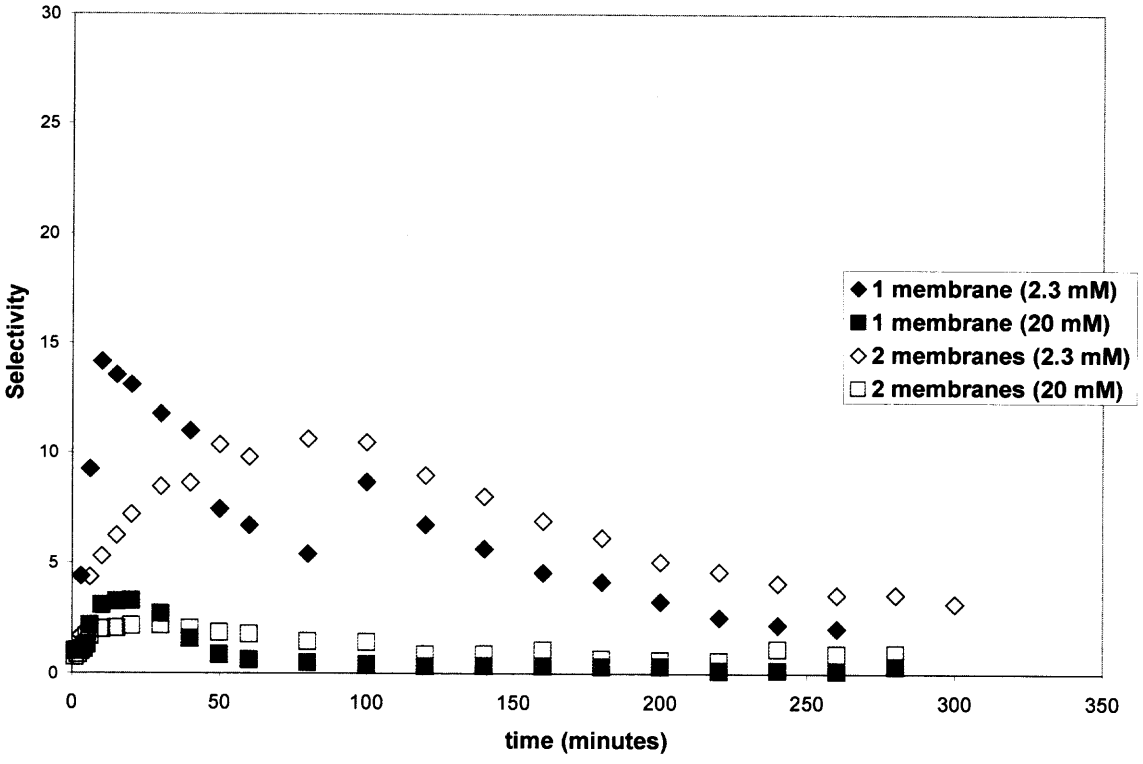

Figure 3.45 Selectivities of YM100 ultrafiltration membranes for different ionic strengths in System 3 (1.0 mg/ml bovine serum albumin and 0.2 mg/ml hemoglobin, pH 6.8, 2.3 mM and 20 mM sodium phosphate buffer; 1.5 psig and 3.0 psig).

The polyethersulfone membranes (Omega) showed much higher adsorption (the more rejected protein (BSA) concentration was ranging from as high as 582 μg/ml for the top membrane to 333 μg/ml for the bottom membrane). Polyethersulfone is a more hydrophobic material, which can be illustrated by a higher contact angle 65° (Hodgins and Samuelson 1990). Due to the higher hydrophobicity, the hydrophobic regions on the proteins will interact with membrane to a greater degree than the regenerated cellulose membranes.

3.4.3.5 Cyclic Experiments. A cyclic experiment was performed to show that the polyethersulfone membrane composite can be cleaned in situ and the ultrafiltration behavior of the proteins observed with fresh membranes can be reproduced with the cleaned membranes. Ultrafiltration was performed with 3 membranes at 4.5 psig, then the *in situ* cleaning procedure was implemented and then ultrafiltration was repeated. The results are shown in Figure 3.46. This means that the membrane composite can be restored to its original performance level without dissembling the apparatus. They can also be used repeatedly, which is cost effective.

3.5 Cleaning *In Situ*

3.5.1 Regenerated Cellulose Membranes

In situ cleaning of YM30 regenerated cellulose membranes was performed (see Section 2.2.4.1) and the pure water fluxes were measured before and after cleaning. Table 3.5 shows the results and the % water flux recovery.

3.5.2 Polyethersulfone Membranes

In situ cleaning of Omega 100K polyethersulfone membranes was also performed (see Subsection 2.2.4.2) and the pure water fluxes were measured before and after cleaning. Table 3.6 shows the results and the % water flux recovery.

Table 3.5 Pure Water Flux Measurements Before and After Cleaning *In Situ* (10 psig, 3 YM30 Membranes)

Virgin membrane water flux (μm/s)	After cleaning water flux (μm/s)	Percent recovery of original flux (%)
16.78	16.25	96.82

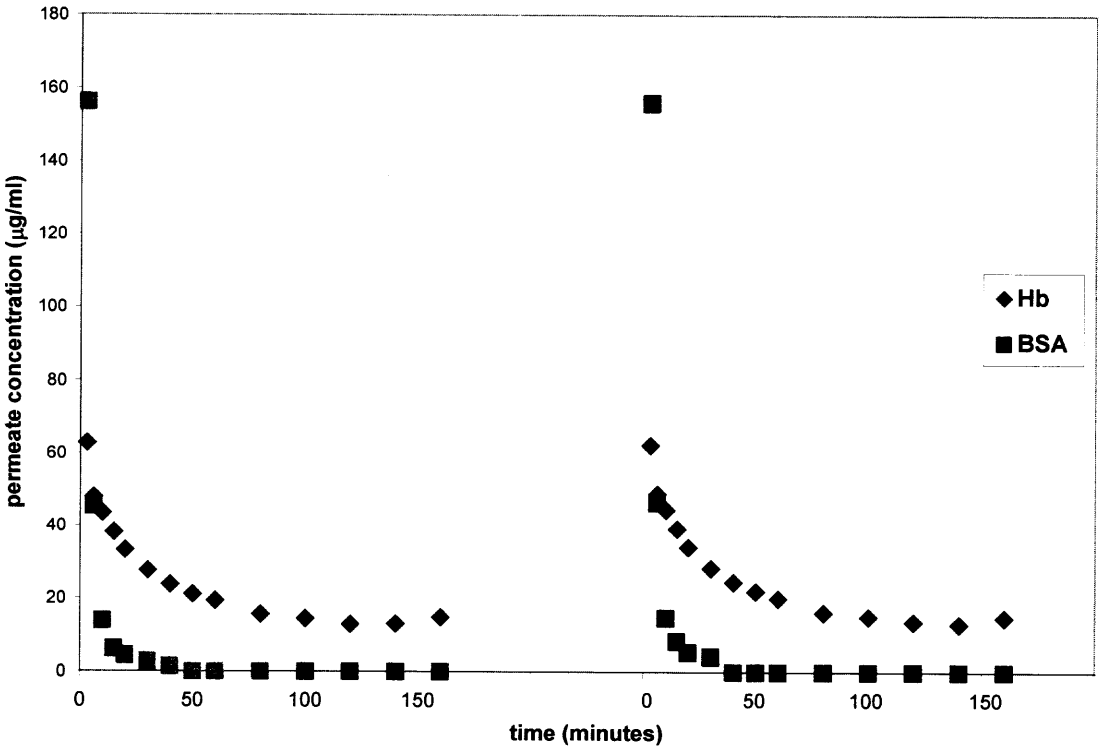

Figure 3.46 Permeate concentration profiles comparing batch ultrafiltration before and after cleaning *in situ* (1.0 mg/ml bovine serum albumin and 0.2 mg/ml hemoglobin, pH 6.8, 2.3 mM sodium phosphate buffer; 3 Omega 100K membranes, 4.5 psig).

Table 3.6 Pure Water Flux Measurements Before and After Cleaning *In Situ* (4.5 psig, 3 Omega 100K Membranes)

Virgin membrane water flux (µm/s)	After cleaning water flux (µm/s)	Percent recovery of original flux (%)
30.16	29.30	97.06

3.6 Concluding Remarks

Through the multimembrane composites, essentially one can create membranes with absolute molecular weight cutoffs (MWCOs) that are unavailable commercially. A multimembrane stack potentially develops a much sharper pore size distribution. When

one needs a smaller MWCO membrane in order to reject a solute completely, the solvent flux can decrease considerably due to a reduction in the pore size since the solvent flux is proportional to the fourth power of the pore diameter. The multimembrane composite investigated here overcomes this problem and allows the development of customized MWCO membranes with less flux reduction than one would find by changing to a smaller MWCO membrane. For example, when switching to the next available smaller size regenerated cellulose membrane (YM10) having a MWCO of 10,000, the flux will be reduced as much as seven times (Amicon, 1995) without a guarantee of complete rejection. The flux reduction in a multimembrane stack for YM30 membrane is only two times lower for two membranes, three times lower for three membranes, etc.. Yet the selectivity enhancement is significant. Unlike chromatography, such a membrane process is continuous, scalable, easily operated, has a small footprint and is likely to be quite inexpensive.

This Chapter presented the experimental results of this research for single membrane and multimembrane configurations. Three different binary protein mixtures, having three different molecular weight ratios (2.05, 1.22, and 1.03) have been effectively separated using the multimembrane composite. Two different molecular weight cutoff membranes were investigated (30,000 and 100,000). Also, in some instances, the overall flux loss encountered when using the multimembrane stack could be recovered by raising the pressure. Both types of membranes could be cleaned *in situ*. At this point, mathematical descriptions are needed for further understanding and description of the process.

CHAPTER 4

MODELING AND SIMULATIONS

In this Chapter, different models will be considered and preliminary modeling results will be presented and discussed. First, the simple lumped model of rejection amplification (described in Section 1.3) will be presented. The results from this basic model provide a fundamental basis of the concept. Beyond this simplistic lumped model, a more detailed model having the requisite equations were developed and will be presented next. These equations use a convection-diffusion model. As a first step, a 2-membrane based multimembrane composite was modeled as two membranes in series both experiencing a boundary layer on the feed side. The effects of MWCO and mass transfer coefficients on protein transmission will be discussed for a single protein. A binary protein mixture of BSA and IgG will also be investigated. Further, a comparison of the two models will be performed.

4.1 Lumped Rejection Amplification Model

Equations 1.3, 1.7, and 1.8 (described in Section 1.3) were used as part of a simple lumped model described in the Introduction to better understand the hypothesis of rejection amplification. These estimates were important in verifying the principle of rejection amplification in a multimembrane stack.

Consider the model of resistances-in-series having the same solvent flux. When a 2-membrane stack is exposed to a certain operating pressure, the pressure imposed on each membrane is approximately one half of the total since the membranes are identical:

any variation will be due to differences in the resistances of the deposits on the membrane. However the flux is the same. Correspondingly, when a 3-membrane stack is exposed to a certain operating pressure, the pressure imposed on each membrane is approximately one third of the total operating pressure. Therefore, single membrane investigations at different pressures were carried out and the results reported in Chapter 3 to help offer useful estimations of rejection values that are otherwise unknown.

4.1.1 System 1

Single membrane experiments were performed on System 1 (consisting of β-lactoglobulin and myoglobin) at different pressures and were presented in Subection 3.3.1.2. These data for YM30 membranes were used to understand what was occurring in the multimembrane stack.

Figure 3.15 illustrated for System 1 the experimental values of R_1 based on a single membrane system at four different operating pressures (10, 5, 3.5, and 2.0 psig) at pH 7.3. The experimental protein rejection versus the calculated protein rejection behavior for System 1 at 10 psig are shown in Figure 4.1 and Figure 4.2, comparing the system performances for one, two, and three membranes in series. The observed rejection values are compared to the values calculated from Equations 2.5 and 2.6 for two and three membranes in series. When a 2- or 3- membrane composite is used, the effective pressure drop per membrane is lower. Therefore the experimental R_1 values from 5 psig data were used to calculate the R_2 for an overall feed pressure of 10 psig for a 2-membrane composite. R_1 values from 3.5 psig data were used to calculate the R_2 and R_3 for an overall pressure of 10 psig for a 3-membrane composite.

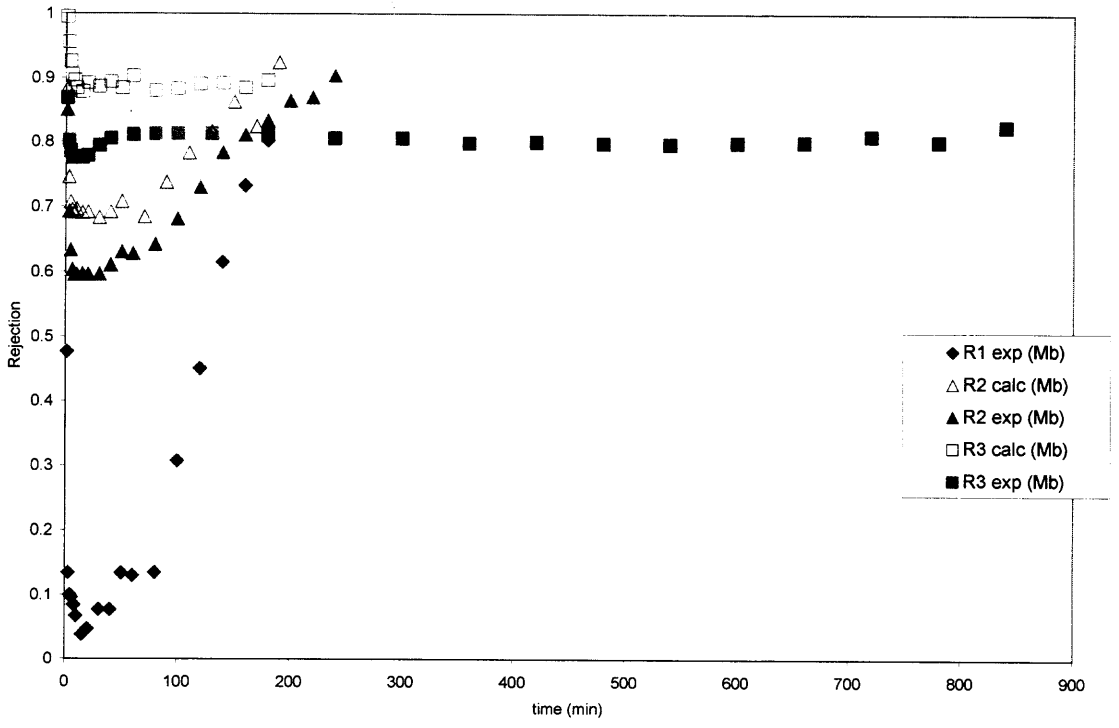

Figure 4.1 Experimental and calculated rejection behaviors of myoglobin for 2 and 3 membranes systems. Batch ultrafiltration of System 1 for YM30 membranes (1.0 mg/ml β-lactoglobulin and 0.2 mg/ml myoglobin, pH 7.3, 10 psig; experimental data from Figure 3.15).

The values comparing the experimental and calculated values of rejections for the more permeable protein, myoglobin, are not identical in Figure 4.1. The experimental values of R_I used for calculation correspond to a certain level of concentration polarization due to particular mixing conditions in the cell in the single membrane. The mixing conditions on top of the second membrane and the third membrane in the 2-membrane and 3-membrane composites are different; the fluids in between the membranes are stagnant (unlike that on membrane 1) which leads to lower rejections. Therefore, the experimentally observed R_2 and R_3 values are lower than the calculated values shown in Figure 4.1. The objective here, however, was to test the crude lumped

model based on the concept of rejection amplification. It appears to provide a good guidance toward the observed rejection increase. More detailed modeling using stagnant conditions in the space between two contiguous membranes in the stack will be discussed later in this chapter. However, the conditions and the dimensions of the inter-membrane space are unknown.

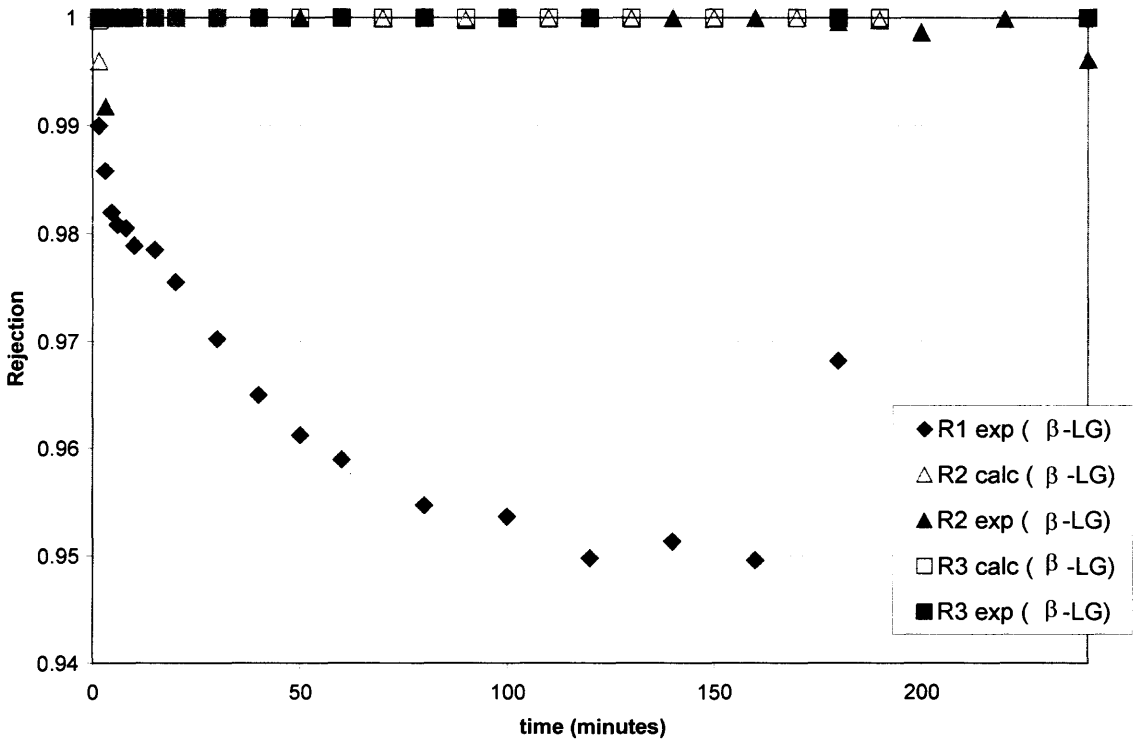

Figure 4.2 Experimental and calculated rejection behaviors of β-lactoglobulin for 2 and 3 membranes systems. Batch ultrafiltration of System 1 for YM30 membranes (1.0 mg/ml β-lactoglobulin and 0.2 mg/ml myoglobin, pH 7.3, 10 psig).

Figure 4.2 compares the calculated rejection values with the observed rejection values for the highly rejected protein β-lactoglobulin. It appears that in this case, the experimentally obtained values are very close to the calculated values. The differences between the two sets are not visible in the scale of Figure 4.2.

4.1.2 System 2

Single membrane experiments were performed on System 2 (consisting of α-lactalbumin and myoglobin) performed at different pressures and were presented in Subection 3.3.2.2. These data were used to understand what was occurring in the multimembrane stack for System 2.

Figure 3.17 illustrated for System 2 the experimental values of R_1 based on a single membrane system at four different operating pressures (10, 5, 3.5, and 2.0 psig). The experimental protein rejection behaviors for myoglobin and α-lactalbumin at 10 psig are shown respectively in Figure 4.3 and Figure 4.4, comparing the system performances for one, two, and three membranes in series. These observed rejection values are compared to calculated values from Equations 1.7 and 1.8 for two and three membranes in series. When a 2- or 3- membrane composite is used, the effective pressure drop per membrane is lower. Therefore the experimental R_1 values from 5 psig data were used to calculate the R_2 for an overall feed pressure of 10 psig for a 2-membrane composite. The values of R_1 values from 3.5 psig data were used to calculate the R_2 and R_3 for an overall pressure of 10 psig for a 3-membrane composite.

The values comparing the experimental and calculated values of rejections for the two proteins are not identical in Figures 4.3 and 4.4 (as seen is Section 4.1.2). The two sets of values are much closer for the more highly rejected protein, myoglobin, in Figure 4.4. The values of R_1 used for calculation correspond to a certain level of concentration polarization due to particular mixing conditions in the cell in the single membrane. The mixing conditions on top of the second membrane and the third membrane in the 2-membrane and 3-membrane composites are different; the conditions are stagnant which

lead to lower rejections. Therefore, the experimentally observed R_2 and R_3 values are lower than the calculated values shown in Figures 4.3 and 4.4; the differences are greater in Figure 4.3 for the more permeable protein whose concentration may get increased substantially on top of the second membrane.

The experimental value of R_1 for α-lactalbumin corresponding to rejection data for one membrane at 10 psig shown in Figure 4.3 is higher than the experimental value of R_1 for α-lactalbumin (corresponding to rejection data for two membranes at 10 psig). This was due to the high degree of fouling / concentration polarization that was observed in System 2 at higher pressures, which caused high rejections.

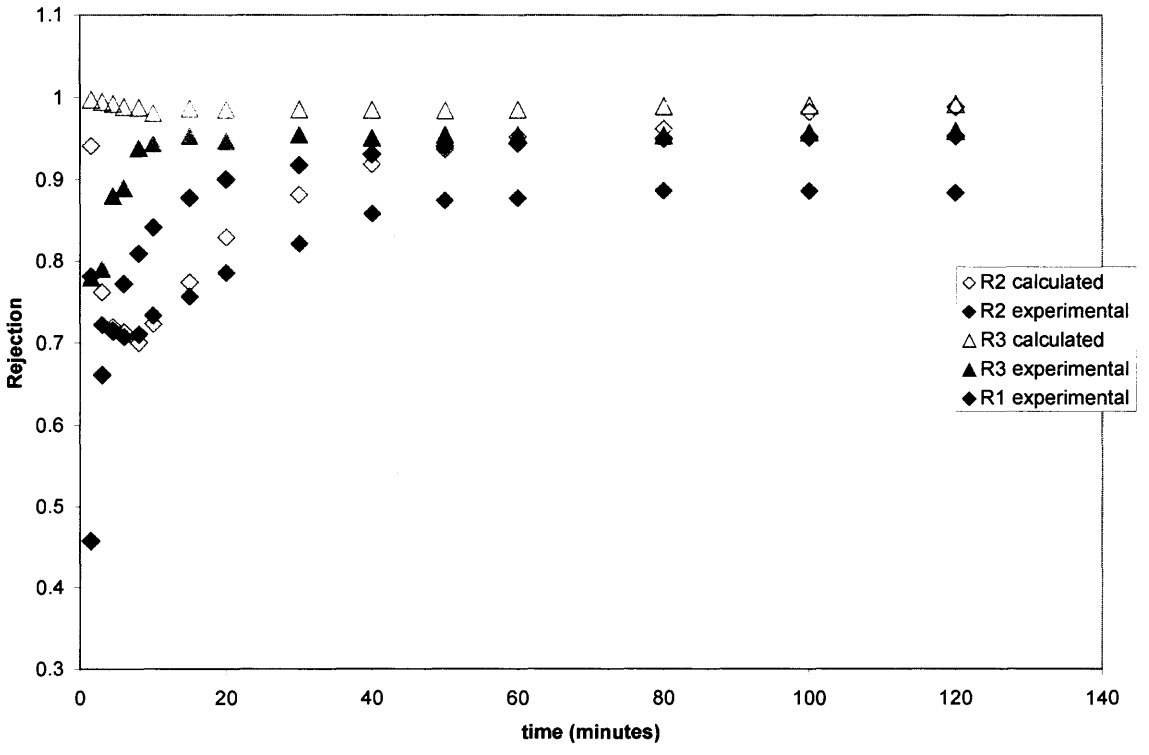

Figure 4.3 Experimental and calculated rejection behaviors of α-lactalbumin for 2 and 3 membranes systems. Batch ultrafiltration of System 2 for YM30 membranes (0.2 mg/ml a-lactalbumin and 0.2 mg/ml myoglobin, pH 4.35, 10 psig).

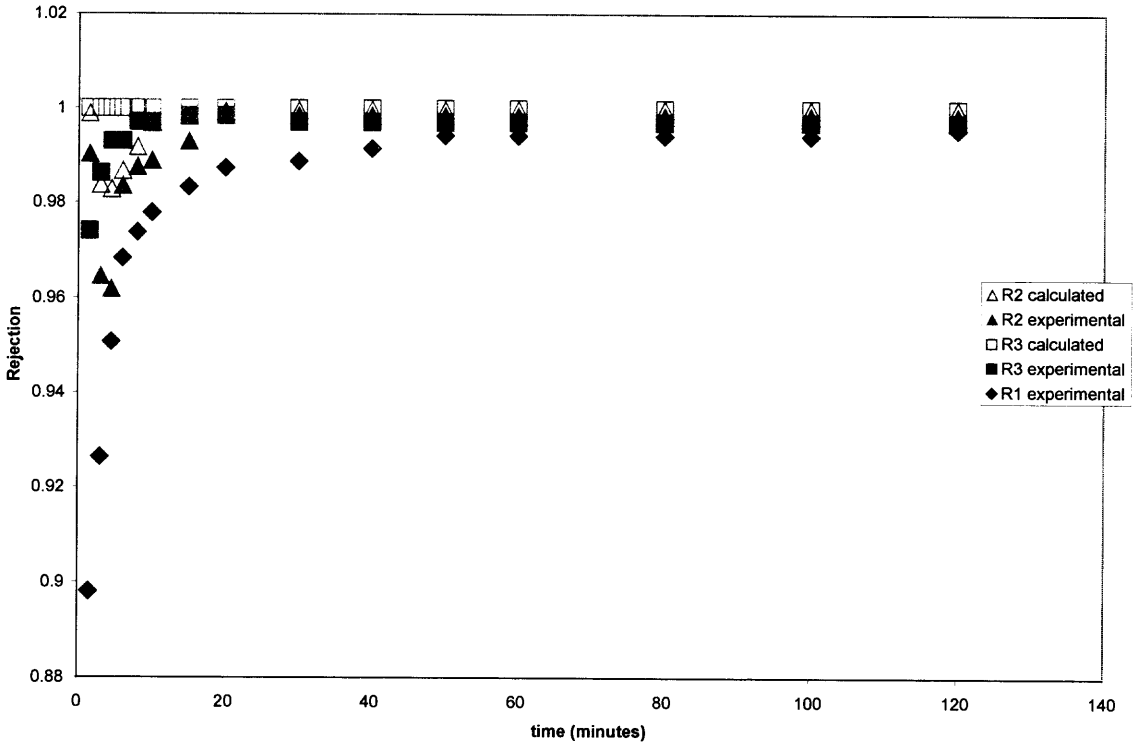

Figure 4.4 Experimental and calculated rejection behaviors of myoglobin for 2 and 3 membranes systems. Batch ultrafiltration of System 2 for YM30 membranes (0.2 mg/ml a-lactalbumin and 0.2 mg/ml myoglobin, pH 4.35, 10 psig).

4.1.3 System 3

Single membrane experiments were performed on System 3 (consisting of bovine serum albumin and hemoglobin) at different pressures and the results were presented in Subsection 3.3.3.2. These data were used to understand what was occurring in the multimembrane stack.

Figure 3.20 illustrates the experimental values of R_I based on a single Omega 100K membrane system for the two proteins at three different operating pressures (4.5, 3, and 1.5 psig) and pH 6.8. The experimental protein rejection behaviors at 4.5, 3, and 1.5

psig and pH 6.8 for hemoglobin and bovine serum albumin are shown respectively in Figure 4.5 and Figure 4.6, comparing the system performances for 1, 2, and 3 Omega 100K membranes in series. These observed rejection values are compared to calculated values calculated from Equations 1.7 and 1.8 for two and three membranes in series. When a 2- or 3- membrane composite is used, the effective pressure drop per membrane is lower. Therefore the experimental R_1 values from 1.5 psig data were used to calculate the R_2 for an overall feed pressure of 3 psig for a 2-membrane composite. R_1 values from 1.5 psig data were used to calculate the R_2 and R_3 for an overall pressure of 4.5 psig for a 3-membrane composite.

The values of experimental and calculated values of rejections for hemoglobin are not identical in Figure 4.5. The values of R_1 used for calculation correspond to a certain level of concentration polarization in the feed due to particular mixing conditions in the cell containing the single membrane. The mixing conditions on top of the second membrane and the third membrane in the 2-membrane and 3-membrane composites are different; stagnant conditions exist which lead to lower rejections. Therefore, the experimentally observed R_2 and R_3 values are lower than the calculated values shown in Figures 4.5 and 4.6. The differences in R_2 and R_3 for BSA are much less since R_1 for BSA is very high; so concentration polarization has much less effect on R_2 and R_3.

Further, in Figure 4.5, the value of experimental R_3 for hemoglobin is less that the experimental value of R_2 due to the very low operating pressures. The total operating pressure was 1.5 psig for a single membrane experiments, 3.0 psig for a 2-membrane composite, and 4.5 psig for a 3-membrane composite; therefore the pressure difference between each experiment was only 1.5 psig. Therefore the small pressure / flux

variations are amplified in System 3. It was observed in Figure 3.41, that the flux for the 3-membrane composite was slightly higher that that obtained for a 2-membrane composite and for a single membrane. This higher flux results in a lower rejection. This was not seen in Systems 1 or 2 because the total operating pressure of all experiments was 10 psig and there was no pressure variation between the single membrane, 2-membrane composite, or 3-membrane composite experiments.

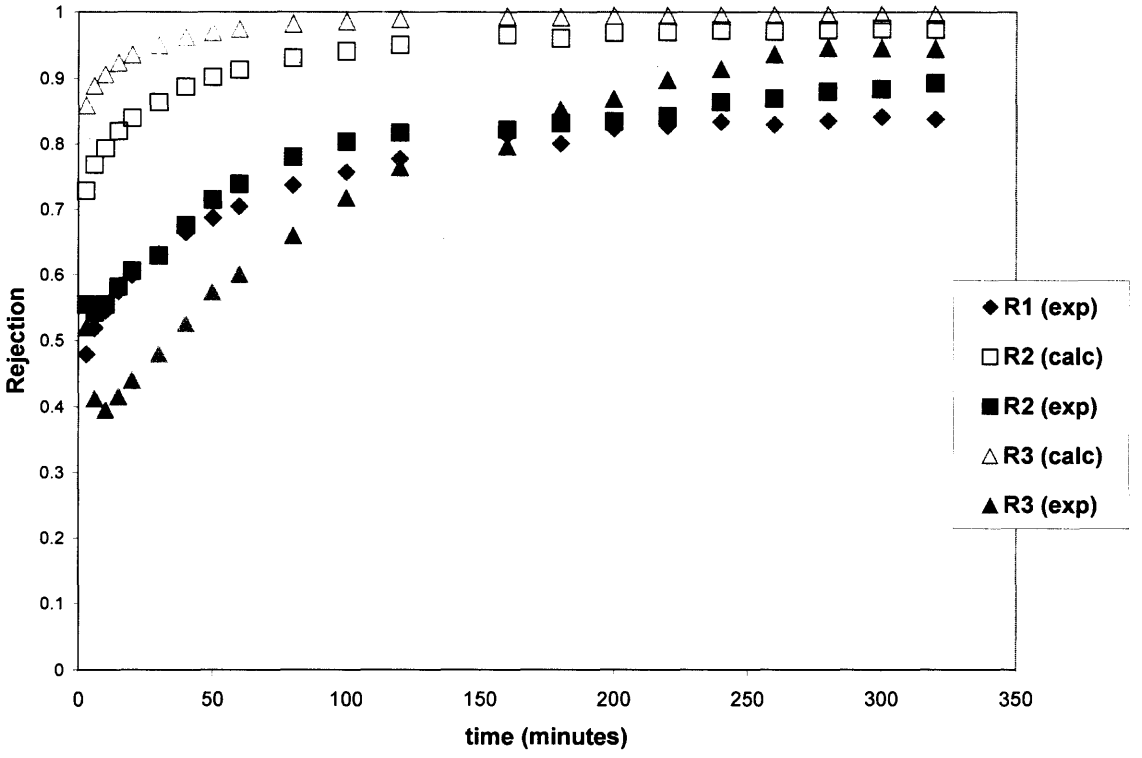

Figure 4.5 Experimental and calculated rejection behaviors of hemoglobin for 1, 2 and 3 membranes systems. Batch ultrafiltration of System 3 (1.0 mg/ml bovine serum albumin and 0.2 mg/ml hemoglobin, pH 6.8, 2.3 mM sodium phosphate buffer; Omega 100K membranes, 1.5, 3, and 4.5 psig).

4.2 Convection-Diffusion Model

4.2.1 Introduction

The model results presented in Section 4.1 provided estimates of rejection in the multimembrane stack, without consideration of a number of factors that affect rejection. Because no measurements can be obtained in-between the membranes, a more realistic model must be considered.

Consider a single ultrafiltration membrane in dead-end or cross flow ultrafiltration mode, as shown in Figure 4.7. As proteins / solutes are brought to the surface of the microporous membrane by convective transport, solvent is removed. When this occurs, a higher concentration of protein (compared to the bulk concentration) builds up at the wall. This increase in concentration happens if the protein is fully, partially, or completely rejected. This increased wall concentration results in the formation of a film of increased protein concentration on the surface of the membrane. After some time, a steady state is reached when this film reaches a constant thickness of δ_f due to the diffusion of the proteins back into the bulk solution. Different factors that affect the characteristics of the film are: concentration of the feed solution, physicochemical properties of the feed solutions, membrane charge, the degree of mixing, and the pressure / flux.

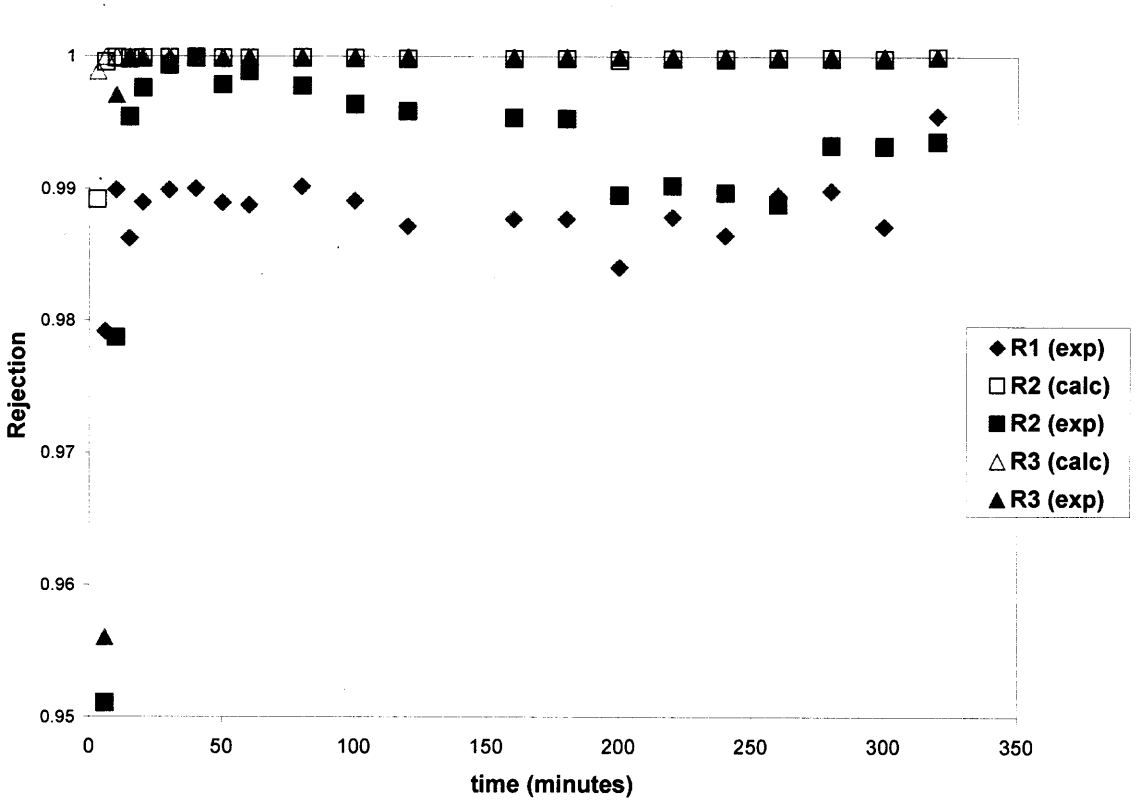

Figure 4.6 Experimental and calculated rejection behaviors of bovine serum albumin for 1, 2 and 3 membranes systems. Batch ultrafiltration of System 3 (1.0 mg/ml bovine serum albumin and 0.2 mg/ml hemoglobin, pH 6.8, 2.3 mM sodium phosphate buffer; Omega 100K membranes, 1.5, 3, and 4.5 psig).

Consider a single ultrafiltration membrane in dead-end or cross flow ultrafiltration mode, as shown in Figure 4.7. As proteins / solutes are brought to the surface of the microporous membrane by convective transport, solvent is removed. When this occurs, a higher concentration of protein (compared to the bulk concentration) builds up at the wall. This increase in concentration happens if the protein is partially or completely rejected. This increased wall concentration results in the formation of a film of increased protein concentration on the surface of the membrane. After some time, a steady state is reached when this film reaches a constant thickness of δ_f due to the diffusion of the

proteins back into the bulk solution. Different factors that effect the characteristics of the film are: concentration of the feed solution, physicochemical properties of the feed solutions, membrane charge, the degree of mixing, and the pressure / flux.

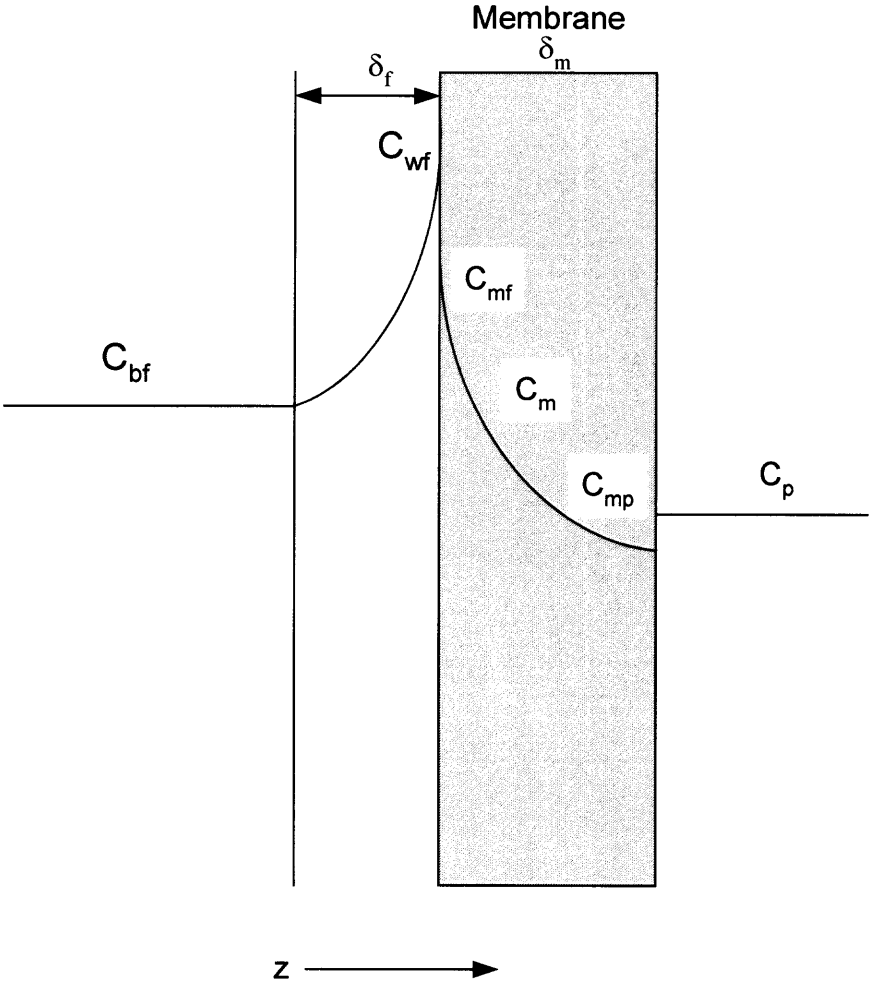

Figure 4.7 Single membrane schematic of ultrafiltration with permeate flow in the z-direction.

By developing a series of steady state equations, a convection-diffusion model was developed to describe a 2-membrane system. This model investigates the effect of

convection and diffusion as well as the effects of mass transfer and film thickness on the overall protein transmission. Such a model is a useful tool to better understand the dynamics of the multimembrane composite. The key assumption here is steady state conditions.

4.2.2 Theoretical Development for a Single Membrane

For a single membrane system (as shown in Figure 4.7), a steady state mass balance in the feed side boundary layer for the protein at any z leads to

$$N_s = J_v C - D_0 \frac{dC}{dz} \tag{4.1a}$$

Boundary conditions:

$$z = 0, \quad C = C_{bf}; \quad z = \delta_f, \quad C = C_{wf}$$

Integrating:

$$\int_{C_{bf}}^{C_{wf}} \frac{dC}{\left(C - N_s/J_v\right)} = \int_0^{\delta_f} \frac{J_v}{D_0} dz$$

$$\frac{C_{wf} - N_s/J_v}{C_{bf} - N_s/J_v} = \exp\left(J_v/k_f\right) \tag{4.1b}$$

where $k_f = D_0/\delta_f$ is the protein mass transfer coefficient in the feed side boundary layer, and J_v/k_f is the Peclet number for the feed side boundary layer. Rewriting Equation 4.1b

$$\frac{N_s}{J_v} = \frac{C_{bf} \exp\left(J_v/k_f\right) - C_{wf}}{\exp\left(J_v/k_f\right) - 1} \tag{4.1c}$$

Next, consider the mass balance through the microporous membrane in the z-direction:

$$N_s = K_c J_v C_m - \varepsilon K_d D_0 \frac{dC_m}{dz} \tag{4.2a}$$

where K_c is the convective hindrance factor, ε is the membrane skin layer porosity, and K_d is the diffusive hindrance factor (Opong and Zydney 1991, Anderson and Quinn 1974).

Boundary conditions:

$$z = 0,\ C_m = \phi C_{wf}; \qquad z = \delta_m,\ C_m = \phi C_p$$

Here ϕ is the partition coefficient for the protein between the external feed solution and the membrane at the membrane-feed solution interface *(z=0)*. The value of the partition coefficient is assumed to be the same at the membrane-solution interface *($z=\delta_m$)* where the external solution concentration is C_p, the permeate concentration.

Integrating Equation 4.2a between $z=0$ and $z=\delta_m$ and utilizing the boundary conditions:

$$\int_{\phi C_{wf}}^{\phi C_p} \frac{dC_m}{C_m - N_s/(J_v K_c)} = \int_0^{\delta_m} \frac{K_c J_v}{\varepsilon K_d D_0} dz$$

$$\frac{\phi C_p - N_s/(J_v K_c)}{\phi C_{wf} - N_s/(J_v K_c)} = \exp\left(\frac{K_c J_v \delta_m}{\varepsilon K_d D_0}\right) = \exp\left(\frac{S_\infty J_v \delta_m}{D_{eff}}\right) = \exp(Pe_m) \tag{4.2b}$$

Here $S_\infty = \phi K_c$, is the asymptotic intrinsic membrane transmission, which is achieved at very high fluxes; $D_{eff} = \phi \varepsilon K_d D_0$, is the effective solute diffusivity in the pore; Pe_m is the membrane Peclet number. Rearranging the above equation results in

$$\frac{N_s}{J_v} = \frac{S_\infty C_{wf} \exp(Pe_m) - S_\infty C_p}{\exp(Pe_m) - 1} \tag{4.2c}$$

In a steady state ultrafiltration process, N_s/J_v is equal to C_p (the permeate protein concentration). From Equation 4.2c the expression for the actual sieving coefficient, S_a, is obtained. This expression was developed by Anderson and Quinn (1974) using classical membrane transport theory (Opong and Zydney 1991, Burns and Zydney 1999).

$$S_a = \frac{C_p}{C_{wf}} = \frac{S_\infty \exp(Pe_m)}{S_\infty + \exp(Pe_m) - 1} \tag{4.3}$$

At very high J_v, $S_a \rightarrow S_\infty$.

Using a stagnant film model (Michaels 1968) and a hydrodynamic model (Deen 1987, Anderson and Quinn 1974) the observed sieving coefficient, S_o, for an ultrafiltration process has been described by Zydney et al. (Saksena and Zydney 1994, Opong and Zydney 1991, Burns and Zydney 1999) and is as follows:

$$S_o = \frac{C_p}{C_{bf}} = \frac{S_\infty \exp(Pe_m) \exp\left(J_v / k_f\right)}{(S_\infty - 1)(1 - \exp(Pe_m)) + S_\infty \exp(Pe_m) \exp\left(J_v / k_f\right)} \tag{4.4}$$

The mass transfer coefficient on the feed side is k_f. At large values of J_v, or large values for Pe_m, $S_o \rightarrow S_\infty$.

Single membrane simulations are useful for understanding the behavior of the multimembrane composite. By comparing single membrane simulation data to 2-membrane composite simulation data, one can observe if rejection amplification is occurring.

4.2.3 Theoretical Development for a Multimembrane Composite

A multimembrane composite of two membranes can be described as four mass transfer resistances in series. Figure 4.8 shows a schematic of the concentration profiles for two of the same ultrafiltration membranes in series, operating in dead-end or cross flow mode. The permeate from the first membrane is the feed for the second membrane. There is a boundary layer that exists on the feed side of each of the membranes. However, different conditions exist for the top membrane and in-between the two membranes.

The top membrane experiences a certain degree of mixing, due to the stirrer that is present in the ultrafiltration cell feed reservoir in the present research. There is also a large bulk volume into which the proteins from the boundary layer can diffuse back. Also, due to the high rejection of one of the proteins, the top membrane has a much higher concentration of the highly rejected protein. In-between the membranes, there is no mixing which affects the boundary layer. There is also not much of a bulk volume in-between the membranes for back diffusion. This will cause an increase in the wall concentration of the second membrane, C_{pw1}, and will increase protein transmission.

Considering the four mass transfer resistances in series, one can derive an expression for the overall observed sieving coefficient for the 2-membrane-based multimembrane ultrafiltration process. The four steady state mass balances can be related because N_s/J_v is considered the same, at a given time, under steady state conditions. The observed sieving coefficient for the multimembrane stack is then compared to single membrane simulation results.

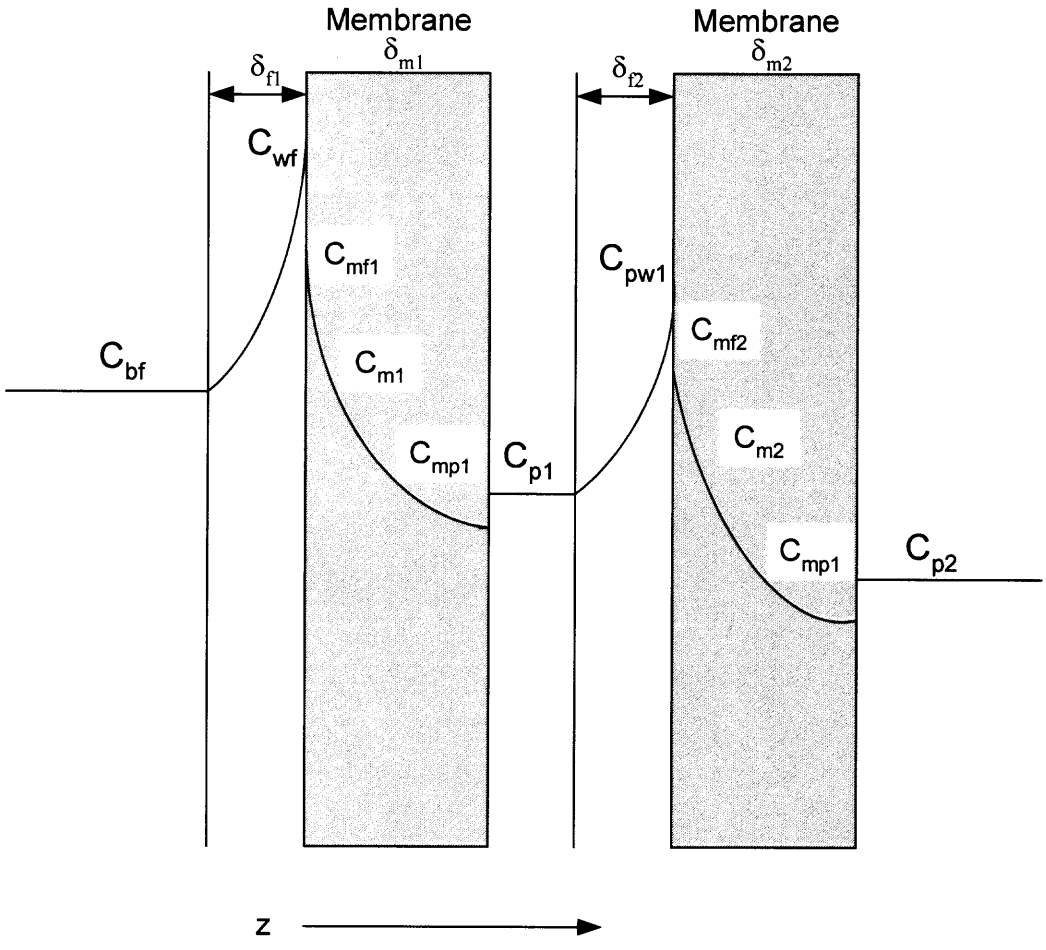

Figure 4.8 A 2- membrane composite schematic of ultrafiltration with permeate flow in the z-direction.

A mass balance in the feed side boundary layer of membrane 1 for the protein solute at any z leads to

$$N_s = J_v C - D_0 \frac{dC}{dz} \tag{4.5a}$$

Boundary conditions:

$$z = 0, \quad C = C_{bf}; \quad z = \delta_{fl}, \quad C = C_{wf} \tag{4.5b}$$

Integrating:

$$\int_{C_{bf}}^{C_{wf}} \frac{dC}{C - N_s/J_v} = \int_0^{\delta f1} \frac{J_v}{D_0} dz$$

$$\frac{C_{wf} - N_s/J_v}{C_{bf} - N_s/J_v} = \exp\left(J_v/k_1\right) \tag{4.5c}$$

where $k_1 = D_0/\delta_{fl}$ is the protein mass transfer coefficient in the boundary layer of the first membrane, and J_v/k_1 is the Peclet number for the feed side boundary layer of the first membrane. Equation 4.5c can be rewritten as

$$\frac{N_s}{J_v} = \frac{C_{bf}\exp\left(J_v/k_1\right) - C_{wf}}{\exp\left(J_v/k_1\right) - 1} \tag{4.5d}$$

Next, consider the mass flux through the through the first ultrafiltration membrane; in the z direction from the membrane-feed interface toward the permeate side of the first membrane:

$$N_s = K_c J_v C_{m1} - \varepsilon K_d D_0 \frac{dC_{m1}}{dz} \tag{4.6a}$$

where K_c is the convective hindrance factor, ε is the membrane skin layer porosity, and K_d is the diffusive hindrance factor (Opong and Zydney 1991, Anderson and Quinn 1974).

Boundary conditions:

$$z = 0, \; C_{m1} = \phi C_{wf}; \qquad z = \delta_{m1}, \; C_{m1} = \phi C_{p1} \tag{4.6b}$$

Here, the partition coefficient, ϕ, for the protein between the feed side of the first membrane and the permeate side of the first membrane is assumed to be the same at both interfaces.

Integrating Equation 4.6a between the two limits:

$$\int_{\phi C_{wf}}^{\phi C_{pl}} \frac{dC_{ml}}{C_{ml} - N_s/(J_v K_c)} = \int_0^{\delta_{ml}} \frac{K_c J_v}{\varepsilon K_d D_0} dz$$

$$\frac{\phi C_{pl} - N_s/(J_v K_c)}{\phi C_{wf} - N_s/(J_v K_c)} = \exp\left(\frac{K_c J_v \delta_{ml}}{\varepsilon K_d D_0}\right) = \exp\left(\frac{S_\infty J_v \delta_m}{D_{eff}}\right) = \exp(Pe_{ml}) \qquad (4.6c)$$

where

$$S_\infty = \phi K_c$$

S_∞ is the asymptotic value of the sieving coefficient; $D_{eff}=\phi\varepsilon K_d D_0$ is the effective solute diffusivity in the pore; Pe_{ml} is the Peclet number of the first membrane. Rearranging Equation 4.6c gives

$$\frac{N_s}{J_v} = \frac{S_\infty C_{wf} \exp(Pe_{ml}) - S_\infty C_{pl}}{\exp(Pe_{ml}) - 1} \qquad (4.6d)$$

A mass balance in the boundary layer of the second membrane for the protein solute at any z leads to

$$N_s = J_v C - D_0 \frac{dC}{dz} \qquad (4.7a)$$

Boundary conditions:

$$z = 0, \quad C = C_{pl}; \quad z = \delta_{f2}, \quad C = C_{pwl} \qquad (4.7b)$$

Here $z=0$ corresponds to the interface between the boundary layer thickness δ_{f2} and the bulk in the inter-membrane gap.

Integrating Equation 4.7a between the two limits:

$$\int_{C_{pl}}^{C_{pw1}} \frac{dC}{C - N_s/J_v} = \int_0^{\delta_{f2}} \frac{J_v}{D_0} dz$$

$$\frac{C_{pw1} - N_s/J_v}{C_{pl} - N_s/J_v} = \exp\left(J_v/k_2\right) \tag{4.7c}$$

where $k_2 = D_0/\delta_{f2}$ is the protein mass transfer coefficient in the boundary layer facing the second membrane, and J_v/k_2 is the Peclet number in the boundary layer of the second membrane. Equation 4.7c can be rewritten as

$$\frac{N_s}{J_v} = \frac{C_{pl}\exp\left(J_v/k_2\right) - C_{pw1}}{\exp\left(J_v/k_2\right) - 1} \tag{4.7d}$$

Next, consider the mass flux through the through the second ultrafiltration membrane; in the z direction from the membrane-feed interface of the second membrane toward the permeate side of the second membrane:

$$N_s = K_c J_v C_{m2} - \varepsilon K_d D_0 \frac{dC_{m2}}{dz} \tag{4.8a}$$

where K_c is the convective hindrance factor, ε is the membrane skin layer porosity, and K_d is the diffusive hindrance factor (Opong and Zydney 1991, Anderson and Quinn 1974).

Boundary conditions:

$$z = 0,\ C_{m2} = \phi C_{pw1}\ ; \qquad z = \delta_{m2},\ C_{m2} = \phi C_{p2} \tag{4.8b}$$

The partition coefficient, ϕ, for the protein between the feed side of the second membrane and permeate side of the second membranes is assumed to be the same at both interfaces. Here $z=0$ corresponds to the feed end of the membrane 2.

Integrating Equation 4.8a between the two limits:

$$\int_{\phi C_{pw1}}^{\phi C_{p2}} \frac{dC_{m2}}{C_{m2} - N_s/(J_v K_c)} = \int_0^{\delta_{m2}} \frac{K_c J_v}{\varepsilon K_d D_0} dz$$

$$\frac{\phi C_{p2} - N_s/(J_v K_c)}{\phi C_{pw1} - N_s/(J_v K_c)} = \exp\left(\frac{K_c J_v \delta_{m2}}{\varepsilon K_d D_0}\right) = \exp\left(\frac{S_\infty J_v \delta_{m2}}{D_{eff}}\right) = \exp(Pe_{m2}) \qquad (4.8c)$$

Here, $S_\infty = \phi K_c$, is the asymptotic intrinsic membrane transmission; $D_{eff} = \phi \varepsilon K_d D_0$, is the effective solute diffusivity in the pore; Pe_{m2} is the membrane Peclet number of the second membrane. Rearranging the above equation gives

$$\frac{N_s}{J_v} = \frac{S_\infty C_{pw1} \exp(Pe_{m2}) - S_\infty C_{p2}}{\exp(Pe_{m2}) - 1} \qquad (4.8d)$$

For a steady state multimembrane ultrafiltration process, N_s/J_v is equal to C_{p2} (the final permeate protein concentration):

$$C_{p2} = \frac{N_s}{J_v} \qquad (4.9)$$

The quantity N_s/J_v provides an estimation of the permeate protein concentration assuming that the transmitted protein was dissolved completely in the permeate solvent. Due to assumed steady-state assumptions, N_s/J_v, can be considered the same at a given z position, at any given time. Therefore, the value of N_s/J_v in Equations 4.5d, 4.6d, 4.7d and 4.8d can be equated and expressions can be developed for the unknown quantities.

By plugging Equation 4.9 into Equation 4.8d, an expression for the unknown quantity, C_{pw1}, was derived as follows:

$$C_{p2} = \frac{N_s}{J_v} = \frac{S_\infty C_{pw1} \exp(Pe_{m2}) - S_\infty C_{p2}}{\exp(Pe_{m2}) - 1}$$

$$C_{pw1} = \frac{C_{p2}(S_\infty + \exp(Pe_{m2} - 1))}{S_\infty \exp(Pe_{m2})} \tag{4.10}$$

Further, by plugging Equation 4.10 into Equation 4.7d, an expression for the unknown quantity, C_{p1}, was derived as follows:

$$C_{p1} = \frac{C_{p2}\left[\left(\frac{S_\infty + (\exp(Pe_{m2}) - 1)}{S_\infty \exp(Pe_{m2})}\right) + \left(\exp\left(J_v / k_2\right) - 1\right)\right]}{\exp\left(J_v / k_2\right)} \tag{4.11}$$

An equation for C_{wf} was also derived from first plugging Equation 4.9 into Equation 4.6d

$$C_{p2} = \frac{N_s}{J_v} = \frac{S_\infty C_{wf} \exp(Pe_{m1}) - S_\infty C_{p1}}{\exp(Pe_{m1}) - 1}$$

then by plugging Equation 4.11 into the above equation, C_{wf} is solved for

$$C_{wf} = \frac{C_{p2}\left[(\exp(Pe_{m1}) - 1) + \left(\frac{S_\infty\left(\left(\frac{S_\infty + \exp(Pe_{m2}) - 1}{S_\infty \exp(Pe_{m2})}\right) + \exp\left(J_v / k_2\right) - 1\right)}{\exp\left(J_v / k_2\right)}\right)\right]}{S_\infty \exp(Pe_{m1})} \tag{4.12}$$

Next, an expression for C_{p2} is derived by plugging Equation 4.9 into Equation 4.5d

$$C_{p2} = \frac{N_s}{J_v} = \frac{C_{bf} \exp\left(J_v / k_1\right) - C_{wf}}{\exp\left(J_v / k_1\right)}$$

$$C_{wf} = C_{bf}\exp\left(\frac{J_v}{k_1}\right) - C_{p2}\exp\left(\frac{J_v}{k_1}\right)$$

Then, plug the above equation expressing C_{wf} as a function of known parameters, C_{bf} and C_{p2}, into Equation 4.12 and solve for C_{p2}:

$$C_{p2} = \frac{C_{bf}\exp\left(J_v/k_1\right)}{\left[\left(\exp\left(J_v/k_1\right)-1\right)+\left(\frac{\left(\exp(Pe_{m1})-1\right)+\left(\frac{S_\infty}{\exp\left(J_v/k_2\right)}\left(\left(\frac{S_\infty+\exp(Pe_{m1})-1}{S_\infty-\exp(Pe_{m1})}\right)+\exp\left(J_v/k_2\right)-1\right)\right)}{S_\infty\exp(Pe_{m1})}\right)\right]} \tag{4.13}$$

Thus one can get the observed transmission for the multimembrane composite:

$$S_o = \frac{N_s/J_v}{C_{bf}} = \frac{C_{p2}}{C_{bf}} \tag{4.14}$$

Therefore an equation for S_o is obtained by rearranging Equation 4.13 and plugging it into Equation 4.14

$$S_o = \frac{C_{p2}}{C_{bf}} = \frac{\exp\left(J_v/k_1\right)}{\left[\left(\exp\left(J_v/k_1\right)-1\right)+\left(\frac{\left(\exp(Pe_{m1})-1\right)+\left(\frac{S_\infty}{\exp\left(J_v/k_2\right)}\left(\left(\frac{S_\infty+\exp(Pe_{m1})-1}{S_\infty-\exp(Pe_{m1})}\right)+\exp\left(J_v/k_2\right)-1\right)\right)}{S_\infty\exp(Pe_{m1})}\right)\right]}$$

(4.15)

Further one can calculate the actual sieving coefficient S_a defined as

$$S_a = \frac{N_s / J_v}{C_{wf}} = \frac{C_{p2}}{C_{wf}}$$

$$S_a = \frac{C_{p2}}{C_{wf}} = \frac{S_\infty \exp(Pe_{m1})}{\left[(\exp(Pe_{m1})-1)+\left(\frac{S_\infty\left(\left(\frac{S_\infty+\exp(Pe_{m2})-1}{S_\infty \exp(Pe_{m2})}\right)+\exp\left(J_v/k_2\right)-1\right)}{\exp\left(J_v/k_2\right)}\right)\right]} \quad (4.16)$$

4.3 Convection-Diffusion Modeling Results and Discussion

The transport of BSA (MW, 66,430 Da) was studied by Opong and Zydney (1991). Omega 100K membranes were utilized. Table 4.1 shows the transport parameters of BSA for an Omega 50K and an Omega 100K membrane. The reported BSA diffusivity in free solution, D_0, was 6.7×10^{-11} m^2/s (Opong and Zydney 1991). The observed sieving coefficients for single membrane are calculated using Equations 4.4. The observed BSA sieving coefficients S_o of multimembrane composites with various parameters are calculated using Equation 4.15. The actual observed BSA sieving coefficients S_a of multimembrane composites with various parameters are calculated using Equation 4.16.

Because the membranes in the multimembrane composite are the same, the parameters are the same. The asymptotic sieving coefficient S_∞ is an intrinsic property of the membrane and the protein; therefore its value will be the same for both membranes.

The solvent flux J_v is equal throughout the composite at steady state; the membrane thicknesses δ_{m1}, δ_{m2} are equal because the membranes are the same, and D_{eff} is the same; therefore Pe_{m1} and Pe_{m2} are equal.

Table 4.1 Transport Parameters of BSA for Two Different Membranes (Opong and Zydney 1991) pH≈7.0, 0.15 M NaCl

Membrane MWCO	S_∞	$\varepsilon\phi K_d$	δ_m (μm)
Omega 50 K	0.001	3.3×10^{-5}	0.5
Omega 100K	0.037	0.4×10^{-2}	0.5

4.3.1 Effect of Pore Size on Protein Sieving

In Figure 4.9, the observed and the actual sieving coefficients of BSA are shown as a function of filtrate flux for both a single membrane and a 2-membrane composite under conditions where $k_1=k_2=5.2 \times 10^{-6}$ m/s. At high filtrate fluxes, both sets of results are the same for actual and observed sieving coefficients. This is due to the domination of convective forces over diffusional forces. Therefore, at high fluxes both a single membrane and a 2-membrane composite perform in the same fashion. However, at lower fluxes, which are the operating flux range for multimembrane composites, the simulation results show that the observed and actual sieving coefficients decreased significantly for a 2-membrane composite vis-à-vis a single membrane. At very low fluxes ($\leq 8.5 \times 10^{-6}$ m/s), the actual and the observed sieving coefficients are equal for both a single membrane and a 2-membrane composite. Then, S_o deviates away from S_a due to the increase in the extent of concentration polarization with increasing flux. The observed sieving coefficient is related to the observed solute rejection by $R=1-S_o$, so the simulation results show that rejection is being amplified in the 2-membrane composite. An example

calculation for a single membrane is illustrated in Appendix B and an example calculation for a 2-membrane composite is illustrated in Appendix C.

Figure 4.10 shows the observed sieving coefficients of BSA as a function of filtrate flux for both a single membrane and a 2-membrane composite for an Omega 50K membrane. Due to the small pore size of this membrane compared to BSA, the sieving coefficient is very low. At high filtrate fluxes, both sets of results are similar. At lower fluxes (which is the operating range of the multimembrane composite), the effect of reduced sieving is observed, verifying the concept of rejection amplification.

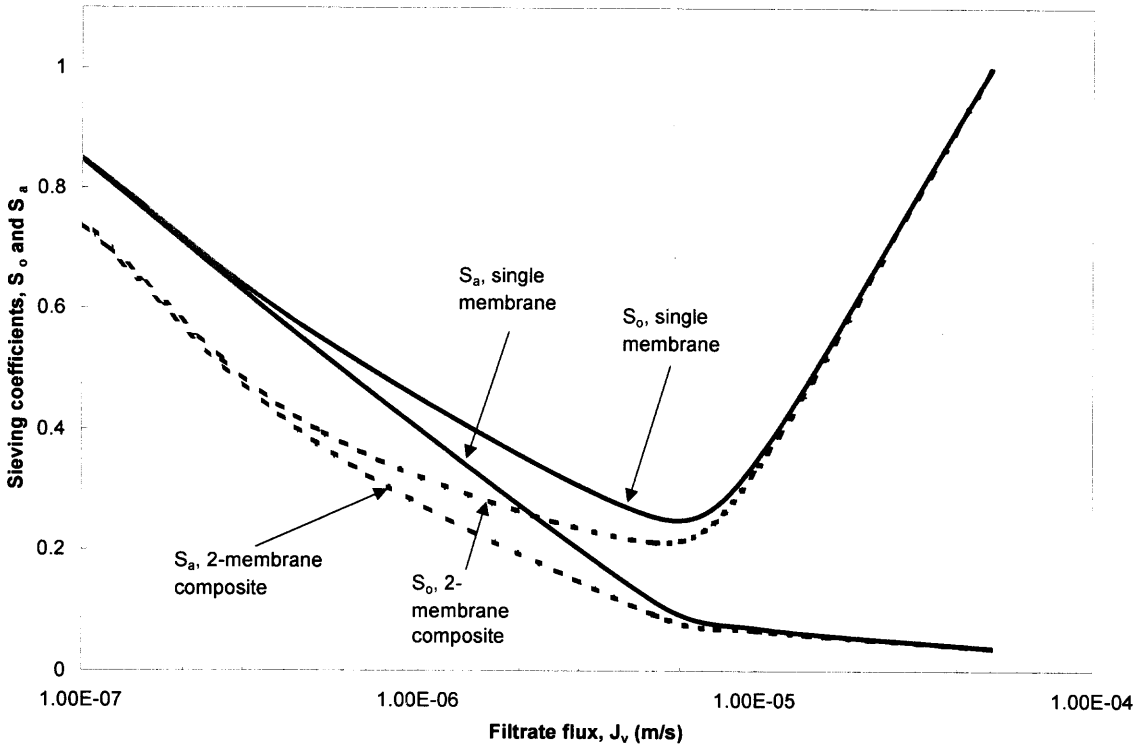

Figure 4.9 Observed and actual sieving coefficients vs. filtrate flux: single membrane and 2-membrane composite (Omega 100K membranes, C_{bf}=5.0 kg/m^3, k_1=k_2=5.2 x 10^{-6} m/s).

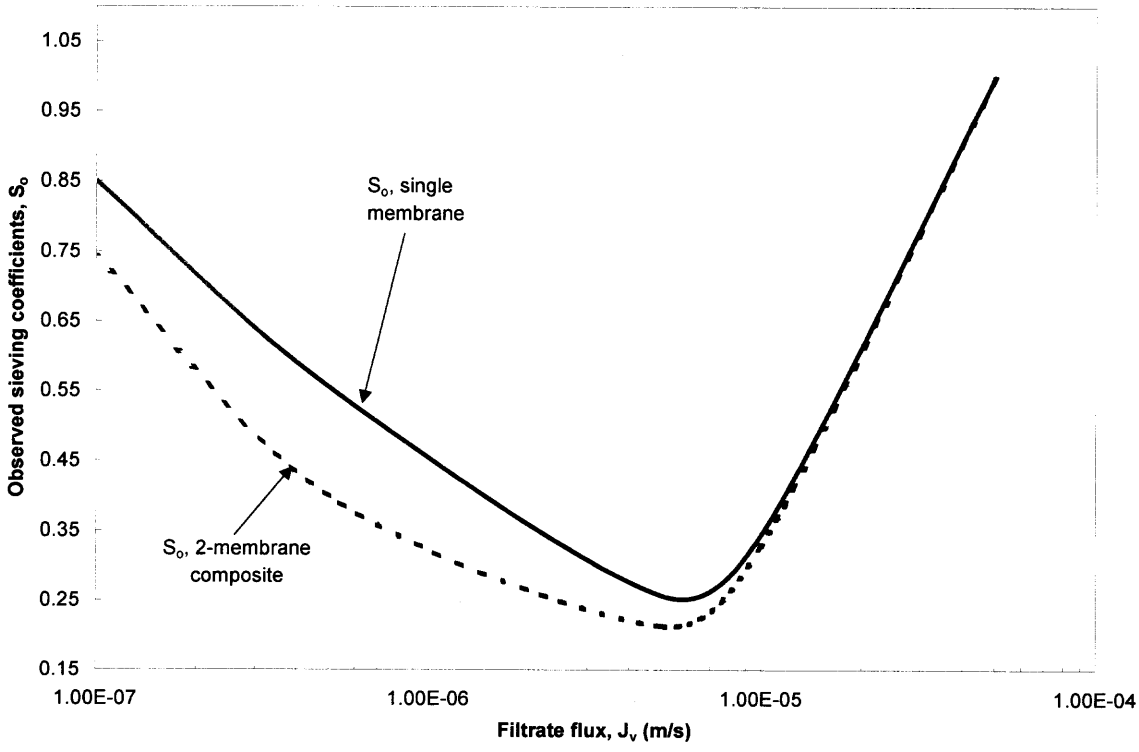

Figure 4.10 Observed sieving coefficient vs. filtrate flux: single membrane and 2-membrane composite (Omega 50K membranes, C_{bf}=5.0 kg/m^3, k_1=k_2=5.2 x 10^{-6} m/s).

4.3.2 Effect of Mass Transfer Coefficient on Protein Sieving

A simulation was performed investigating different mass transfer coefficients for the second boundary layer, k_2. The mass transfer coefficient of the first boundary layer, k_1,was kept constant at k_1 =5.2 x 10^{-6} m/s and three different values of k_2 were used. The value of $k_2=D_o/\delta_2$; therefore k_2 is inversely proportional to the thickness of the boundary layer on the second membrane. The thicknesses of the boundary layers on the second membrane for different mass transfer coefficients are shown in Table 4.2.

Table 4.2 Thickness of the Boundary Layer for Different k_2 Values: Omega 100K Membranes, k_1=5.2 x 10^{-6} m/s, BSA Feed Concentration=5.0 kg/m^3

Mass transfer coefficient, k_2 (m/s)	Boundary layer thickness (μm)
0.00001	6.70
0.0000052	12.88
0.0000001	670.00

Results for these simulations are shown in Figure 4.11. At k_2 = 1x10^{-7} m/s, the multimembrane stack performs very similar to a single membrane except at very low fluxes (≤ 3.0 x 10^{-7} m./s) where diffusion is dominant over convection, there is an effect of reduced protein transmission. At this low mass transfer coefficient (k_2 = 1x10^{-7} m/s), the boundary layer thickness is very high, 670 μm. The boundary layer on the second membrane would not exhibit such low mass transfer (or posses such a thick boundary layer) even without the effects of stirring, because most of the protein rejection is imposed on the first membrane. The distance between the membranes is also very small, which may not allow such a thick boundary layer (as seen with k_2 = 1x10^{-7} m/s).

At higher values of the mass transfer coefficient k_2, the effect of a reduced sieving coefficient, or increased rejection, is observed at flux levels between 1 x 10^{-5} and 1 x 10^{-7} m/s. The two values of k_2 (1 x 10^{-5}, 5.2 x 10^{-6}) show similar profiles, however there is additional reduced sieving for k_2=1 x 10^{-5} m/s at flux levels between 1 x 10^{-6} and 1 x 10^{-5} m/s. This effect is minimal due to the thin boundary layer for both values of k_2 (1 x 10^{-5}, 5.2 x 10^{-6}). Figure 4.11 shows that having a mass transfer coefficient of the second boundary layer equal to or greater than that of the first boundary layer results in a more reduced sieving coefficient or amplified rejection.

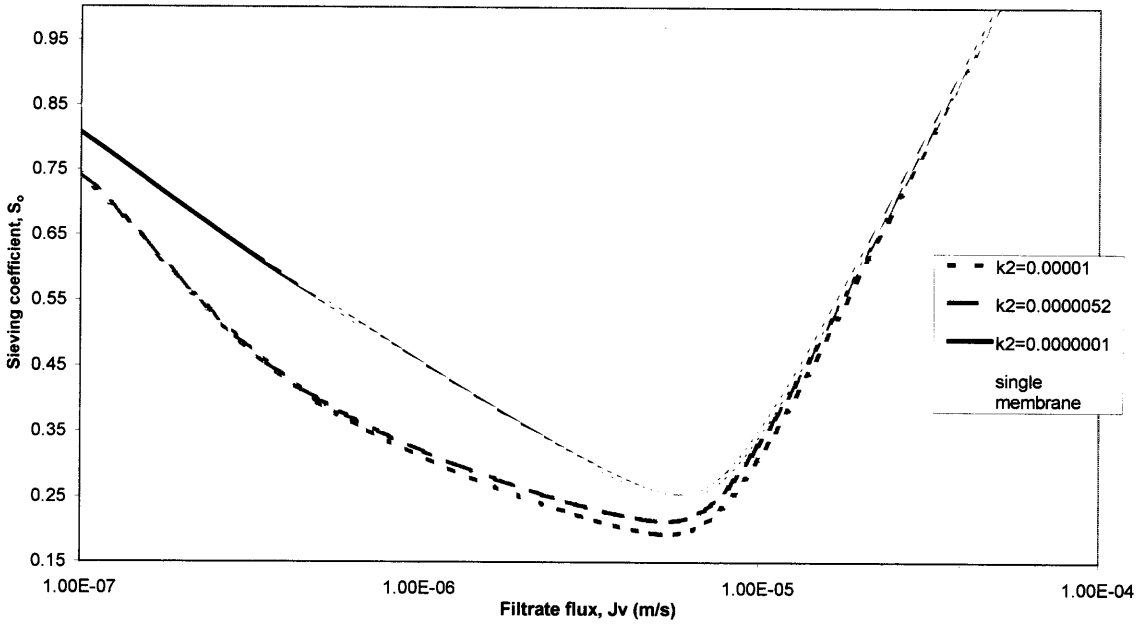

Figure 4.11 Effect of mass transfer coefficient of the boundary layer over the second membrane on the observed sieving coefficient: Omega 100K membranes, BSA feed concentration=5.0 kg/m^3, k_l=5.2 x 10^{-6}.

4.3.3 Simulation of Binary System

The transport of BSA (MW 66,430) and immunoglobulin G (IgG; MW 15,5000) was studied by Saksena and Zydney (1994). Omega 100K membranes were utilized. Table 5.1 shows the transport parameters of BSA and IgG. The observed sieving coefficients for a single membrane for BSA and IgG were calculated using Equation 4.4. The BSA and IgG observed sieving coefficients of multimembrane composites were calculated using Equation 4.15.

Results for the simulation of the separation of BSA and IgG are shown in Figure 4.12. There is an assumption that there is no interaction between the two proteins or between the proteins and the membrane. These results show that there is reduction in the observed sieving coefficient (or increase in the rejection via amplification) for BSA at

fluxes lower than 1 x 10^{-5} m/s (which is the operating range of multimembrane UF). The observed sieving coefficient of IgG is also reduced (or the rejection is increased) at lower fluxes. However, the sieving coefficient of IgG is low due to the large size of the proteins compared to the average size of the pores (illustrated by the low value of S_∞=0.0026).

Table 4.3 Transport Parameters of BSA and IgG for Omega 100K Membranes, pH≈7.0, 0.15 M NaCl (Saksena and Zydney 1994)

Protein	S_∞	D_o (m^2/s)	D_{eff} (m^2/s)
BSA	0.016	6.7 x 10^{-11}	1.0 x 10^{-13}
IgG	0.0026	4.55 x 10^{-11}	4.0 x 10^{-15}

4.4 Concluding Remarks on Modeling Results

The simple rejection amplification model presented in Section 4.1 compared experimental rejection data at different pressures to calculated values of rejection. The calculated data always overpredicted the experimental rejection data. This is due to the different mixing conditions and different levels of concentration polarization present, vis-à-vis the second membrane.

A steady state model was developed using a convection-diffusion model for two membranes in series. The results from the simulations cannot be directly compared to the lumped rejection amplification model described in Section 4.1, due to different experimental conditions. However, some calculations can be developed to compare the two models.

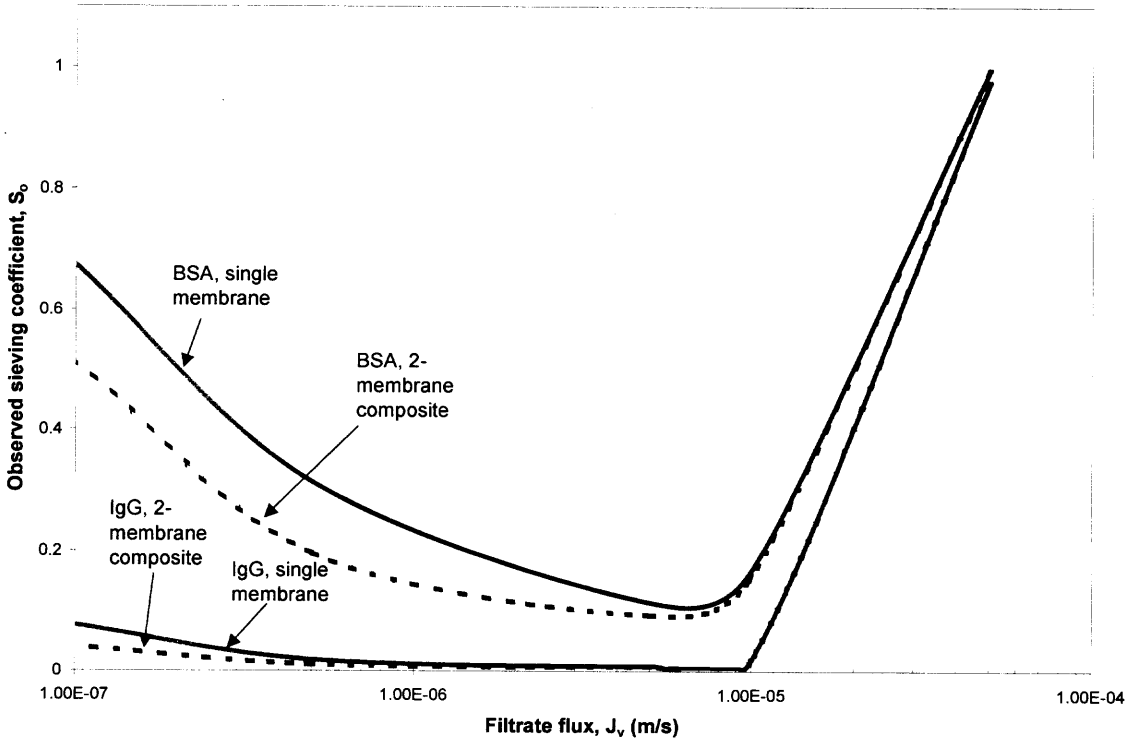

Figure 4.12 Observed sieving coefficient vs. filtrate flux in a binary system: single membrane and 2-membrane composite: Omega 100K membranes, Feed concentrations: 5.0 kg/m^3 BSA and 5.0 kg/m^3 IgG, $k_1=k_2=5.2 \times 10^{-6}$ m/s.

First the observed sieving coefficients are converted to rejection values ($R=1-S_o$). Further, the single membrane rejections obtained from the convection-diffusion model can be amplified with the lumped rejection amplification equation ($R_2=1-(1-R_1)^2$). This value of R_2 can be compared directly with those obtained for the 2-membrane composite calculated with the convection-diffusion model. These results are shown in Figure 4.13.

The results from the comparison of the two models (Figure 4.13) demonstrate the extent of overprediction of the rejection calculated by the rejection amplification equation. Although direct comparison with the experimental data cannot be performed

due to different operating conditions, the comparison between the two models confirms the overprediction observed in Section 4.1. However, direct comparison to experimental data is needed to confirm the performance of the convection-diffusion model.

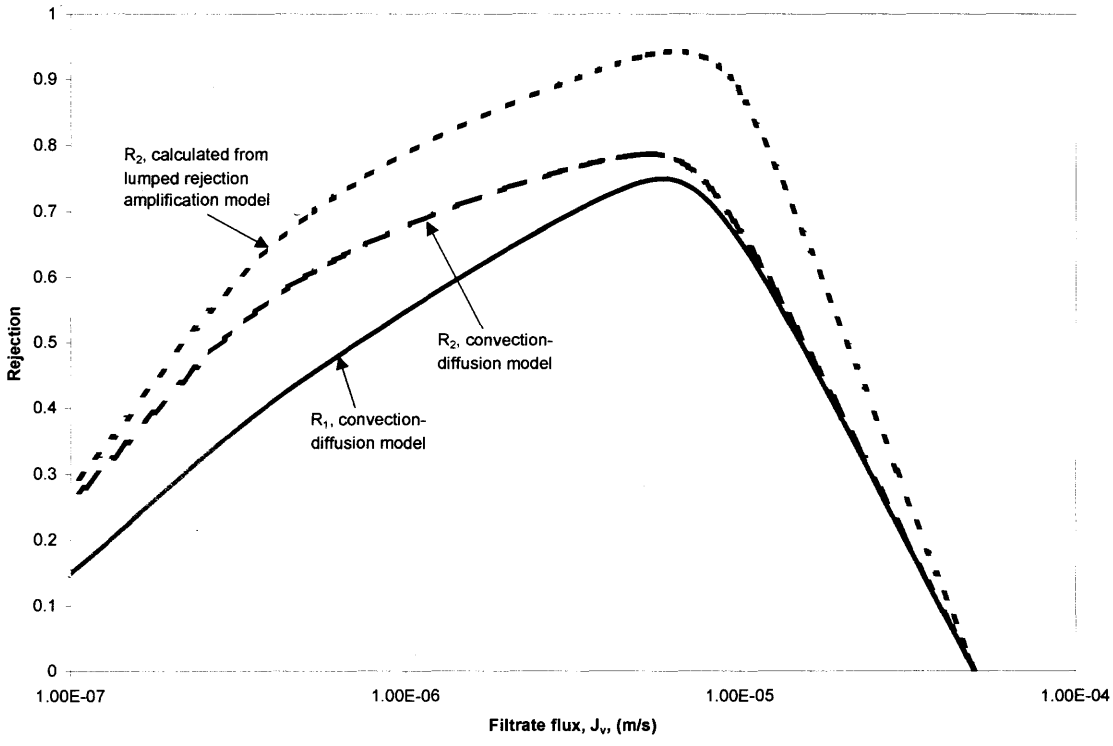

Figure 4.13 Rejection values of BSA vs. flux comparing two different models: Omega 100K membranes, C_{bf}=5.0 kg/m^3, k_1=k_2=5.2 x 10^{-6} m/s.

CHAPTER 5

CONCLUSIONS AND RECOMMENDATIONS FOR FUTURE STUDIES

A new multimembrane composite was developed for ultrafiltration processes by sandwiching the same UF membranes together, one above another in the fashion of skin-backing-skin-backing-skin-backing, etc.. Rejection amplification was observed resulting in complete purification of a binary protein mixture. Different configurations were studied and an optimal sandwich design was utilized. Three different protein mixtures were studied. Single membrane, 2- membrane composite, and 3-membrane composites were investigated.

A new ultrafiltration technique to effectively fractionate biomolecules has been developed by stacking flat UF membranes of the same MWCO in series. The technique may be called internally-staged ultrafiltration (ISUF). The results obtained clearly demonstrate that the rejection characteristics observed for a single membrane were substantially amplified in a multimembrane stack resulting in a pure permeated product in both buffer optimized batch UF (Systems 1 and 2) and nonoptimized systems (System 1); further for System 1, this behavior was observed in pulse-fed UF as well.

In System 1, the operating pressure may be increased to compensate for solvent flux loss encountered with the addition of each new membrane in the stack. It was also shown that the solvent flux was constant over a considerably extended period of time as long as 15 hours. Different feed concentrations as well as continuous feed experiments resulted in complete purification of the permeated protein from the mixture. *In situ* cleaning was carried out to allow cleaning of the stack without disrupting the process and

allowing pure water flux to be essentially completely recovered and cyclic processes to be utilized effectively.

To explore the validity of these conclusions for other systems containing larger proteins and more open UF membranes, 100,000 MWCO membranes were examined along larger proteins (System 3). The results obtained clearly demonstrate that the rejection characteristics observed for a single membrane are substantially amplified in a multimembrane stack resulting in a pure product in buffer and membrane optimized systems. It was also shown that for such a multimembrane stack of, say, 3 membranes to succeed in producing a pure protein in the permeate, the rejection by a single membrane had to be substantial. Thus optimization of the pH, ionic strength, etc. are important to achieving the goal of getting one pure protein in the permeate, as is selecting the membrane with the right membrane charge level. The operating pressure may be increased to compensate for solvent flux loss encountered with the addition of each new membrane in the stack. It was also shown that the solvent flux was constant over a period of time as long as 5 hours. *In situ* cleaning was carried out to allow cleaning of the stack without disrupting the process and allowing pure water flux to be essentially completely recovered and cyclic processes to be utilized effectively.

It was observed that some selectivity in a single membrane system needs to exist in order to undergo rejection amplification. A selectivity of around 15 was found to be the minimum for System 3. However, it is important to understand why rejection amplification does not occur when there is low selectivity (i.e., if the selectivity of a binary system is 2). This can be attributed to the effect of concentration polarization on

the second membrane. The increased wall concentration on the second membrane will increase protein transmission, reducing the overall selectivity of the mixture.

Two mathematical models were described to simulate the effect of the multimembrane composite. First, a simple lumped model was explored and experimental data were compared to the model-based calculated results. This model illustrated the effect of rejection amplification. This simple model revealed the general trends of rejection; however, the lumped model overpredicted the experimental data. This is due to the different conditions imposed on the membranes. Increased concentration polarization on the middle and bottom membranes in the stack, will result in increased sieving, or reduced rejection. The increased concentration polarization can be attributed to the lack of mixing present, as well as a lack of a substantial amount of bulk volume for the solutes to diffuse.

In order to explain the effects of the boundary layer that is present on the membranes, a steady state convection-diffusion model was developed. This model consisted of two membranes in series, both experiencing a concentration boundary layer on the respective feed side. Expressions for the wall concentrations of both membranes, as well as the solute concentration in the interstitial space were developed. Simulations were performed using literature data to illustrate the multimembrane performance at different fluxes. Data for different MWCO membranes were utilized and increased sieving was observed for both scenarios at the operating flux range of multimembrane ultrafiltration. Variation of the mass transfer coefficient of the second membrane displayed that at very low mass transfer coefficients, the multimembrane composite

behaved similar to a single membrane. A binary system of BSA and IgG was also simulated and reduced sieving was observed with both solutes.

Although experimental data were not utilized in the convection-diffusion model, the performance of the two models could be directly compared. When single membrane simulation results were amplified with the lumped model and compared to the simulation results obtained for two membranes using the convection-diffusion model, it was observed that the lumped model overpredicted the results from the convection-diffusion model. It can be inferred that the convection-diffusion model better describes the multimembrane process, however, experimental data are needed to confirm this statement.

Future studies should explore the validity of the convection-diffusion model. The parameters of the proteins of study need to be found and applied to the model. Further the model should be expanded to a 3-membrane system.

Some fundamental experiments should be explored to better understand a number of aspects of the multimembrane stack, such as the volume present in-between the membranes. More knowledge of the characteristics of the space in-between the membranes needs to be obtained due to the inability to measure the parameters; such as mass transfer, concentration, and volume.

An unsteady state model of the process is also needed. In the convection-diffusion model, a steady state assumption is made. An unsteady state model would better describe the behavior of the multimembrane composite due to the potential time-based accumulation of proteins in the inter-membrane space. Other parameters should be considered as well, such as the effect of charge on the sieving of the protein.

Other applications, such as multicomponent systems should be investigated. This was an initial investigation into the technique, and therefore focused on binary systems to better understand the process. However, other systems (i.e., whey protein) could be explored. A synthetic broth is also an option.

Improved yields of the more permeable protein are desirable for industrial purposes. The purpose of this research was an initial investigation, and therefore a high yield was not an important aspect of the research. A high yield may be achieved by employing longer operating time. High operating pressure may also aid in increasing the yield.

Experiments other than batch ultrafiltration are desirable as well. A continuous experiment that maintains the feed concentration constant is a valuable asset for system design when applying it to manufacturing processes.

APPENDIX A

METHOD FOR CALCULATING PROTEIN CONCENTRATION

Presented below is an example calculation for determining protein concentrations in a binary mixture of Mb and β-LG using calibration curves identified in Table 2.5. For example, to determine the concentrations from raw absorbance data, assume the experimentally determined absorbance values of 0.121 at 410 nm and 0.049 at 280 nm.

Experimentally determined absorbances at 280 and 410 nm:

1. Absorbance of a binary mixture of Mb and β-LG at 280 nm=A_{280T}=0.049
2. Absorbance of a binary mixture of Mb and β-LG at 410 nm=A_{410T}=A_{410Mb} (β-LG has no absorbance at 410 nm)=0.121

Calculations for individual protein concentrations:

1. Concentration of Mb, C_{Mb} (from Figure 2.6)=0.150 x A_{410Mb}
   = 0.150 x 0.121=18.126 μg/ml
2. The corresponding Mb absorbance at 280 nm (from Figure 2.7)
   $A_{280Mb} = C_{Mb} / 0.670 = 18.126 / 0.670 = 0.027$
3. Absorbance of β-LG at 280 nm
   $A_{280\beta\text{-LG}} = A_{280T} - A_{280Mb} = 0.049 - 0.027 = 0.022$
4. Concentration of β-LG, $C_{\beta\text{-LG}}$ (from Figure 2.12) = 1.260 x $A_{280\beta\text{-LG}}$
   =1.260 x 0.022=27.632 μg/ml

APPENDIX B

METHOD FOR CALCULATING SIEVING COEFFICIENTS USING THE CONVECTION DIFFUSION MODEL FOR A SINGLE MEMBRANE

Presented below is an example calculation for the observed and actual sieving coefficients for BSA at a given flux using the convection diffusion model for a single membrane. Microsoft® Excel 2000 was used for the simulations. Parameters are taken from Table 4.1 for an Omega 100K membrane.

Parameters (single membrane)

J_v (m/s)	D_0 (m^2/s)	ϕKc	$\varepsilon\phi Kd$	δ_m (m)	C_{bf} (mg/ml)
1.00E-07	6.70E-11	0.037	0.004	5.00E-07	5.0

k_f (m/s)	Pe_{m1}	J_v/k_f
5.20E-06	6.90E-03	1.92E-02

$\exp(Pe_{m1})$	$\exp(J_v/k_f)$
1.007	1.019

Where
$Pe_m = (\phi Kc \times J_v \times \delta_m) / (\varepsilon\phi Kd \times D_0)$
J_v/k_f=1.0E-0.7 / 5.2E-6=1.92E-2

Calculations of BSA concentrations and sieving coefficients

C_{wf} (mg/ml)
5.015

C_{p1}(mg/ml)
4.253

$S_{o,\ single\ membrane}$
0.851

$S_{a,\ single\ membrane}$
0.848

Where

$C_p=(C_{bf}*\phi Kc*\exp(Pe_m)*\exp(J_v/k_f))/((\phi Kc-1)*(1-\exp(Pe_m)+(\phi Kc*\exp(Pe_m)*\exp(J_v/k_f))$

$=(5*0.037*1.007*1.019)/((0.037-1)*(1-1.007)+(0.037*1.007*1.019)) =4.246$

$Cwf=(C_p*(\phi Kc+\exp(Pe_{m1})-1))/((\phi Kc*\exp(Pe_{m1}))=(4.246*(0.037+1.007-1))/((0.037*1.007))= 5.015$

$S_o=C_p/C_{bf}=4.246/5.0=0.851$

$Sa=C_{wf}/C_{bf}=5.015/5.0=0.848$

APPENDIX C

METHOD FOR CALCULATING SIEVING COEFFICIENTS USING THE CONVECTION DIFFUSION MODEL FOR A 2-MEMBRANE COMPOSITE

Presented below is an example calculation for the observed and actual sieving coefficients for BSA at a given flux using the convection diffusion model for a 2-membrane composite. Microsoft® Excel 2000 was used for the simulations. Parameters are taken from Table 4.1 for an Omega 100K membrane.

Parameters (2-membrane composite)

J_v (m/s)	D_0 (m^2/s)	$\phi Kc=S_{infinity}$	$\varepsilon\phi Kd$	δ_m (m)	C_{bf} (mg/ml)
1.00E-07	6.70E-11	0.037	0.004	5.00E-07	5.0

k_1 (m/s)	k_2 (m/s)	Pe_{m1}	J_v/k_1	J_v/k_2
5.20E-06	5.20E-06	6.90E-03	1.92E-02	1.92E-02

$\exp(Pe_{m1})$	$\exp(J_v/k_1)$	$\exp(J_v/k_2)$
1.007	1.019	1.019

Where

$Pe_{m1} = (\phi Kc \times J_v \times \delta_m) / (\varepsilon\phi Kd \times D_0)$

J_v/k_1=1.0E-0.7 / 5.2E-6=1.92E-2

J_v/k_2=1.0E-0.7 / 5.2E-6=1.92E-2

Calculations of BSA concentrations and sieving coefficients

C_{wf} (mg/ml)

5.025

C_{p1}(mg/ml)

4.365

C_{pw1}(mg/ml)
4.377

C_{p2}=(mg/ml)
3.713

$S_{o,2\text{-membrane composite}}$
0.743
$S_{a,2\text{-membrane composite}}$
0.739

Where

$C_{p2}(mg/ml)=(\exp(J_v/k_1)*C_{bf})/((\exp(J_v/k_1)-1)+(((\exp(Pe_{m1})-1)+(((\phi Kc*(\phi Kc+\exp(Pe_{m2})-1)/(\phi Kc*\exp(Pe_{m1}))+\exp(J_v/k_2)-1))/\exp(J_v/k_2))))/(\phi Kc*\exp(Pe_{m1})))=(1.019*5.0)/((1.019-1)+(((1.007-1)+(((0.037*(((0.037+1.007-1)/(0.039*1.007))+1.019-1))/1.019)))/(0.037*1.007)))= 3.713$

$C_{fw}=(C_{p2}*((\exp(Pe_{m1})-1)+(((\phi Kc*(\phi Kc+\exp(Pe_{m2})-1)/(\phi Kc*\exp(Pe_{m1}))+\exp(J_v/k_2)-1))/\exp(J_v/K_2)))))/(\phi Kc*\exp(Pe_{m1}))=(3.713*((1.007-1)+(((0.037*((0.037+1.007-1)/(0.037*1.007)+1.017-1))/1.017))))/(0.037*1.007)= 5.025$

$C_{p1}=(C_{p2}*((\phi Kc+\exp(Pe_{m2})-1)/(\phi Kc*\exp(Pe_{m1})+(\exp(J_v/k_2)-1)))/\exp(J_v/k_2)=$
$(3.713*((0.037+1.007-1)/(0.037*1.007)+(1.019-1)))/1.019=4.365$

$C_{pw1}=(C_{p2}*(\phi Kc+\exp(Pe_{m2})-1))/(\phi Kc*\exp(Pe_{m2}))=(3.713*(0.037+1.007-1))/(0.037*1.007)=4.377$

$S_o=C_{p2}/C_{bf}=3.713/5.0=0.743$

$Sa=C_{wf}/C_{bf}=5.025/5.0=0.739$

REFERENCES

Amicon Corporation. 1995. *Membrane Filtration Chromatography Catalog.*

Anderson, J. L. and J. A. Quinn 1974. "Restricted Transport in Small Pores: A Model for Steric Exclusion and Hindered Particle Motion." *Biophys. J.* **14**: 130.

Barker, P. E. and A. Till 1992. "Using Multistage Techniques to Improve Diafiltration Fractionation Efficiency." *J. Membr. Sci.* **72**:1-11.

Boyd, R. F. and A. L. Zydney 1997. "Sieving Characteristics of Multilayer Ultrafiltration Membranes." *J. Membr. Sci.* **131**:155-165.

Burba, P, B. Aster, T. Nifant'eva, V. Shkivnev and B. Spivakov 1998. "Membrane Filtration Studies of Aquatic Humic Substances and their Metal Species: a Concise Overview Part 1. Analytical Fractionation by Means of Sequential-Stage Ultrafiltration." *Talanta* **45**:977-988.

Burns, D. B. and A. L. Zydney 1999. "Effect of Solution pH on Protein Transport through Ultrafiltration Membranes." *Biotechnol. Bioeng.* **64**(1): 27-37.

Burns, D. B. and A.L. Zydney 2000. "Buffer Effects on the Zeta Potential of Ultrafiltration Membranes. " *J. Membr. Sci.* **172**:39-48.

Chan, K. and T. Matsuura 1983. "Determination of Pore Sizes at the Skin Layer of Aromatic Polyamidohydrazide Ultrafiltration Membranes." *J. Polym Sci. Lett. Ed.* **21**:417-422.

Cheang, B. and A. L. Zydney 2003. "Separation of Alpha-Lactalbumin and Beta-Lactoglobulin Using Membrane Ultrafiltration." *Biotechnology and Bioengineering* **83**(2): 201-209.

Cherkasov, A. N. and A. E. Polotsky 1996. "The Resolving Power of Ultrafiltration." *J. Membr. Sci.* **110**:79-82.

Cheryan, M 1998. *Ultrafiltration and Microfiltration Handbook.* Pennsylvania. Technomic Publishing Company, Inc.

Darbre, PD, A. E. Romero-Herrera and H. Lehmann 1975. "Comparison of the Myoglobin of the Zebra (Equis Burchelli) With that of the Horse (Equis Caballus)." *Biochemica et Biophysica Acta* **393**:201-204.

Deen, W. M. 1987. "Hindered Transport of Large Molecules in Liquid-Filled Pores." *AIChE J.* **33**: 1409.

Dickerson, R. E. and I. Geis, 1969 *The Structure and Action of Proteins.* New York, Harper and Row Publisher.

Fane, A. G., C. J. D. Fell and A. G. Waters 1981. "The Relationship Between Membrane Surface Pore Characteristics and Flux." *J. Membr. Sci.* **9**:245-262.

Gebauer, K. H., J. Thömmes and M. R. Kula 1997. "Plasma Protein Fractionation with Advanced Membrane Adsorbents." *Biotechnol. Bioeng.* **54**:181-189.

Ghosh, R. 2003 "Novel Cascade Ultrafiltration Configuration for Continuous, High-Resolution Protein-Protein Fractionation: a Simulation Study." *J. Membr. Sci.* **226**:85-99.

Ghosh, R. and Z.F. Cui, 2000. "Simulation Study of the Fractionation of Proteins Using Ultrafiltration." *J. Membr. Sci.* **180**:29.

Harrison, R. G., Ed. 1994. *Protein Purification Process Engineering*. Bioprocess Technol. New York, Marcel Dekker.

Hirayama, K., S. Akashi, M. Furuya and K. Fukuharak 1990. "Rapid Confirmation and Revision of the Primary Structure of Bovine Serum Albumin by Esims and Frit-Fab LC/MS." *Biochemical and Biophysical Research Communications* **173**:639-646.

Hodgins, L. and E. Samuelson 1990. "Hydrophilic Article and Method of Producing Same." US Patent: 4,906,379.

Jucker, C. and M. Clark 1994. "Adsorption of Aquatic Humic Substances on Hydrophobic Ultrafiltration Membranes." *J. Membr. Sci.* **97**:37-52.

Kaplan, L. J. and J. F. Foster 1971. "Isoelectric Focusing Behavior of Bovine Plasma Albumin, Mercaptalbumin, and Beta-Lactoglobulins A and B." *Biochemistry* **10**:630-636.

Kim, K. J, A. G. Fane, M. Nystrom, A. Pihlajamaki, W. R. Bowen and H. Mukhtar 1996. "Evaluation of Electroosmosis and Streaming Potential for Measurement of Electrical Charges of Polymeric Membranes." *J. Membr. Sci.* **116**:149-159.

Kronman, M. J. and R. F. Andreotti 1964. "Inter- and Intramolecular Interactions of α-Lactalbumin. I. The Apparent Heterogeneity at Acid pH." *Biochemistry* **3**(8): 1145-1151.

Kulkarni, S. S., E. W. Funk and N. N. Li. 2001. Ultrafiltration. *Membrane Handbook.* W. S. W. Ho and K. K. Sirkar. Boston, Kluwer Academic Publishers: 393-453.

Kurnik, R. T., A. W. Yu, G. S. Blank, A. R. Burton, D. Smith, A. M. Athalye and R. van Reis 1995. "Buffer Exchange Using Size Exclusion Chromatography, Countercurrent Dialysis, and Tangential Flow Filtration: Models, Development, and Industrial Application." *Biotechnol. Bioeng.* **45**:149-157.

Lehninger, A. L. 1975. *Biochemistry.* 2nd edition. New York, Worth Publisher.

Longsworth, L. G. and C. F. Jacobsen 1949. "An Electrophoretic Study of the Binding of Salt Ion by β-Lactoglobulin and Bovine Serum Albumin." *J. Phys. Colloid Chem.* **53**: 126-135.

Merin, U. and M. Cheryan 1980. "Ultrastructure of the Surface of a Polysulfone Ultrafiltration Membrane." *J. Appl. Polym. Sci.* **25**:2139-2142

Millipore 2000.*Ultrafiltration Membranes Operating Instructions.*

Mochizuki, S. and A. Zydney 1992. "Dextran Transport Through Asymmetric Ultrafiltration Membranes: Comparison with Hydrodynamic Models." *J. Membr. Sci.* **68**:21-41.

Myers, J. 2000. "Economic Considerations in the Development of Downstream Steps for Large Scale Commercial Biopharmaceutical Processes." IBC Production and Economics of Biopharmaceuticals; November 13-15; La Jolla CA.

Nyström, M., P. Aimar, S. Luque, M. Kulovaara and S. Metsämuuronen 1998. "Fractionation of Model Proteins using their Physiochemical Properties." *Colloids and Surfaces A: Physiochemical and Engineering Aspects* **138**:185-205.

Opong, W. S. and A. L. Zydney 1991. "Diffusive and Convective Protein Transport through Asymmetric Membranes." *AIChE J.* **37**(10): 1497-510.

Pall Corporation 2001. *Ultrafitration Membrane Disc Filters.*

Pfeiffer, J. F., Chen J. C., and J. T. Hsu 1996. "Permeability of Gigaporous Particles." *AIChE J.* **42**:932-939.

Prazeres, D. M. F. 1997. "A Theoretical Analogy Between Multistage Ultrafiltration and Size-Exclusion Chromatography." *Chem. Eng. Sci.* **52**:953-960.

Radola, B. J. 1973. "Isoelectric Focusing in Layers of Granulated Gels: I. Thin-Layer Isoelectric Focusing of Proteins." *Biochimica et Biophysica Acta* **295**: 412 -428.

Rathore, A. S., P. Latham, H. Levine, J. Curling and O. Kaltenbrunner 2004. "Costing Issues in the Production of Biopharmaceuticals." *BioPharm Int.* **17**(2): 46-55.

Saksena, S. and A. L. Zydney 1994. "Effect of Solution pH and Ionic Strength on the Separation of Albumin from Immunoglobulins (IgG) by Selective Filtration." *Biotechnol. Bioeng.* **43**(10): 960-968.

Sarfert, F. T. and M. R. Etzel 1997 "Mass Transfer Limitations in Protein Separations Using Ion-Exchange Membranes." *J. Chromatogr. A* **764**:3-20.

Scopes R. K. 1994. *Protein Purification Principles and Practice.* 3rd edition. New York, Springer Verlag.

Sirkar, K. K. and R. Prasad. 1986. Protein Ultrafiltration-Some Neglected Considerations. In: W. C. McGregor, editor. *Membrane Separations in Biotechnology.* 1st edition. New York, Marcel Dekker.

Sofer, G. and L. Hagel 1997. *Handbook of Process Chromatography: A Guide to Optimization, Scale up, and Validation.* New York, Academic Press.

Sokol, F., L. Hána and P. Albreacht 1961. "Fluorescent Antibody Method: Quantitative Determination of 1-Dimethylaminonaphthalene-5-Sulphonic Acid and Protein in Labeled γ-Globulin." *Folia Microbiologica.* **6**:145-150.

Swaminathan, T., M. Chaudhuri, and K. K. Sirkar 1981. "Effect of Solvent Flux During Stirred Cell Ultrafiltration of Proteins." *Biotechnol. Bioeng.* **23**:1873-1880.

Thömmes, J. and M. R. Kula 1995. "Membrane Chromatography - An Integrated Concept in the Downstream Processing of Proteins." *Biotechnol. Prog.* **11**:357-367.

Townend, R., L. Weinberger, and S. N. Timasheff 1960. "Molecular Interactions in β-Lactoglobulin. I. The Electrophoretic Heterogeneity of β-Lactoglobulin Close to its Isoelectric Point." *J. Am. Chem. Soc.* **82**:3157.

van Eijndhoven, R. H., S. Saksena and A. L. Zydney 1995 "Protein Fractionation Using Electrostatic Interactions in Membrane Filtration." Biotechnol Bioeng **48**:406-414.

van Reis, R, S. Gadam, L. N. Frautschy, S. Orlando, E. M. Goodrich, S. Saksena, R. Kuriyel, C. M. Simpson, S. Pearl, and A. L. Zydney 1997. "High Performance Tangential Flow Filtration." *Biotechnol. Bioeng.* **56**:71-82.

van Reis, R., E. M. Goodrich, C. L. Yson, L. N. Frautschy, R. Whiteley and A. L. Zydney 1997. "Constant C_{wall} Ultrafiltration Process Control." *J. Membr. Sci.* **130**(1-2): 123-140.

Vanaman, T. C., K. Brew and R. L. Hill 1970. "The Complete Amino Acid Sequence of Bovine Alpha-Lactalbumin." *The Journal of Biological Chemistry* **245**: 4570-82.

Zydney, A. L. and R. van Reis. 2001. High-Performance Tangential-Flow Filtration. *Membrane Separations in Biotechnology.* W. K. Wang. New York, Marcel Dekker: 277-298.